Modelling the response of channel and vegetation patterns to extreme discharge events

Master thesis

Y. R. Bossenbroek

TU Delft

Deltares
Enabling Delta Life

Modelling the response of channel and vegetation patterns to extreme discharge events

Master thesis

by

Y. R. Bossenbroek

Student number:	4219341	
Thesis committee:	Prof. dr. ir. Z. B. Wang,	TU Delft, supervisor
	Dr. ir. C. J. Sloff,	TU Delft
	Dr. T. A. Bogaard,	TU Delft
	Dr. ir. J. T. Dijkstra,	Deltares
	Dr. ir. M. van Oorschot	Deltares

Deltares
Enabling Delta Life

TU Delft Delft University of Technology

Preface

In this master thesis, my graduation work about the effects of extreme flood events on the vegetation and morphology in a natural river is presented. With this thesis I conclude my MSc studies in Hydraulic Engineering at the Faculty of Civil Engineering and Geosciences of Delft University of Technology. I have carried out this thesis in cooperation with Deltares.

First, I would to thank my thesis committee. I would not have been able to complete my thesis without the time, support and guidance of everyone on my thesis committee. Zheng Bing Wang for chairing the committee and your valuable feedback during the committee meetings. Jasper Dijkstra, for your time and support as my daily-supervisor at Deltares, your help in how to approach this thesis and giving me the ability to graduate at Deltares. Kees Sloff for your help with Delft3D and making time for our weekly online meetings during the corona-crises to discuss my results and progress, this has helped me a lot in finishing my thesis. Mijke van Oorschot for your critical read-throughs, your help in developing the vegetation model and for your time going through all that code. Thom Bogaard for your fresh look at the subject which helped me to improve my thesis.

Second, to all my friends, thank you for making my time in Delft such a great time! Without you guys my time outside the TU Delft lecture halls would never been as fun as they have been. For this thesis, I want to especially thank my friends Cas, Gerben, David, as you guys never got tired to read new parts of my thesis.

Third, I want to thank my mom and wonderful sisters Merle, Myrte, Mayra and Myrza. They all had no idea what I was researching all this time during my thesis, but I could always count on their unconditional love, support and trust in me. I also want to thank my dad even though he is no longer on this earth and I unfortunately never got to know him. The reason I still want to thank him is because I must have inherited my technical and mathematical skills from him, as it is very unlikely that I have them from my mom (sorry mom). And as you can imagine, those skills were pretty useful in this thesis and study. Last, but not least, I want to thank my girlfriend Inez, thank you for your endless patience, trust and support during the ups and downs of this thesis.

Yoram Bossenbroek
Delft, November 2020

Summary

River systems are under pressure worldwide because of human intervention, which often reduces or eliminates the natural dynamics of a river. This has led to a large reduction of riparian vegetation worldwide because the life-cycle of riparian vegetation is closely related with the natural dynamics of a river. Riparian vegetation plays an important role in ecosystems, as it provides habitat for wildlife and recreational value (Johnson et al., 1977; Knopf et al., 1988). Not only human alterations, but also climate change can pose a threat to natural rivers and riparian vegetation. The predictions are that climate change will lead to a general trend towards lower mean river discharges and more extreme discharge events. The aim of this study is to understand how extreme flood events affect the channel and vegetation patterns, and how vegetation recovers after an extreme flood.

An extreme flood event cause a sudden change in the river flow and affects both morphology and vegetation development. The interaction between those drivers is complex and difficult to predict. Van Oorschot et al. (2016) were the first to develop a model that is able to simulate the interaction between river flow, morphodynamics, and vegetation development. They used a separate vegetation-development model and coupled that with a hydro-morphodynamic model. However, in this coupled model the drought stresses and vegetation growth in the first year are not accurately simulated. To address those shortcomings a new vegetation-development model is introduced in this study, which bases the drought stresses on root lengths and estimated groundwater levels. Furthermore, this new vegetation-development is able to simulate the vegetation growth during the first year after germination. This enables the model to take the higher mortality resistance of more mature seedlings into account. Together with the improved drought process, this provides the possibility to simulate more reliable seedling recruitment rates. An added advantage is that the new model uses a different coupling method which results in 7 to 10 times faster computation times than the model of Van Oorschot et al. (2016).

A model schematization based on the Allier River (France) at Moulins is used as a case-study. The Allier River is one of the last European unregulated vegetated rivers, which behaves still as a natural meandering river. Two of the most dominant riparian tree species along the Allier river are simulated: the *Salix alba* and *Populus nigra*. Riparian tree species are used because they have the most morphological impact on dynamic vegetated rivers (Gurnell, 2014). The river discharges used in the model are based on 51 years of discharge measurements.

To investigate the effects of extreme flood events on channel and vegetation patterns with the introduced model, the following steps are taken: First, the most important vegetation characteristics of the *S. alba* and *P. nigra* are investigated so that that those can be used in the model. Second, to gain a deeper understanding of the sensitivity of the found vegetation characteristics in the model, a sensitivity analysis is carried out. Third, the effects of extreme floods are investigated by comparing two extreme floods events with a default scenario without extreme floods.

The model results of the default scenario show realistic vegetation patterns and vegetation age distributions compared to field observations reported in literature and observed in the Allier river. The results show that the vegetation in the Allier river creates and maintains an active meandering system, and thereby confirms the earlier findings of Van Oorschot et al. (2016). Simulating dynamic vegetation results in a more dynamic river because it influences the flow and morphology of the river, ultimately resulting in islands, chute cut-offs and secondary channels. In the no coupling scenario, where the hydro-morphodynamic model is not influenced by vegetation, a very static behaviour of the river channel is observed. This finding is contrary to previous studies which have suggested that without vegetation channel dynamics increase. This static behaviour of the model is probably caused by the fixed upstream boundary condition in the Delft3D FM model and as a result propagating bars and migrating meander bends from upstream are excluded from the model.

The sensitivity analysis shows a strong interaction between vegetation and morphology, and found that vegetation characteristics can have a large influence on the river morphology in the model. In general, a higher vegetation coverage leads to a more dynamic river behaviour in the model. An exception is vegetation with characteristics that allows it to colonize the river banks very quickly: rapid colonization leads to stabilization of the river banks, which in turn leads to static behaviour and narrowing of the river channel. This effect is most pronounced in the scenario with fast growing seedlings. The vegetation coverage is most sensitive to the flood threshold of the vegetation, which specifies the number of consecutive flooding days after which the vegetation starts to decease. The flooding threshold strongly influences both the mortality as the seedling recruitment rates. The uproot resistance of the vegetation has a much smaller effect on the vegetation coverage. Results also show that shortening of the seed dispersal period can significantly reduce the chances of successful seedling recruitment.

To investigate the effects of an extreme flood event, two scenarios are examined. Both scenarios use a single extreme flood event with a maximum discharge of 1900 m^3/s, but the moment of flood occurrence differs. Based on this study it can be concluded that the direct effects of an extreme flood are relatively low, with almost no vegetation removed during a flood event. However, the extreme floods lead to an increased area suitable for seedling colonization within the river floodplain, which is partly caused by the formation of a secondary channel in both extreme flood scenarios. This causes an increase in the seedling recruitment rate in the years directly after an extreme flood and in a higher vegetation coverage.

The higher vegetation coverage in the years after an extreme flood causes a narrowing of the river channel and eventually forces the river to become single-threaded. This results in a reduction of the area in the floodplain that is suitable for the colonization of seedlings and consequently to a decrease in seedling recruitment. Depending on how successfully the vegetation colonizes the secondary streams, this leads to equal or lower vegetation coverage than in the default scenario. However, the results show that the reduction of the area in the floodplain that is suitable for the colonization of seedlings is likely to be temporary, as this area starts to increase again after about 20 years of the extreme flood event.

This research showed the advantage of using a coupled model to investigate morphological and vegetational changes. Because of the model's relatively fast computation times it is possible to quickly investigate multiple scenarios with slightly different vegetation characteristics and discharge regimes. This makes the model applicable for river management purposes, as an envelope of model results is more informative than a single, never exactly right model outcome. Furthermore, crucial biological processes, like drought and growth processes, were added or improved which improved the reliability of seedling recruitment rates. While many vegetation processes are simulated in the model, it is not possible to implement all complex interactions. As a result, it remains unclear what the absolute value for vegetation coverage is. However, the relative difference between scenarios with different vegetation characteristics or discharge regimes can be well simulated. With few modifications, the model can be applied to other meandering vegetated rivers and used to investigate long-term effects of climate change, human interventions, and river adjustments on riparian vegetation.

Contents

1 Introduction

1.1. Background

Rivers constitute some of the most dynamic earth surface systems, transporting sediment and water from their catchment area towards the sea and creating valuable ecosystems that provide habitats and food for countless fluvial species. Besides this, rivers play an important role in human societies by providing fresh water for drinking, irrigation and industry, travel routes for goods and people, and fertile soils for farming.

River systems are under pressure worldwide because of human intervention. Human alterations, such as the building of dams or the modification of river courses for navigational purposes, often reduce or eliminate the natural dynamics of a river. In industrialised parts of the world, such as Europe, only a small number of natural rivers remain (Dynesius and Nilsson, 1994). This has led to a large reduction of riparian vegetation, as the life-cycle of riparian vegetation is closely related with the natural dynamics of a river. However, riparian vegetation is an important part of a healthy natural river, because it provides habitat for wildlife, including endangered species, as well as recreational value (Johnson et al., 1977; Knopf et al., 1988). The last decades have seen an increase in river restoration projects to restore human altered rivers to their more natural conditions (Szałkiewicz et al., 2018). This is, for instance, achieved by removing dams or reversing the river canalization by giving the river more space.

However, not only human alterations but also climate change can create a threat to natural rivers and the riparian vegetation. The predictions are that climate change will lead to a general trend towards lower mean river discharges and more extreme discharge events (IPCC, 2014; Van Vliet et al., 2013; Hirabayashi et al., 2013). This could have severe consequences on the ecological processes within the riparian zones. The hypothesis is that riparian vegetation is particularly vulnerable to climate change, due to its dependency on the river discharge regime (Schneider et al., 2011; Capon et al., 2013; Garófano-Gómez et al., 2017). To understand the effects of a changing discharge regime on a natural river, it is of vital importance to understand the

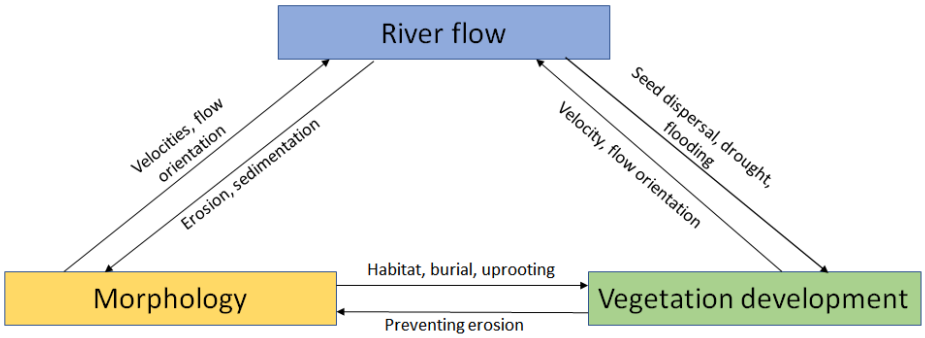

Figure 1.1: Main drivers of the feedback loop between vegetation and a river.

natural dynamics of a river. This understanding can contribute to preserve the sparse natural rivers left in Europe and help to improve future restoration projects.

River dynamics in a natural river are determined by three main drivers and their interactions: (1) river flow, (2) vegetation development in the river floodplain and (3) the morphology of the river (see Fig. 1.1). The interaction between river flow and morphology is a well-established field of research (e.g., van Rijn, 1993; Engelund and Hansen, 1967), and can be simulated reasonably well with morphodynamic models (e.g., Siviglia and Crosato, 2016; Schuurman et al., 2018). The interaction of vegetation with river flow and morphology is more difficult to simulate due to the complex interaction between the three drivers.

Vegetation affects the river flow by creating a hydraulic roughness and thereby slowing down the flow (Baptist, 2005). This leads to sedimentation behind the vegetation and as a result indirectly affects the bed level. River flow itself can have both positive and negative effects on the vegetation. Mortality processes related to the river flow, such as drought and flooding, can decrease the vegetation. Furthermore, river flow can also help vegetation colonise to new areas by transporting seeds downstream (Gurnell, 2014). Riparian vegetation also has direct feedback loops with the bed level in a river. The below-ground biomass, such as roots, affects the hydraulic and mechanical properties of the river bed and consequentially reduces the erosion susceptibility of the bed level. However, changes in the bed level caused by erosion and sedimentation can subject vegetation to mortality processes such as scour, excavation, uprooting, and burial.

1.2. Problem statement

This thesis focusses on the effects of extreme flood events on the channels and vegetation patterns of natural vegetated rivers. As such, this study highlights a different aspect than an earlier similar study that looked at a gradually changing discharge regime and mainly assessed the effects of increasing droughts on riparian vegetation (Martínez-Fernández et al., 2018).

The timing of an extreme flood event is unpredictable which makes it difficult to investigate the effects of a flood event on the vegetation and morphology in the field. To investigate the effects both the pre and post-flood vegetation coverage must be known. The pre-flood vegetation coverage is often unknown, and therefore few studies have addressed the immediate impact of an extreme flood (Bendix, 1998). Understanding the effects of extreme flood events could improve river restoration projects in the future, but also give insight in what the impact will be on existing natural rivers. Therefore, it is important to not only understand how these extreme discharge events affect vegetation and morphodynamic patterns but also understand how vegetation re-establishes itself and in which time window.

To investigate those effects a model is needed that is able to simulate the interaction between river flow, morphodynamics and vegetation development. In an earlier study a vegetation development model was developed and coupled to a hydro-morphodynamic model (Van Oorschot et al., 2016). In this study this coupled model is referred to as the MvO2016 model. Studies showed that the MvO2016 model is able to simulate a realistic morphology and vegetation development (Van Oorschot et al., 2016; Martínez-Fernández et al., 2018).

The downside of the MvO2016 model is that it uses a Matlab based vegetation-development model which is then coupled with a Delft3D 4.0 hydrodynamic model. This coupling only possible with the use of files. This reduces the computational efficiency of the model and consequently results in long computation times. This reduces the applicability of the model for river managers. From a river management point of view, an envelope of model results is more informative than a single model outcome, as the vegetation characteristics and the future river discharge are never exactly known. This means that fast computation times are required to increase the applicability of the model in the field.

Another point of improvement in the MvO2016 model is the simulation of the drought process. In the MvO2016 model drought stresses are modelled in a simplified way, using the days when the vegetation is not flooded as a measure of whether or not drought stress occurs. In reality drought stresses are related to the groundwater levels and root lengths. Lastly, the growth of young vegetation in their first year is not simulated in MvO2016 model. Studies showed that the survival chances of newly recruited vegetation is strongly related to the growth rate in its first year and the occurring groundwater levels (eq. Mahoney and Rood (1998); Guilloy et al. (2011)). This indicates that the survival changes of young vegetation and therefore the recruitment

of new vegetation is not accurately simulated in the MvO2016 model, while the simulation of vegetation recruitment is important when looking at how quickly vegetation recovers after an extreme flood event.

1.3. Research objective

The primary objective of this thesis is to investigate how extreme discharge events can affect the channel and vegetation patterns of a vegetated meandering river. This study also looks at how the vegetation recovers after a flood event.

To achieve this goal, a new vegetation development model is developed and coupled with a hydro-morphodynamic model. The vegetation development model uses both newly developed vegetation processes and processes based on that of the MvO2016 model. In this way, the interactions and dependencies between the physical and biological processes of vegetation, and the morphological processes of a river can be assessed.

1.4. Research questions

Two main research question are formulated to achieve the objectives of this thesis. The second main research questions is divided in three sub-questions.

Q1 What effect can an extreme flood event have on the long-term riparian vegetation development and larger-scale morphology of a meandering river and what is the recovery time of such an event?

Q2 How can question Q1 be answered with a coupled hydrodynamic vegetation-development model?

- Q2.1 What processes influence channel and vegetation patterns and need to be included in the numerical and vegetation-development model??
- Q2.2 How can the processes and computational efficiency of the vegetation development model of Van Oorschot et al. (2016) be improved?
- Q2.3 How sensitive are the model results on the formation of vegetation and morphological patterns to the model settings?

1.5. Scientific relevance

The developed model will use a different modelling approach than the earlier mentioned MvO2016 model. The vegetation model in this study will be entirely process-based (see Ch. 2). This means that all vegetation processes, but also vegetation properties such as mortalities thresholds will be based on processes found in literature. This differs from the MvO2016 model which used the vegetation mortality thresholds as calibration parameters in order to broadly fit their model results on measured vegetation occurrence data (Van Oorschot et al., 2016).

The approach used in this study gives the model a broader usage due to two advantages: (1) the model can be used independently of its location as long as the characteristics of the vegetation are known, and (2) it makes the model more flexible, as new vegetation species can be added easily without changing the characteristics of the already modelled vegetation.

1.6. Case study

This research can not include all aspects of the complex interaction of riparian vegetation and its environment. Numerous different riparian vegetation species exist, as do rivers, each with different characteristics. In order to investigate this complex and broad subject, a case study is studied. A model schematization based on the Allier River (France) at Moulins is used as a case-study (see also Ch. 3 and Fig. 1.2). The Allier River is one of the last European unregulated vegetated rivers, which behaves still as a natural meandering river (Garófano-Gómez et al., 2017). This makes the Allier River an ideal case-study to investigate the effects of extreme flood events on larger-scale morphology and vegetation patterns in a natural vegetated river.

A large amount of riparian species exists within the riparian zone of the Allier River. Therefore a simplification had to be made. For this study two of the most dominant riparian tree species are selected: the *Salix alba* (*S. alba*) and the *Populus nigra* (*P. nigra*). Riparian tree species are modelled because they have the most morphological impact on dynamic vegetated rivers, compared to, for example, grasses or herbs species (Gurnell, 2014). An additional advantage is that these species belong to the vegetation type Salicacea, which is a typical

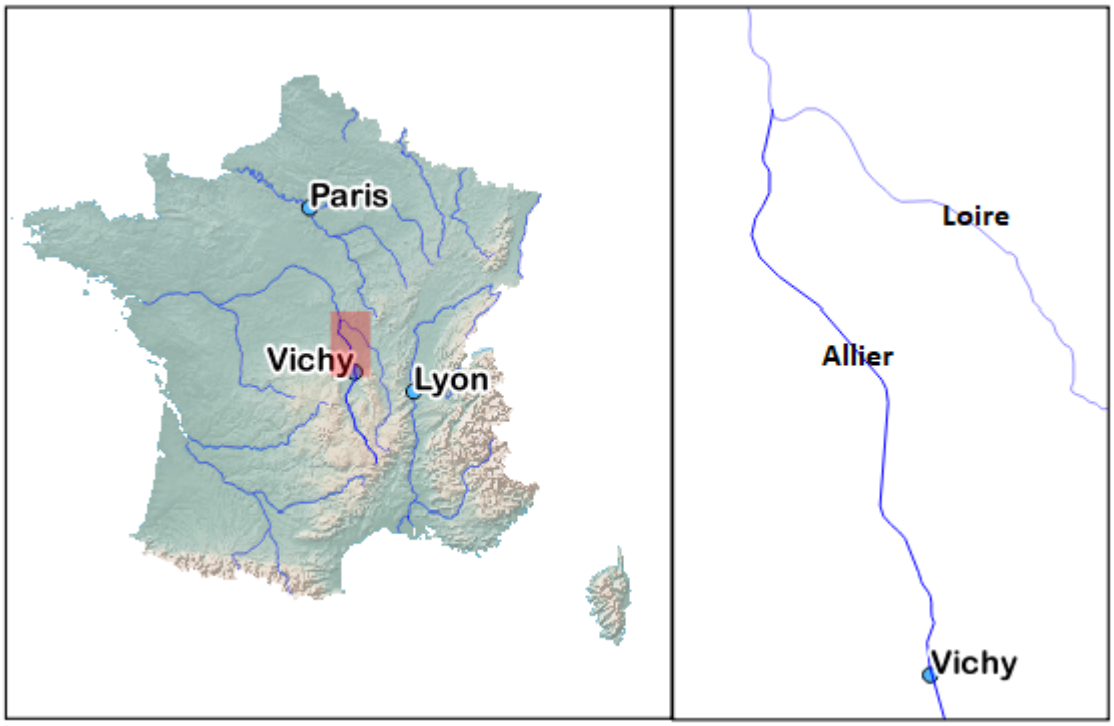

Figure 1.2: Location of the Allier river in France

type of riparian tree found in north-western Europe. (Van Oorschot et al., 2016). This makes the translation of literature into input parameters also useful for future riparian vegetation modelling studies in other parts of Europe.

1.7. Thesis outline

To answer the research questions proposed in Section 1.3, this study is composed of several steps. A literature study is carried out in Chapter 2 to investigate which vegetation processes and characteristics are important for riparian vegetation development, which will provide for a large part the answers to sub-questions Q2.1 and Q2.2. After the literature review the vegetation development model is developed and coupled with the hydro-morphodynamic model of the Allier River. Chapter 3 shows the results of the default run, which uses the vegetation characteristics as found in literature. To investigate the influence of different model settings on the model results, a sensitivity analysis is performed in Chapter 4, which provides an answer to research question Q2.3. In Chapter 5 the model is used to investigate the effect of extreme discharges on the long-term riparian vegetation development and the larger-scale morphology, which gives an answer to research question Q1.

The report concludes with a discussion of the results and the model itself in Chapter 6. This discussion forms the basis of Chapter 7 in which the conclusions and recommendations are drawn.

2

Vegetation modelling

Predicting or even understanding the effects of extreme flood events on riparian vegetation is difficult due to the amount of different processes involved, which also bear some uncertainties. Extreme flood events are unpredictable, which makes it difficult to study them in the field. Models can be used to investigate the effects of extreme flood events on the riparian vegetation and can also give insight in how the vegetation development will be after such a flood. In this chapter, a short introduction is given on vegetation modelling in general and which processes are important to include in the riparian vegetation development model. The second part focusses on explaining the different vegetation processes and how they are included in the vegetation model.

2.1. Vegetation models

Ideally, a model should simulate all climate and environmental conditions, such as water and nutrients availability and temperature. The model would include all occurring vegetation processes such as establishment, grow, reproduction and persistence as well as vegetation competition. It would take into account the effects of disturbances on vegetation distributions and growth. The model would not only give the final vegetation cover but also the rate of changes, the intermediate conditions, and insight in the mechanisms producing change. However, such ideal models do not currently exist due to its complexities and the need for extensive computational power (Kerns and Peterson, 2014). Therefore, current models only focus on one or a few aspects of vegetation related processes. A model can, for instance, focus on one environmental niche or focus mainly on simulating competition and examine spatial variation while other aspects are being simplified.

Generally, vegetation models can be divided in statistics-based and process-based models. Statistics-based models estimate changes in vegetation by using a (known) relationship between vegetation occurrence data and the corresponding environmental conditions. By looking only at a relationship statistical models often do not directly include vegetation processes or mechanisms. Detailed vegetation occurrence data is scarce for riparian environments and if it is available it has often large time intervals of several years between the datasets (e.g., Garófano-Gómez et al. (2017)). This lack of vegetation data makes it difficult to create a statistics-based vegetation model for riparian vegetation.

Process-based models simulate some or many of the underlying physical and ecosystem processes that influence vegetation aspects like growth and mortality in order to estimate vegetation coverage. A lot of research has been done on the different processes that influence riparian vegetation growth. This allows the use of a process-based vegetation model, which will also be used in this thesis. The different vegetation processes will be treated in detail in section 2.2.

2.1.1. Requirements and limitations

When developing a process-based vegetation model it is important to consider which vegetation processes need to be included. This study focusses on how extreme flood events will affect the interaction between riparian vegetation and the morphology of a river. Processes on leaf or even cell scale are too detailed for the

research questions in this study and will make the model too complex and computationally intensive. Those small scale processes will therefore be neglected in this study. However, processes on plant cluster scale such as colonisation or mortality due to droughts and flooding are important to include.

It is important to consider that the vegetation model in this study will be coupled with a morphodynamic river model. This gives detailed information about the hydro- and morphodynamics of the river as input for the vegetation model. However, the input for the vegetation model is limited by the morphodynamic model, because information about temperature, available nutrients and groundwater levels is not modelled and is therefore not available as input. Those parameters could be included by using for instance also a water quality and groundwater model, but this is outside the scope of this study

The lack of vegetation occurrence data makes it difficult to validate a vegetation model. To obtain a realistic vegetation model without detailed validation data, the used processes in this thesis rely heavily on field observations and experiment data found in literature.

2.1.2. Time scale

It is important to consider which time scale is used in the model. This research focusses on the effects of extreme flood events. An approach could be to only look at the direct effects of one extreme flood. The duration of an extreme flood is often in the order of days, which significantly reduces modelling time. However, extreme floods zorgen vaak voor veel morfologische activiteit in een rivier. Deze verandering in de morfologie hebben ook effect op de vegetation colonisation, development and recovery. Those processes happen on much larger time scales and depend on the vegetation species. For instance, a herb matures earlier than a tree. Depending on the species this process can take months to decades before vegetation is completely developed.

In this research riparian tree species are modelled (see Sec. 1.6). In their first years riparian trees often occur as densely populated shrubs and after around ten years they start to develop into larger single trees. In order to investigate and understand the effects of colonisation, growth and mortality of riparian trees at least 10-20 years needs to be modelled. The vegetation model has relative fast computation times compared to a morphological river model. This means that the morphological model is often the limiting factor in computation time.

		Salix alba					Populus nigra					
Vegetation characteristic	Unit	Seedling	Young sapling	Sapling	Adult	Old Adult	Seedling	Young sapling	Sapling	Adult	Old Adult	Reference
Number of years in lifestage	yr	1	2	7	40	10	1	2	7	130	10	Adaption from Van Oorschot et al. (2016)
Stem density	stems/m2	25	15	15	0.16	0.16	25	13	13	0.27	0.27	Van Oorschot et al. (2016)
Area fraction	-	0.8	0.8	0.8	0.8	0.8	0.8	0.8	0.8	0.8	0.8	Van Oorschot et al. (2016)
Drag coefficient	-	1	1	1	1	1	1	1	1	1	1	-
Drought threshold	days	5	30	30	45	45	7	45	45	60	60	Guilloy et al. (2011); Scott et al. (1997b, 2000)
100 % drought mortality	days	18	363	363	378	145	36	378	378	393	160	
Flooding threshold	days	50	100	120	130	130	30	70	70	80	80	Siebel and Blom (1998); Glenz et al. (2006)
100% flooding mortality	days	107	200	320	330	230	80	137	237	247	180	
Root lenght start		-	0.6	1	1.1	1.1	0.1	-	1	1.3	1.3	Corenblit et al. (2014)
Root lenght end		-	1	1.1	1.1	1.1	0.6	-	1.3	1.3	1.3	Corenblit et al. (2014)
Uproot factor		0.3	0.2	0.2	0.2	0.2	0.2	0.1	0.1	0.1	0.1	Crow and Houston (2004)

Table 2.1: Table with the default vegetation characteristics. There are five different life stages defined: Seedling, Young sapling, Sapling, Adult, Old adult. Each life stages has different characteristics.

Parameter	Salix alba	Populus nigra	Reference
Maximum age	60 year	150 year	Van Oorschot et al. (2016)
Logaritmic growth factor shoot (Eq. 2.1)	11.5	14	Van Oorschot et al. (2016)
Logaritmic growth factor diameter (Eq. 2.1)	0.41	0.6	Van Oorschot et al. (2016)
Dispersal period	15 April-15 June	1 May-1 July	Van Splunder et al. (1995); Guilloy-Froget et al. (2002)
Fitting parameters seedling stem growth (Eq. 2.2)	a=6.42, b=-0.0506, c=0.848, d= 0.002	a=6.74, b=-0.0534, c=1.05, d= 0.005	Guilloy et al. (2011); Stromberg (1997); Horton and Clark (2001)
Fitting parameters seedling stem growth (Eq. 2.5)	k=0.015, c=0.5, d=0.02	k=0.012, c=0.6, d=0.03	Guilloy et al. (2011); Ying Liu et al. (2011); Corenblit et al. (2014)

Table 2.2: Table with the default growth and dispersal parameters per vegetation species.

2.2. Vegetation processes

The hydrogeomorphic characteristics controlling riparian vegetation succession are the flow and sediment transport regimes, sediment erosion and deposition, sediment texture, and topography (Corenblit et al., 2007). When developing a riparian vegetation model it is important to investigate which vegetation processes need to be included in the model. The following processes are incorporated in the vegetation model:

- Seedling recruitment: The recruitment of new vegetation
- Growth: the growth of vegetation
- Seedling growth: Detailed seedling growth in their first year
- Flooding: mortality due to prolonged flooding
- Drought: mortality due to drought stresses
- Uprooting: mortality due to uprooting of roots caused by scour
- Burial: mortality due to burial of vegetation under sediment deposits

The selection of those processes are for a large part based on the work of Van Oorschot et al. (2016). However the drought and uprooting processes are improved in the vegetation model, so that the vegetation can be modelled in a more realistic way. There is also an important process added which is a more detailed simulation of the seedling growth (see Sec. 2.2.3). This because seedling survival depends for a large part on its growth rate (Mahoney and Rood, 1998; Corenblit et al., 2014; Karrenberg et al., 2002).

As described in Section 1.6 two riparian tree species are implemented in the vegetation model: the Populus nigra (*P. nigra*) and Salix Alba (*S. alba*) species. In the following paragraphs the above processes are described in more detail for both vegetation species.

2.2.1. Seedling recruitment

Riparian vegetation has two ways of colonization, sexual and vegetative reproduction. Sexual reproduction is reproduction through seeds, while vegetative reproduction is reproduction through regeneration from shoots and roots.

The preference between sexual or vegetative reproduction differs between populations and place (Karrenberg et al., 2002). Legionnet et al. (1997) found that *P. nigra* trees at the Loire, Allier and Durance rivers mostly originated from seedlings, with few clonal individuals. Based on these findings it is assumed that sexual reproduction is the main process of reproduction for the *P. nigra* species in the Allier River and that neglecting the vegetative reproduction will have no major effects on the results. The reproduction strategy of the *S. alba* species is very similar to the *P. nigra* species. For this reason it is assumed that sexual reproduction is also the main reproduction process for the *S. alba* species in the Allier.

Successful sexual reproduction for riparian trees depends largely on the river discharge. During the seed dispersal period Salicaceae species produces hundreds of thousands or even millions of seeds which are initially wind-dispersed but will also land in the river stream (Karrenberg et al., 2002; Mahoney and Rood, 1998). During this period thousands of seeds float in the river and in combination with a receding water level those seeds are deposited on the river banks. The moist river banks are ideal for seedling establishment. Successful seedling establishment happens when the seed release occurs after a peak flow and during the falling limb of the hydrograph. Seedling recruitment in the vegetation model is based on this concept. The model assumes that during the seed dispersal period new seedlings will establish themselves on any receding riverbank with sufficient space for the establishment of new vegetation.

The wind dispersed seeds that do not end up in the river have not been included in this study. This is a simplification because rainfall can also create moist substrates that could allow these seeds to germinate.However, these seedlings are even more susceptible to drought stress than seedlings close to the river bank because they germinate further away from the river stream and their roots are unlikely to reach the groundwater level. It is assumed that their chances of survival are very low and that neglecting those seeds will not affect the results.

Species	Duration of seed dispersal period	Start seed dispersal period	Authors	Location
Populus nigra	9 weeks	unkown	Legionnet et al. (1997)	Loire River, France
Populus nigra	9 weeks	unkown	Guilloy-Froget et al. (2002)	Drome River, France
Populus nigra	2-3 weeks	June	Van Splunder et al. (1995)	Waal River, The Netherlands
Populus nigra	2-3 weeks	unkown	Guilloy-Froget et al. (2002)	Isere and Drac Rivers, France
Populus nigra	8-13 weeks	late April and mid-May	Guilloy-Froget et al. (2002)	Garonne River, France
Salix alba	2-7 weeks	mid-May and June	Van Splunder et al. (1995)	Waal River, The Netherlands

Table 2.3: The duration and start of the dispersal period for the *P. nigra* and *S. alba* species at different locations

Although sexual reproduction is the main reproduction process in the Allier, the start and duration of the seed dispersal period can differ between species. Table 2.3 gives an overview of the duration and starting month of the seed dispersal period of the *P. nigra* and *S. alba* species found in literature. The exact time of the seed dispersal period is only known for the studies of Van Splunder et al. (1995) and Guilloy-Froget et al. (2002). Guilloy-Froget et al. (2002) studied the *P. nigra* species at the Garonne River and found a dispersal period of 8-13 weeks starting around begin May. The Garonne River is like the Allier River located in the Southern part of France. Guilloy-Froget et al. (2002)'s findings are therefore the most representative for the Allier River and used in this study,. Van Splunder et al. (1995) states that the seeding period *S. alba* start slightly earlier than the *P. nigra*. Therefore, it is assumed that the seed dispersal period of the *S. alba* species in the Allier River starts in mid-April.

2.2.2. Growth

The size of vegetation, such as the stem height, stem diameter and root length, has a major impact on the mortality of vegetation. The older and larger the vegetation is, the more resilient it is to mortality processes such as drought, burial and uprooting. Vegetation growth is thus an important process in vegetation modelling. This study makes a distinction between vegetation up to one year old and vegetation of one year and older. In this study, each tree up to one year old is referred to as a seedling. The development of a seedling starts with the germination of a seedling, after which the stem height can grow to more than 1 metre in one growing season (Stromberg, 1997). This means that the growth of the seedlings must be modelled in detail (see Sec. 2.2.3).

For vegetation of one year and older, the growth within a year is relative small. Therefore vegetation properties such as stem height and root length are only updated once a year. This is a similar method as used in the work of Van Oorschot et al. (2016). To determine the size in stem height, stem diameter and root length of vegetation of one year and older, the formula proposed by Van Oorschot et al. (2016) is used:

$$G = F_v log(a) \tag{2.1}$$

Where G is the size in meters, F_v is the vegetation-type dependent logarithmic growth factor and a is the vegetation age in years. The used parameters for the *S. alba* and *P. nigra* species can be found in Table 2.2, those parameters are adopted from Van Oorschot et al. (2016).

2.2.3. Seedling growth

In its first year a seedling grows rapidly. Directly after germination, the roots and stems of a seedling are small, but a seedling can reach a stem height of more than one meter in one growing season (Stromberg, 1997). A typical growth season lasts around 6 months. The seedling characteristics such as stem height and root length thus differ greatly throughout the growing season. It is important to model seedling growth in detail because those characteristics determine the resistance of the vegetation to mortality processes such as uprooting and drought. Despite its rapid growth the seedling mortality of trees in the Salicacea family, in which the *S. alba* and *P. nigra* belong, are often high, with mortality rates ranging from 77 to 100 percent (Karrenberg et al., 2002).

Experimental and field data found in literature is used to get an insight in the seedling growth rate. For both vegetation species a different growth curve is defined for the shoot height and root length.

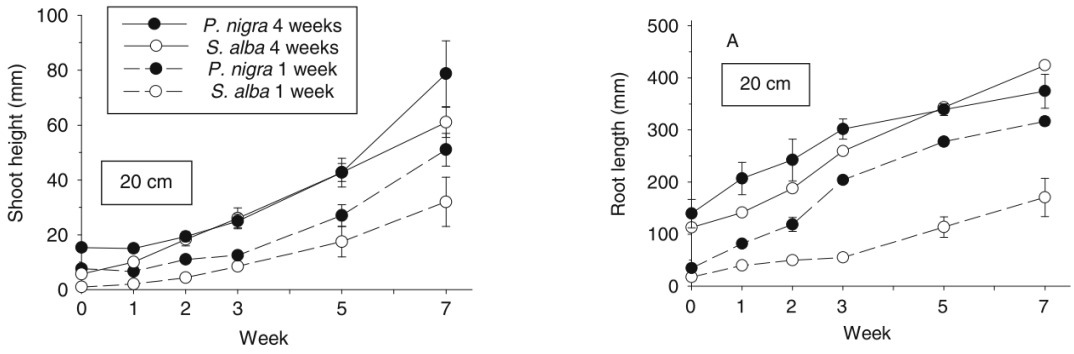

(a) Shoot height

(b) Root length

Figure 2.1: Shoot height and root length growth of *P. nigra* and *S. alba* one- and four- week old seedlings in a scenario where the groundwater level is 20 cm below soil level Each point represents mean shoot height. The error bars represent 1 standard error of the mean. Adopted from Guilloy et al. (2011)

Shoot growth

Experimental data of Guilloy et al. (2011) gives a good insight of early shoot growth for both species (see Fig. 2.1a). No additional growth data of the species *S. alba* and *P. nigra* could be found in literature. Therefore, growth data of similar riparian trees is used to create a shoot growth curve. Field observations of the *S. gooddingii* species showed that the seedling growth is initially slow with reaching stem heights of 12-47 mm after 60 days and grew more rapidly later in the season with reaching heights of 50-125 mm after 90 days (Horton and Clark, 2001). Field observations by Stromberg (1997) show that this rapid growth continues until the end of the growing season with stem heights reaching 0.75 to 1 meter for the *S. gooddingii* and *P. fremontii* species.

To summarize, seedling growth is slow in the first months but their growth rate accelerates rapidly later in the growth season. Therefore, a sigmoid growth curve is proposed to describe the vegetation growth in the first year:

$$y(t) = \frac{c}{1 + e^{(a+bt)}} + d \tag{2.2}$$

Where t is time in days, y is the shoot height at time t, a and b are fitting parameters, $c + d$ is the maximum shoot height after one growth season, and d is the initial shoot height directly after germination. This equation describes the stem growth in the first year, after the first year the stem height is described by Equation 2.1. Equation 2.2 is similar to the method employed by Badhwar (1984) and Zhang et al. (2003). They used it to approximate the variance in time of the spectral reflectance for respectively corn and soybeans crop during the growth season. The seedling growth rate shows a similar combination of exponential and logistic growth, therefore this formula is adopted to describe the stem height growth of seedlings.

Figure 2.2 shows the combined growth data for both vegetation species found in literature. The blue dots represent the experiment data of Guilloy et al. (2011) for the reference scenario without water stresses. The orange lines are the range of shoot heights for the *S. gooddingii* recorded by Horton and Clark (2001). The grey lines represent field data of the shoot height ranges after one growing season found by Stromberg (1997) for the species *S. gooddingii* and *P. fremontii*.

The growth rate of *S. alba* is slightly slower than the *P. nigra*, as a result the shoot heights for the *S. alba* species are taken from on the lower part of the observed shoot height range and vice versa for the *P. nigra* species. The yellow dots represent the shoot heights which were used to create a growth curve for both species. A standard non-linear least square function in Python was used to create a shoot growth curve for both species, resulting in the following growth curves:

$$y_{P.\,nigra}(t) = \frac{1.045}{1 + e^{(6.745 - 0.0534t)}} + 0.005 \tag{2.3}$$

$$y(t)_{S.\,Alba} = \frac{0.848}{1 + e^{(6.417 - 0.0506t)}} + 0.002 \tag{2.4}$$

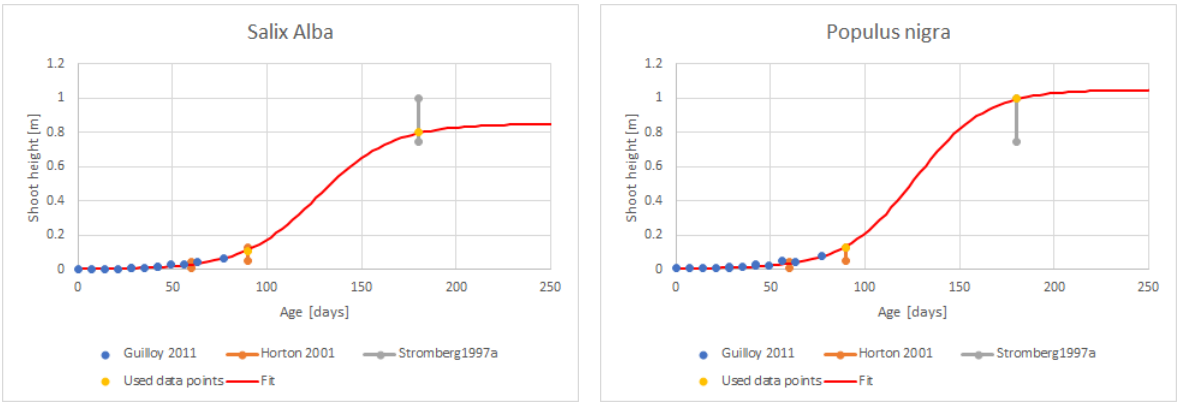

(a) *S. Alba* (b) *P. nigra*

Figure 2.2: The shoot height growth curve of the *S. alba* (a) and *P. nigra* (b) species. The blue dots represent the growth data from the research of Guilloy et al. (2011). The orange and grey lines represent the range of shoot height field data for similar riparian trees from the research of respectively Horton and Clark (2001) and Stromberg (1997). The yellow dots represent the used data to in those ranges to create a growth curve.

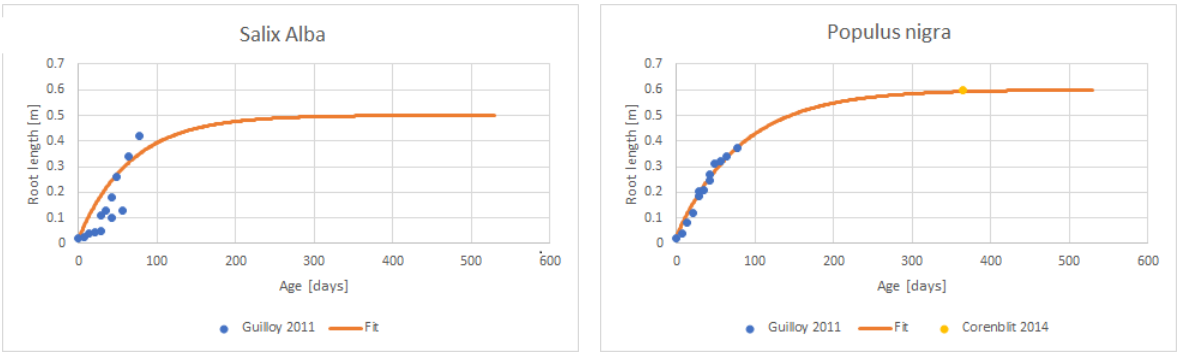

(a) *S. Alba* (b) *P. nigra*

Figure 2.3: The root length growth curve of the *S. alba* (a) and *P. nigra* (b) species. The blue dots represent the growth data from the research of Guilloy et al. (2011), the yellow dot represents the root length of the *P. nigra* at the end of the growing season as reported by Corenblit et al. (2014).

Species	Flooding threshold	Location
Salix Alba	142 days/growth season	Upper Rhine, Iffezheim, Germany
Salix viminalis	165 days/year	Elbe river, Lezen-Wustrow, Germany
Salix rubra	238 days/year	Elbe river, Lezen-Wustrow, Germany
softwood	150 days/year	Elbe river, unknown
hardwood	50 days/year	Elbe river, unknown

Table 2.4: Flooding tolerances as reviewed by Glenz et al. (2006)

Root growth
The timeline of root growth is completely different from shoot growth. Drought and erosion are often the main mortality causes and therefore seedlings prioritize root growth over shoot growth in their first years to improve their resource acquisition and anchorage (Braatne et al., 1996).

Looking at the experimental data of Guilloy et al. (2011) it can be seen that root growth is indeed faster in the first months (Figure 2.1b). Root length data of the *S. alba* and *P. nigra* species during the growing season could not be found. Corenblit et al. (2014) mentions however that *P. nigra* species reach root lengths of 60-100 cm after 2-3 years. Based on this information it is assumed that *P. nigra* seedlings have a root length of 60 cm at the end of the first growing season.

For the *S. alba* species no root data could be found at the end of the season. However, Ying Liu et al. (2011) investigated the root lengths of 4 year old *S. Albatristis* trees, which is an hybrid between *S. alba* and *S. babylonica*. They found maximum rooting depths of only 72 cm. Assuming that the *S. alba* will have similar root lengths, this field data shows that *S. alba* have shallower roots than the *P. nigra* species. For this reason it is assumed that at the end of the growing season the *S. alba* species will have a maximum root length of 0.5 meter.

Despite the lack of root length data during the growth season, a logarithmic growth curve can be expected for root growth. Based on the work of Guilloy et al. (2011) it is known that seedling roots grow rapidly in the first 11 weeks to a length of about 40 cm. After the first growth season the root length is however around 50-60 cm. Therefore, the seedling root growth is represented with a simple logarithmic growth function:

$$y(t) = c \cdot \left(1 - e^{-k}\right) + d \tag{2.5}$$

Where t is time in days, y is the root length, k is a fitting parameter, $c+d$ is the maximum root growth after one growth season, and d is the initial root length directly after germination. The fitting parameter is manually fitted to the root data of Guilloy et al. (2011) and the assumed root lengths at the end of the growth season. Figure 2.3 shows the root growth formula's for both species, the used fitting parameters can be found in Table 2.2.

2.2.4. Flooding

Prolonged flooding of vegetation is an important cause of vegetation mortality in rivers. The model uses the continuous time that vegetation is flooded as an indicator whether flooding mortalities occur. Flooding mortality occurs gradually in the model at the moment the consecutive flooding time exceeds the flooding threshold. This can be best explained by looking at Figure 2.5. The rate at which a plant dies is affected by the flooding slope, the steeper the slope, the faster the vegetation dies. Flood tolerance increases with the age of vegetation, but also varies between vegetation species. While it is widely know that riparian trees such as *P. nigra* and *S. alba* species are more resistant to flooding than 'hardwood' tree species (e.g, Corenblit et al. (2007),Gurnell (2014)), detailed information about flooding mortality is sparse, especially for matured trees. The following two paragraphs list the literature found on vegetation flood tolerance.

Seedlings and young vegetation
Flooding experiments of one and two year old *P. nigra* vegetation showed mortality rates of 50 percent after respectively 11 and 15 weeks (Siebel and Blom, 1998). They also stated that six week old *P. nigra* seedlings acquire about the same degree of flood tolerance under favourable growth conditions as the *Q. robur* species, for which they found a 50 percent mortality rate after 8 weeks. While no flooding data could be found for the

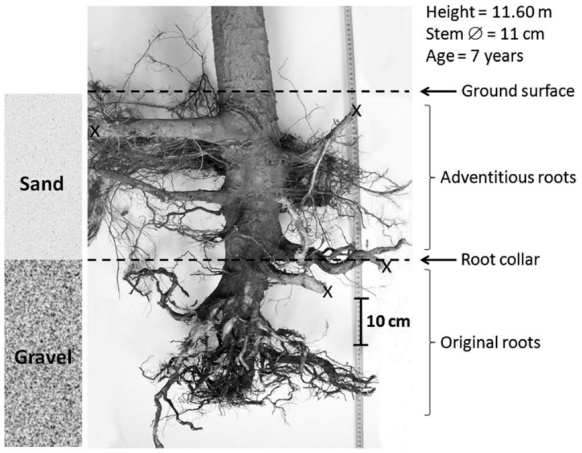

Figure 2.4: Root system of a 7 year old *P. nigra* tree. Adapted from Corenblit et al. (2014).

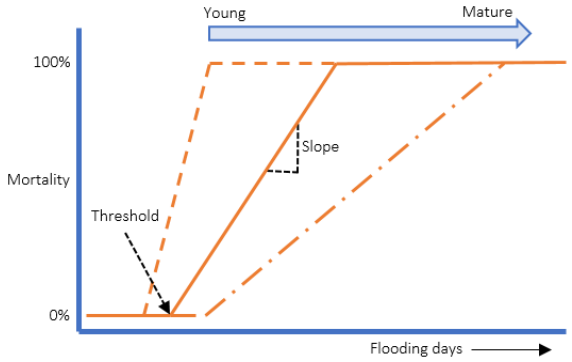

Figure 2.5: Flooding mortality graph. Flooding mortality occurs after the flooding threshold is exceeded. The slope indicates how fast the vegetation dies after the flooding threshold is exceeded.

S. alba species, it is known that the *S. alba* species is more flood tolerant than the *P. nigra* species (Glenz et al., 2006). Therefore, the flooding thresholds of the *S. alba* for young seedlings are chosen higher (see Tab. 2.1)

Adults

The flooding thresholds for more matured trees are based on field data. Those flooding thresholds are often based on the total amount of flooding days in a growing season or year. Table 2.4 summarizes the flooding thresholds as reviewed by Glenz et al. (2006). Field observations show that *S. alba* species can withstand flooding durations of 95 percent of the growth season. This results in 142 days of flooding, based on a growth season of 5 months. Pott (2000) found flooding thresholds of around 150 days/year for softwood and 50 days/year for hardwood (as reviewed by Glenz et al. (2006)). Because the moment of mortality can differ between individual trees the flooding threshold of the *S. alba* species is set at 130 days, after which the mortality occurs gradually. Studies also showed that the flooding resistance of vegetation is lower during the growing season than during the winter period (Glenz et al., 2006). In the vegetation model however the flooding threshold can not be varied between seasons. Therefore it is chosen to use a relatively low flooding slope of 0.5 for the *S. alba* species, so that the vegetation mortality occurs very gradually.

No specific flooding data for *P. nigra* trees older than 2 year could be found, only that *P. nigra* trees are less tolerant to flooding than *S. alba* trees. To estimate the flooding thresholds for adult *P. nigra* trees, information about the *S. alba* flooding thresholds was used. The flood threshold for adult *S. alba* species is 2.6 times higher than that of the seedlings. This ratio was then used to estimate the flooding threshold of adult *P. nigra* trees. A period of 80 days was found.

2.2.5. Droughts

Drought stresses are another important cause of vegetation mortality. The drought tolerance of vegetation increases with age and differ per vegetation species. Rapidly declining water levels in a river can result in drought stresses due to limited water availability and subsequently cause vegetation mortality. The length of the roots and the age of the vegetation largely determine the drought resistance of the vegetation.

Seedlings

Experiments have shown that there was no survival possible for young *P. nigra* seedlings if dry conditions persist more than one week (Guilloy-Froget et al., 2002). Experiments by Guilloy et al. (2011) found similar results where they looked how abrupt water level drops influenced the survival rate of *S. alba* and *P. nigra* seedlings. Figure 2.6 shows the two most extreme scenarios where the water level drops 60 and 90 cm beneath the root depth. It can clearly be seen that *S. alba* is less resistant to drought and dies after one or two weeks, where the *P. nigra* seedlings survive the drought stresses slightly longer. This is also in line with the experimental results of Splunder et al. (1996) where *P. nigra* seedlings had a better drought resistance than *S. alba* seedlings.

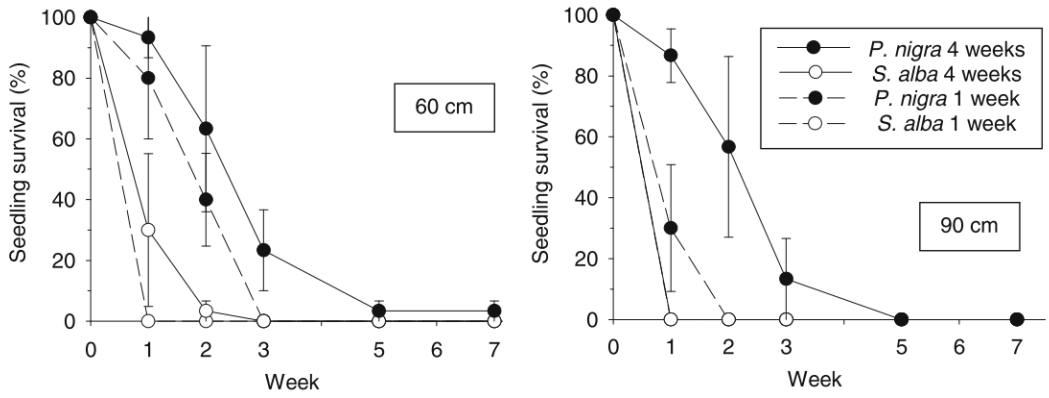

Figure 2.6: The survival rate of *P. nigra* and *S. alba* for one- and four-week old seedlings following the abrupt drops in water table levels from 20 cm below ground level to respectively 60 and 90 cm below ground level. The error bars represent ± 1 standard error of the mean. Adapted from Guilloy et al. (2011).

Adults

Detailed drought tolerance thresholds for more matured riparian trees could not be found in literature. This is a more widely encountered problem in research as described by McDowell et al. (2008):

> "Essentially, we cannot address questions such as: how severe must a drought be to kill a tree; and during drought, which trees will die and which will survive? Consequently, our current ability to predict when regional-scale plant stress will exceed a threshold that results in widespread mortality is lacking."

Drought mortality of matured trees only seems to occur after large and sustained groundwater level declines. However, it remains uncertain how drought mortality develops over time. A field study at a riparian site in Colorado, USA, demonstrated that a sustained groundwater decline of more than 1 meter lead to leaf desiccation and branch dieback within three weeks and an 88 percent mortality over a three-year period for the *P. deltoides* var. *monilifera* species (Scott et al., 1997b). They also found that groundwater level declines of around 0.5 meter had no significant effect on tree mortality. Similar results were found along the Mojave River, California, where a groundwater level decline of more than 1.5 meter resulted in mortality ranges between 58 and 93 percent after 4 years (Scott et al., 2000). In areas with groundwater level declines of less than 1 meter the mortality rate was around 7-13 percent. Unfortunately, both studies do not present more detailed information about how tree mortality develops over time. As a result, it remains uncertain at which point in time tree mortality starts to occur. Chances are that the mortality already occurred earlier than the 3-4 years mentioned in both studies.

It is important to mention that the root distribution and length is believed to be related to the site-specific groundwater level. Several studies show that the historic variation in groundwater levels very likely determines the root length of riparian trees (Scott et al., 1997b, 2000; Shafroth et al., 2000; Sprackling and Read, 1979). Therefore, mainly abrupt and large drops of the water table in relation to the historical levels seem to induce high mortality rates.

However, in the vegetation model the root lengths depend on the age of the vegetation and not on the historical groundwater levels. Drought stresses occur in the model when roots fail to reach the capillary fringe layer above the groundwater level. Because the *P. nigra* and *S. alba* species grow near the river bed with relatively high groundwater levels it is assumed that even matured trees have relatively shallow root systems with maximum root lengths of respectively 1.3 and 1.1 meter. Therefore, drought stresses due to large groundwater level drops can still affect matured trees.

The drought thresholds in the model for matured *P. nigra* and *S. alba* trees are set on respectively 45 and 30 days (see also Table 2.1). *S. alba* species are more prone to drought mortality, therefore, a lower threshold is chosen for this species (Splunder et al., 1996). Those thresholds are roughly based on the study of Scott et al. (1997b) which mentions the first drought effects such as leaf desiccation within 3 weeks of drought for the *P. deltoides* var. *monilifera* species. Leaf desiccation does not directly lead to tree mortality, but shows

the first signs of drought stresses. It is assumed that if a drought period last more than 6 weeks, the first matured *P. nigra* species will die. Due to the fact that only drought mortalities rates are known after three years a low mortality slope of 0.3 is chosen, meaning that the mortality slowly increases to 100 percent after more or less one year. Drought mortalities are incorporated in the vegetation model in the same way as flooding mortalities (See also Figure 2.5).

2.2.6. Uprooting

While floods can eliminate vegetation due to inundation, vegetation can also be removed by physical scouring, this process is called uprooting or wash-out (Braatne et al., 1996). It is assumed that when a certain percentage of the roots is exposed by scouring, the vegetation is washed away or dies. This percentage varies per species and is mainly based on the resistance of the vegetation to uprooting.

Bywater-Reyes et al. (2015) showed with a field experiment that the vulnerability of seedlings is closely related to the size and root length of the seedlings. They also conclude that the scour depth is the main cause of uprooting, because the drag force induced by the water velocity alone is unlikely to uproot seedlings. Therefore, only scour depth is considered as uprooting process in this study.

Also adult trees can be removed due to erosion. A field study in a non-riparian environment showed that typically 75-95 percent of the willow and poplar roots occur in the first 35 centimetre of the soil (Crow and Houston, 2004). In riparian environments parts of the stem are often buried beneath the sediment and will become part of the root system. Figure 2.4 shows the roots of a 7 year old *P. nigra* tree, which clearly shows that the largest lateral roots are formed in the later deposited soil. Similar results were found in another field study, where the largest part of the roots were formed in the deposited soil above the root collar (Holloway et al., 2017). Therefore, it is assumed that only a small part of the original roots needs to be eroded to remove an adult tree. The chosen percentages of the root length that needs to be eroded is respectively 10 and 20 percent for the *P. nigra* and *S. alba* (see also Table 2.1).

2.2.7. Burial

Mortality due to sediment burial is only relevant in the early life stage of a tree. Young trees have the highest chance to die by partial or complete sediment burial, due to their smaller stem heights. No experimental data could be found about tree mortality rates due to burial. However it is mentioned in literature as an important mortality cause for young seedlings (eg. Mahoney and Rood (1998); Corenblit et al. (2014); Braatne et al. (1996)). Due to the lack of experimental data it is assumed that vegetation dies if the complete stem is buried beneath sediment. This is based on the fact that if a stem is completely buried, no photosynthesis can take place which is essential for vegetation to survive.

2.3. River modelling

As stated in Section 1.1, riparian vegetation is heavily influenced by the flow and morphology of a river. In order to include those effects, a morphological model needs to be coupled with the vegetation model. Numerical models can simulate hydrodynamics and morphology in two-dimensional (2D) depth-averaged or three-dimensional (3D) flow computations. However, the computation times of three-dimensional simulations are often very high. To reduce the computation time most studies on rivers use depth-averaged two-dimensional models, which will also be used in this study.

Earlier vegetation modelling studies have used a Matlab-based vegetation model coupled with Delft3D 4 (eg. (Van Oorschot et al., 2016; Martínez-Fernández et al., 2018)). This set-up has however two large drawbacks: large modelling times due to the inefficient sharing of data between both models and the model were not user-friendly. Due to recent developments in Delft3D Flexible Mesh (Delft3D FM) separate Python-based models can be coupled with Delft3D FM. Therefore Delft3D FM will be used as a morphodynamic model and coupled with the Python-based vegetation model. Vegetation can have a significant effect on the flow by slowing it down and changing the turbulent flow field. Vegetated rivers can therefore behave different from non-vegetated rivers, due to differences in flow resistance and sediment dynamics. Within Delft3D FM four formulae are implemented to describe vegetation, two based on the research of Klopstra et al. (1996) and two based on the research of Baptist (2005). The second formula based on the work of Baptist (2005) will be used in this study because this formula is capable of modelling both emerged and submerged vegetation. This for-

mula is briefly explained below, for a more extensive overview of the formulae in Delft3D FM one is referred to the Delft3D FM User Manual (Deltares, 2018).

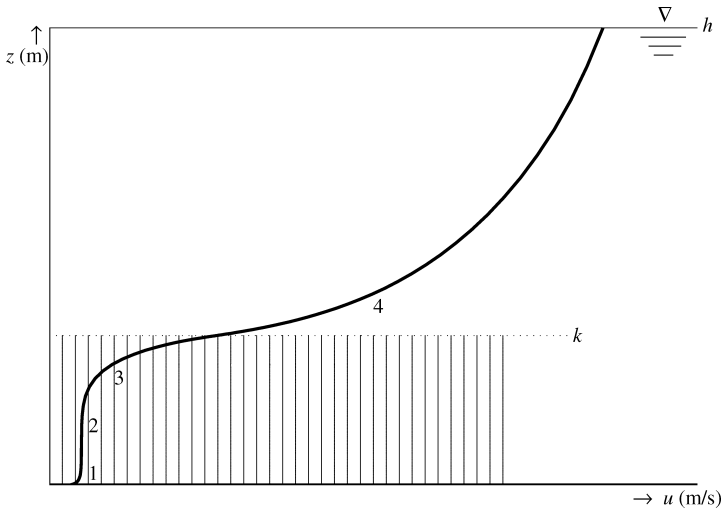

Figure 2.7: The four zones of the vertical profile for a horizontal velocity, $u(z)$, through and over the vegetation with h = water depth (m), k = vegetation height (m). The description of each zone can be found in section 2.3. Adapted from Baptist et al. (2007)

Flow resistance
In rivers there is a momentum balance in stream-wise direction. The gravitational forces drive the flow downstream while the vegetation and bed roughness hinders the flow. Those forces are expressed in shear stresses. The magnitude of those shear stresses are often characterized by a roughness coefficient like Chezy, Manning or White-Colebrook.

In the main channel shear stresses are mainly determined by the bed composition and bed characteristics. On vegetated river banks and floodplains the flow resistance is determined by a combination of bedforms and the vegetation. Figure 2.7 shows a schematisation of the time-averaged vertical velocity profile for a floodplain with vegetation where four different zones can be identified (Baptist et al., 2007):

1. In the first zone the velocity is highly influenced by roughness of the bed.
2. The second zone far enough from the bed the velocity is uniform.
3. In the third zone there is a shift in the velocity profile from uniform to the logarithmic profile above it.
4. The fourth zone is the zone above the vegetation that shows a logarithmic velocity profile.

Flow conditions for non-submerged vegetation, so only considering zone 1 and 2, can be described analytically. The total shear stress on the fluid is equal to the sum of the bed shear stress and the shear stress due to drag of the vegetation (Baptist et al., 2007):

$$\tau_t = \tau_b + \tau_v \tag{2.6}$$

where τ_t is the total fluid shear stress:

$$\tau_t = \rho g h i \tag{2.7}$$

τ_b is the bed shear stress and is given by:

$$\tau_b = \rho g \frac{u^2}{C_b^2} \tag{2.8}$$

and τ_v is the vegetation resistance per unit horizontal area:

$$\tau_v = \frac{1}{2} \rho C_D m D h u^2 \tag{2.9}$$

where m is the number of stems per square meter and D is the stem diameter. The vegetation is thus modelled as a staggered or random array of uniform cylinders with the same drag coefficient C_D. Using the momentum

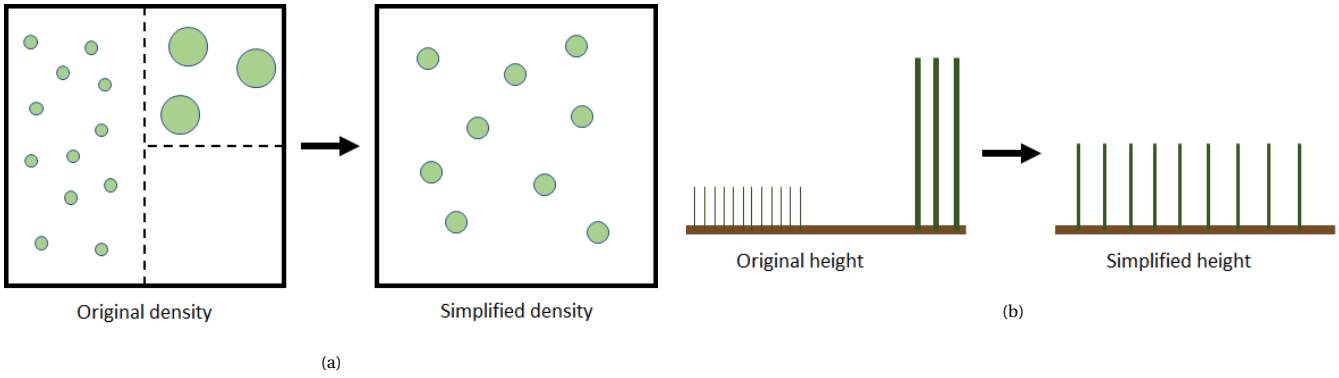

Figure 2.8: A schematization of how the density (a), stem height (b) and diameter (a and b) of two vegetation groups are simplified per Delft3D FM grid cell. This simplification is done by taking a weighted average the density, stem height and diameter, were the weights are equal to the fraction each vegetation group in the grid cell.

balance of equation 2.6 the uniform velocity through non-submerged vegetation u_{cb} is given by:

$$u_{cb} = \sqrt{\frac{hi}{1/C_b^2 + (C_D m D h)/(2g)}} \tag{2.10}$$

The discharge per unit width is given by $q = hu_{cb}$, using this formula the corresponding Chezy value can be calculated with the following equation:

$$C = \frac{q}{h\sqrt{hi}} \tag{2.11}$$

With those formulae the representative Chezy value for the combination of bed shear stress and vegetation drag becomes:

$$C_{cb} = \sqrt{\frac{1}{1/C_b^2 + (C_D m D h)/(2g)}} \tag{2.12}$$

Fully submerged vegetation is however more difficult to describe because also the zones 3 and 4 have to be included in the formula. Baptist et al. (2007) used genetic programming, which is a technique that can be used to find the symbolic form of an equation, to derive a roughness formula for fully submerged vegetation:

$$C_v = \sqrt{\frac{1}{1/C_b^2 + (C_D m D h)/(2g)}} + \frac{\sqrt{g}}{\kappa} \ln\left(\frac{h}{h_v}\right) \tag{2.13}$$

where h is the water depth and h_v the vegetation height. This formula was found to be in good agreement with experimental data and is theoretically well-founded Baptist et al. (2007). The second term goes to zero at the transition from submerged to emerged vegetation and equals formula 2.12 earlier found.

Including vegetation in Delft3D FM

Vegetation can vary in height, density and diameter depending on the age and type of vegetation. Each difference in height, density or diameter is called a vegetation group from now on. The most realistic way to model vegetation in Delft3D FM is to define a different trachytope class for each vegetation group. Trachytopes are used to model vegetation in Delft3D FM with equation 2.13. For more detailed information about trachytopes in Delft3D FM the reader is referred to the D-Flow Flexible Mesh User Manual (Deltares, 2020a).In this study a Python-based vegetation model is used and coupled with Delft3D FM. To couple both models the Basic Model Interface (BMI) is used, which allows Python to directly communicate with Delft3D FM via memory. The BMI is originally developed in the Community Surface Dynamics Modeling System (Peckham et al., 2013)[1]. Currently, the BMI wrapper supports only one trachytope class per grid cell, thereby only one vegetation height, density and diameter can be specified for each Delft3D FM grid cell.

In the vegetation model a grid cell can contain different groups of vegetation, as the species and also vegetation age can differ within a cell. Each vegetation group has their own height, density and diameter. Because

[1]The BMI Python package used in this study can be found at: `https://github.com/openearth/bmi-python`.

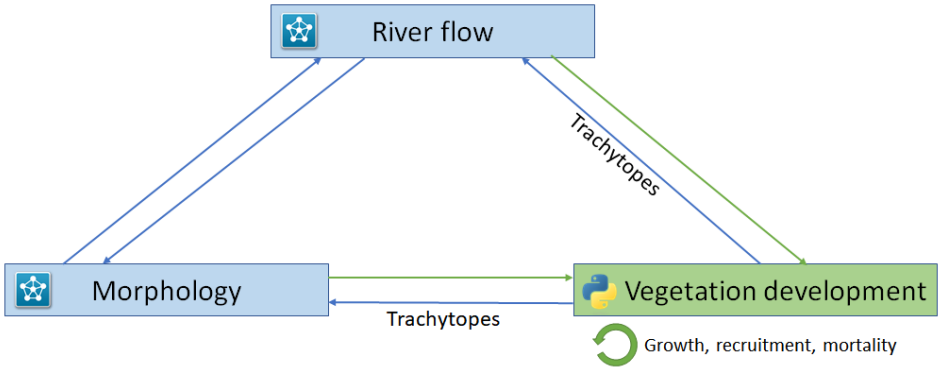

Figure 2.9: Main drivers of the feedback loop between the vegetation and a river. The river flow and morphology is modelled using Delft3D FM (blue shaded boxes) and vegetation development is modelled in a python-based vegetation model. The blue arrows indicate the interactions within Delft3D FM. The green arrows indicate the new interactions created by the coupling with the vegetation development model.

only one trachytope class can be defined per Delft3D FM cell, a simplification step has to be made. This simplification is done by taking a weighted average over each vegetation group property (height, density and diameter) in a grid cell (see Fig. 2.8). The weights are equal to the fraction each vegetation groups occupies in the cell.

2.4. Model framework

The coupled model exist of a coupling between a vegetation model and the morphodynamic Delft3D FM model. The coupled model is capable of simulating the three main drivers: (1) water flow, (2) morphology and (3) vegetation. The Delft3D FM model simulates the river flow as well as the morphology. The Delft3D FM model also takes into account the effect of vegetation on the flow and morphology of the river with the so-called trachytope module. The vegetation development model simulates the feedback from river flow and morphology to vegetation and uses this feedback to simulate vegetation growth, recruitment and mortality (see Fig. 2.9).

The vegetation model uses the same grid as the Delft3D FM model, see Section 3.2 for more information about the used Delft3D FM grid. The vegetation model simulates for each Delft3D FM cell the vegetation recruitment, growth and mortality. The vegetation coverage within a cell can range between 0 (no vegetation) and 1 (completely filled with vegetation), this number is called the vegetation fraction.

The vegetation development model uses the following processes to simulate riparian vegetation: (1) seedling recruitment growth, (2) growth, (3) seedling growth, (4) uprooting, (5) burial, (6) flooding and (7) drought. The text below briefly explains for each process how it is incorporated into the model. A more detailed description can be found in Appendix A.

2.4.1. Seedling recruitment

The recruitment of new vegetation takes place during the seed dispersal period of a species. If a cell was wet in the previous vegetation time step and is currently dry, seeds are deposited in this cell if it has space left for new vegetation. When cells are already completely filled with vegetation, new vegetation can not establish in those cells. Vegetation is added to a cell until the maximum surface fraction of the vegetation species concerned is reached. For both species the maximum surface fraction is equal to 0.8. For example, if a cell is already filled for 80% with *S. alba* species, no new seeds will be dispersed in this cell because the maximum surface fraction has already been reached. Figure 2.11 shows some examples of how seedling recruitment will take place with and without existing vegetation. If two or more vegetation species disperse their seeds at the same time, the available space in a cell will be shared equally between the vegetation species. At the moment a seed is dispersed in a cell the then occurring bed level is stored. This bed level will be used in the uprooting process.

2.4.2. Growth and seedling growth

As described in Section 2.2.2 the properties of the shoot, root and stem diameter of vegetation older than one year are updated once a year with equation 2.1. This process simulates the growth for vegetation older than one year old. The moment of the vegetation growth is set at the first of April. This moment has been chosen because the first seed dispersal takes place in mid-April (see Table 2.2). The use of 1 April makes it easier to follow the development of the seedlings throughout their first year of life, because at the moment of growth the survived seedling become part of the older vegetation.

At the moment of growth the vegetation increases in age. This means that the resistance of the vegetation to certain mortalities can change. Life stages are used to define certain vegetation characteristics, such as drought and flood thresholds (Table 2.1). Each year, the vegetation model checks the corresponding life stage for each tree. A tree may be in the same life stage for several years, which is defined by 'Number of years in the life stage'. The life stage in which a tree finds itself determines what vegetation characteristics the tree has at that moment. In this study, five different life stages are defined for each vegetation species.

De modelling of the seedling growth differs from the rest of the vegetation. Because seedlings have an rapid growth rate the size of the stem and roots are updated every vegetation time step within the vegetation model, instead of only once a year. The stem and root growth of seedlings are modelled with respectively equation 2.2 and 2.5.

2.4.3. Uprooting and burial

Removal of vegetation due to uprooting occurs when a part of the roots are uprooted due to erosion. The uprooting uses the germination height as reference level to keep track of how much erosion has occurred. If this erosion is larger than the root length times the uproot factor, the vegetation is removed in the model. Removal of vegetation due to burial occurs when the vegetation is completely buried beneath sediment. For the burial process is also the germination height used as reference level to check whether the vegetation is completely buried.

2.4.4. Flooding

Mortality by flooding starts to take place if the consecutive days of flooding in a grid-cell exceeds a threshold. For each cell the consecutive days of flooding is counted and stored within the model. Each vegetation step the model checks whether a Delft3D FM cell is flooded. A cell is identified as flooded when the mean water depth during the vegetation time step is 5 cm or higher and the maximum flow velocity has been higher than 0.01 m/s. The velocity threshold is used to eliminate cells that were flooded during a flood but are not completely drained after the flood and act as some unrealistic pools of water. If a cell becomes dry again after the next vegetation time step, the flooding time of that cell is reset. If the consecutive flooding time in exceeds the flooding threshold vegetation will be gradually be removed from the model (see Fig. 2.5). The flooding slope determines the rate at which vegetation is removed.

2.4.5. Drought

Drought stresses occur in the model when the roots of the vegetation cannot reach the capillary fringe layer above the groundwater level (see Fig. 2.10). The groundwater level in a floodplain cell is calculated by distance averaging the water level of the 3 nearest water containing grid-cells. Drought stresses occur in a similar way as those in the flooding process. The model keeps track of the continuous days that the vegetation is affected by drought stresses. If the consecutive days of drought stresses in exceeds the drought threshold, vegetation will be gradually be removed from the model.

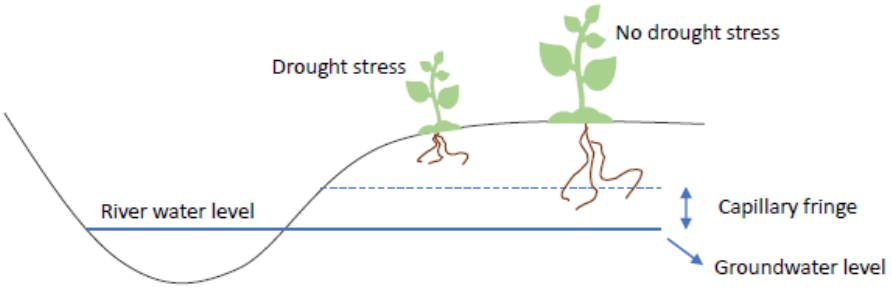

Figure 2.10: Schematic representation of the groundwater level related to the vegetation drought stresses.

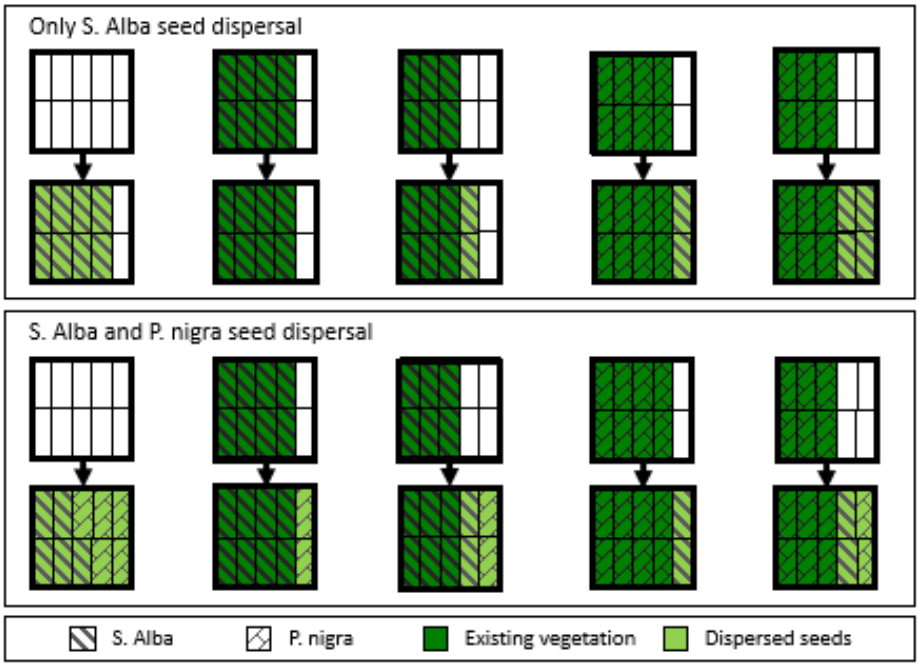

Figure 2.11: Examples of how a Delft3D FM cell is filled with vegetation in the model. For both the *S. alba* as the *P. nigra* species the maximum surface fraction is equal to 80 percent of a Delft3D FM cell. The figure shows how this influences the seed dispersal within a cell.

3

Case study

3.1. Introduction

As case-study a model schematization based on the Allier River (France) at Moulins is used (Figure 1.2). The Allier river is one of the last unregulated vegetated rivers in Europe, which still behaves as a natural river meandering river. Van Oorschot et al. (2016) showed that it is possible to model a realistic representation of riparian vegetation in the Allier and their hydrodynamic model was made available for this study. Therefore the Allier river was chosen as a case study.

The Allier River is a vegetated meandering river with a length of approximately 421 km with a total catchment area of 14,350 km^2. Its source is in the Margeride mountain range in the south of France. The river bed sediment is heterogeneous and consist mostly of gravel with a D50 of 5-8mm and a D90 of around 9-20 mm (van Dijk et al., 2014).

The Allier River has a mean annual river discharge of around 130 m^3/s with a very irregular discharge regime. The maximum discharges can vary highly between years, as does the moment at which this maximum occurs within a year (Onde, 1923; Garófano-Gómez et al., 2017). Occasionally this can lead to both extreme floods, which usually occur in winter or spring, as severe low discharges, usually in summer. Figure 3.1 shows the mean daily measured river discharge between 1968 and 2019. The Allier River has the following characteristic floods: HQ2 (2-yr recurrence interval flood): 669 m^3/s, HQ5 (5-yr recurrence interval flood): 937 m^3/s, HQ10 (10-yr recurrence interval flood): 1,110 m^3/s and HQ20 (20-yr recurrence interval flood): 1,280 m^3/s (Garófano-Gómez et al., 2017).

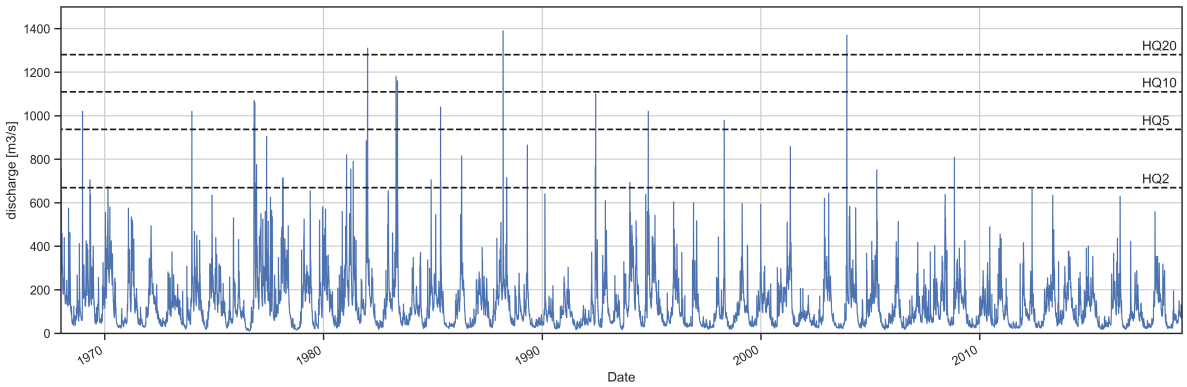

Figure 3.1: Mean daily discharge at Moulins recorded for the period 1968-2019. Missing periods at Moulins where replaced by measurements at Châtel-de-Neuvre (source: Banque Hydro). The dashed lines corresponds with the characteristic floods: HQ2 (2-yr recurrence interval flood): 669 m^3/s, HQ5 (5-yr recurrence interval flood): 937 m^3/s, HQ10 (10-yr recurrence interval flood): 1,110 m^3/s and HQ20 (20-yr recurrence interval flood): 1,280 m^3/s (source: Garófano-Gómez et al. (2017)).

In the years 1790, 1846, 1856, 1866 some catastrophic floods occurred in the Allier River with discharges estimated as high as 7,500 m3/s (Gautier et al., 2000). Those high discharges resulted from a combination of a Mediterranean storm from the south-east with a westerly oceanic storm coming in from the Atlantic coast.

3.2. Model set-up

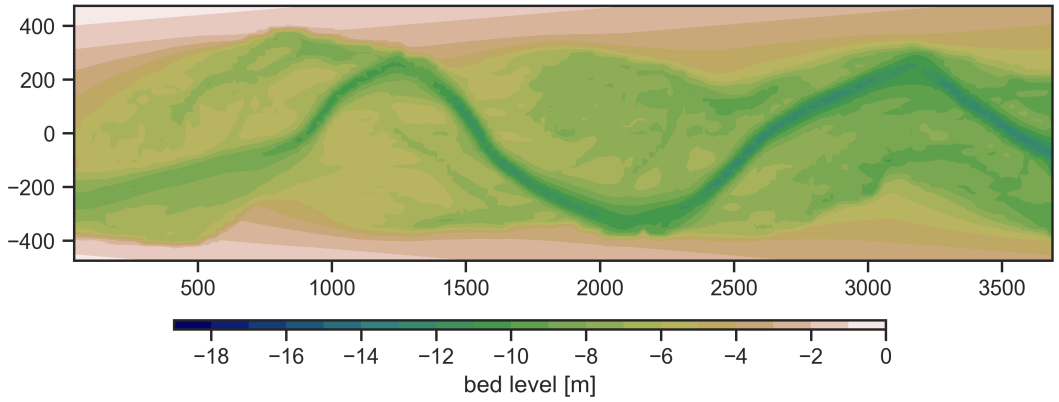

Figure 3.2: The initial bed level

In this study a two-dimensional (2D) depth-averaged Delft3D FM model is used. However, secondary flow (spiral flow), which is a 3D-effect, is essential for the formation of pointbars in river bends. To include secondary flow within the depth-averaged Delft3D FM model, a parametrization of the spiral flow effect on the direction of sediment is used by setting the Espir parameter in Delft3D FM to 1. The transverse bed-slope effect, which changes the sediment transport towards the downslope direction, is calculated by using the formula of Flokstra and Koch (1980) with an Ashld parameter of 0.7. A morphological acceleration factor of 30 was used similar to Van Oorschot et al. (2016). Morphological acceleration factors can be used to reduce computation times, because morphological developments take place on a time scale several times longer than typical flow changes. For more detailed information on how spiral flow, transverse bed-slope effects and morphological acceleration factors are incorporated in Delft3D FM the reader is referred to the D-Morphology User Manual (Deltares, 2020b).

Figure 3.2 shows the initial bed level used in the model. This bed level is based on bed level data from the model of Van Oorschot et al. (2016). The model in that study started with a manually created bed level that after modelling 150 years developed into a realistic channel lay-out, typical for the Allier river. The next step was to model 22 years using the measured Allier discharge from 1968 till 1990 with the coupled Delft3D FM model, starting with the bed level data of Van Oorschot et al. (2016). The resulting bed level after those 22 years is used as initial bed level for the rest of the study. This additional modelling was done to level out potential large morphological modifications due to the differences between the Van Oorschot et al. (2016) model and the coupled model used in this study, which could significantly influence the model results.

At both ends of the model boundary conditions need to be prescribed for the flow and transport of sediment. The upstream boundary is defined by a 250 m long discharge boundary, equal to the discharge measurements showed in Figure 3.1. The downstream boundary is a discharge related water level boundary based on the model of Van Oorschot et al. (2016).

Uniform fine gravel with a D50 of 5 mm is used as sediment in the model with an initial sediment layer of 5 m thick. The sediment transport is calculated with the Engelund and Hansen (1967) formula. For the upstream sediment boundary condition a Neumann boundary condition is used, which is the default setting in Delft3D FM (Deltares, 2018). With a Neumann boundary condition, sediment concentrations at the inflow boundary are set equal to those just inside the domain, leading to very little sedimentation or erosion at the boundary.

Parameter	Unit	Value
Grid width	m	950
Grid length	m	3700
D_{50}	mm	5
Chezy	$m^{1/2}/s$	25
Grid cell size lxw	m	25x25
Initial sediment thickness	m	5
Hydronamic time step	s	12
Morphodynamic time step	s	360
Vegetation time step	$days$	7
Espir	-	1
Ashld	-	0.7
ThetSD	-	0.5

Table 3.1: Used Delft3D FM model settings

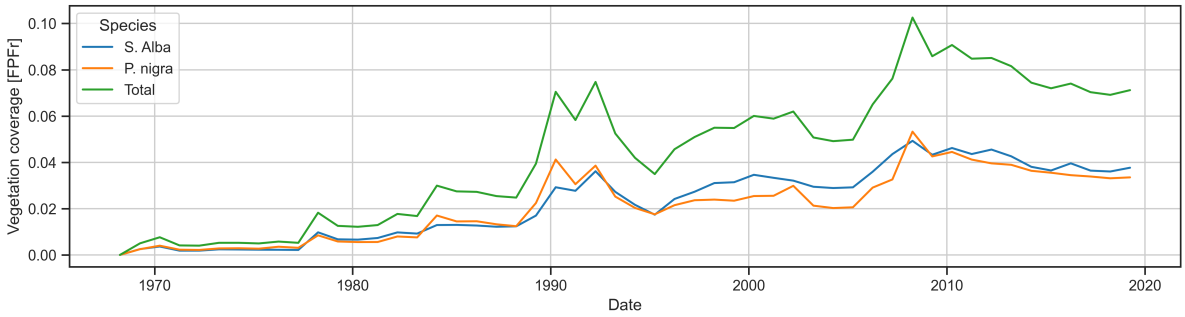

Figure 3.3: The development of vegetation coverage in time. The vegetation coverage is showed as fraction of the floodplain (FPFr). In this figure the seedling coverage is not included.

Sediment transport is only calculated at cells with a water depth of 0.05 m or more, grid cells with lower water depths are considered as inactive for sediment motion in the used model. Grid cells are reactivated when the water depth threshold is exceeded or when subject to the bank erosion. Bank erosion occurs when a wet cell is adjacent to one or more dry cells. In that case 50 percent of the erosion of a wet cell is assigned to the adjacent dry cells.

3.3. Results

This section shows the results of the default vegetation and model settings. The Delft3D FM model settings can be found in Table 3.1. The used vegetation settings are equal to those shown in Tables 2.1 and 2.2. This means that two vegetation species are modelled, the *S. alba* and the *P. nigra*. The model starts without any initial vegetation.

Figure 3.3 shows the vegetation coverage in time for both species, as well as the total vegetation coverage. The seedling coverage is not included in this figure because the amount of seedlings can highly fluctuate within a year, making the figure unreadable. The vegetation coverage is shown as a fraction of the total floodplain (FPFr):

$$FPFr = \frac{\text{Area vegetation in the floodplain}}{\text{Total area floodplain}} \tag{3.1}$$

The floodplain is defined as the area that has shown morphological activity between 1968 and 2019. To avoid boundary effects the first and last 20 cells are clipped from the floodplain. The vegetation cover itself is calculated by adding up the part of each cell that is occupied by vegetation and divide this number by the total amount of cells in the floodplain.

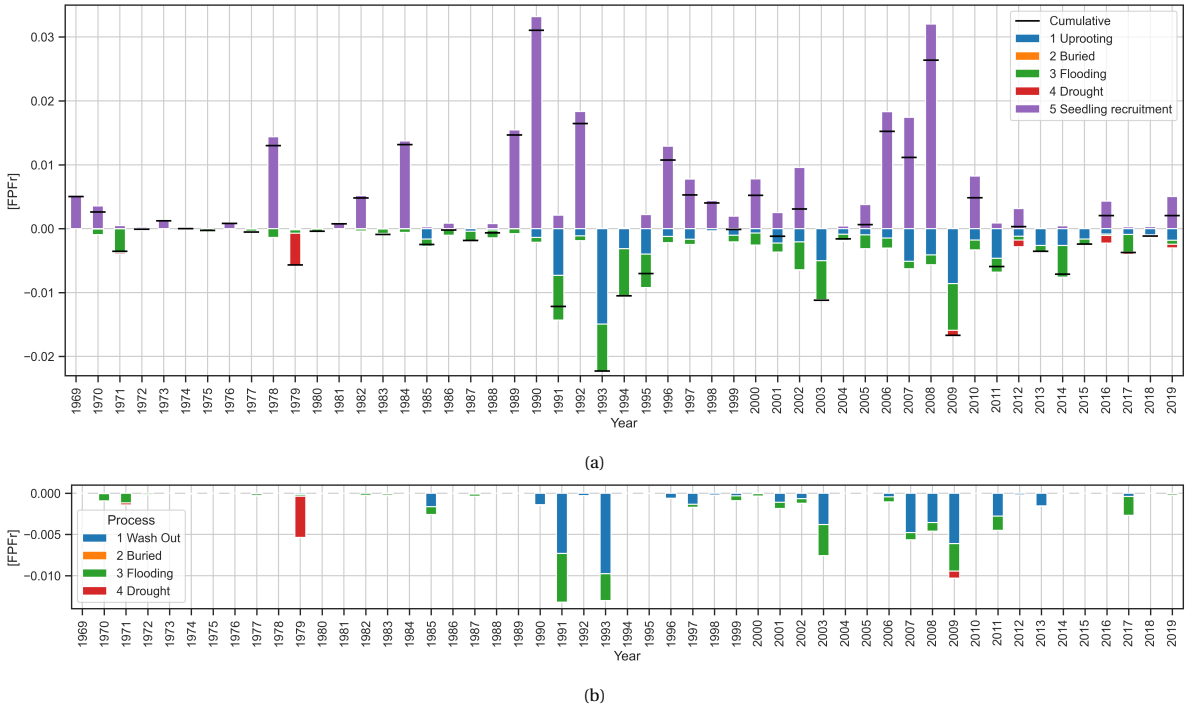

Figure 3.4: The total seedling recruitment and vegetation removal for each year in fraction of the floodplain (a). Figure (b) shows the vegetation removal of one year old vegetation.

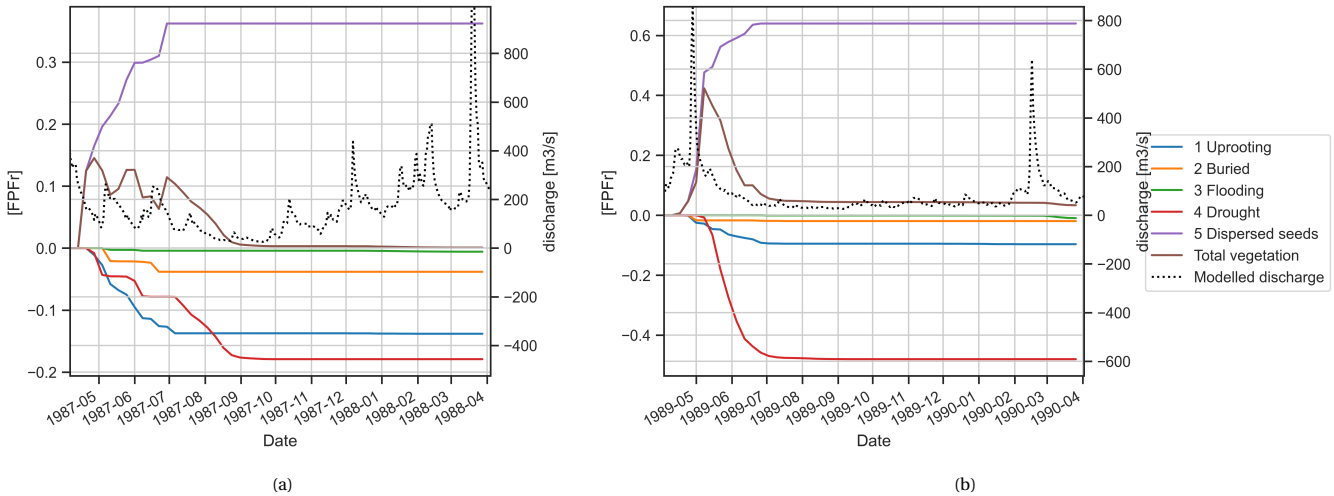

Figure 3.5: The seedling development in time from 1-4-1987 till 1-4-1988 (a) and 1-4-1989 till 1-4-1990 (b). The brown line shows the seedling coverage over time for the Default scenario. The blue, orange, green en red lines represent the the cumulative removal of vegetation in fraction of the floodplain (FPFr), where the purple line represent the cumulative seed deposition. The dotted black line represent the modelled discharge.

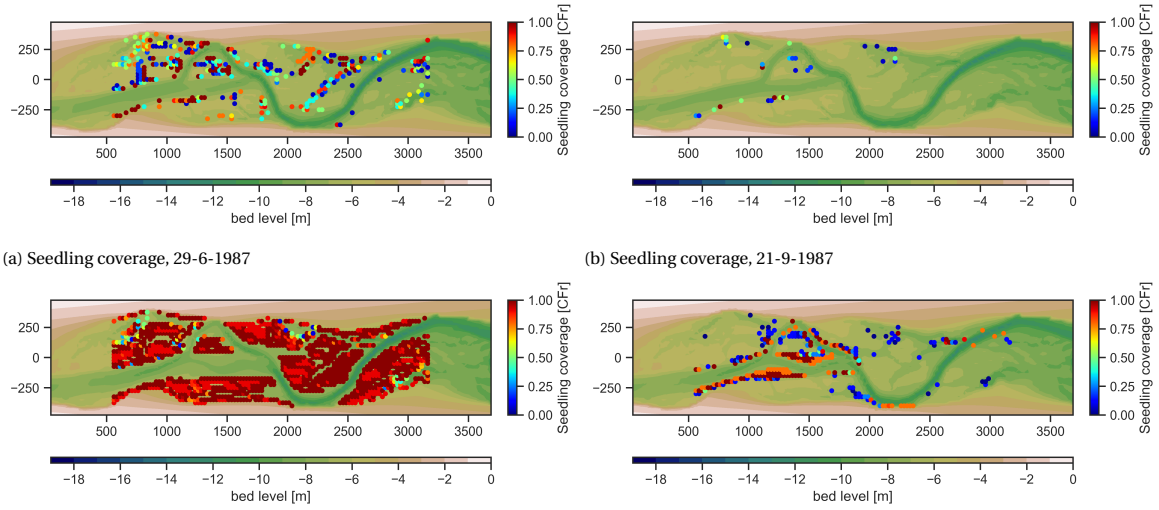

(a) Seedling coverage, 29-6-1987

(b) Seedling coverage, 21-9-1987

(c) Seedling coverage, 15-5-1989

(d) Seedling coverage, 17-7-1989

Figure 3.6: Map plots of seedling coverage in the years 1987 and 1989. The highest seedling coverage in both years are shown (a an c) and the seedling coverage just after the high mortalities due to drought (b and d). The seedling coverage is shown as fraction of a Delft3D FM cell (CFr).

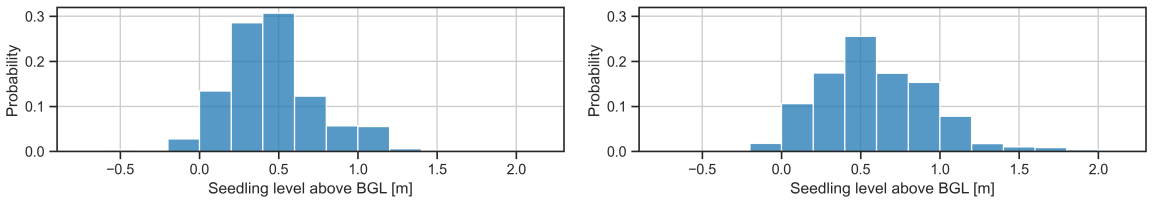

(a) *S. alba*

(b) *P. nigra*

Figure 3.7: The seedling elevation distribution in mid-July of all seedlings that have successfully survived their first year. The figures show the probability of which elevation above BGL a surviving seedling is located.

During the first 15-20 years the vegetation coverage is relatively low and the fraction of the floodplain covered with vegetation stays below 0.03. Around 1988 there is a sudden increase in vegetation coverage for both species after which the fraction of the floodplain that is covered with vegetation fluctuates between the 0.04 and 0.10.

Figure 3.4a shows for each vegetation year the vegetation mortality and seedling recruitment. A vegetation year is defined as the period between two growth moments (1 April-31 March, see section 2.2.2). The difference between the seedling recruitment and the total vegetation mortality determines the change in vegetation coverage, which is showed by a black line. Both the vegetation mortality as the seedling recruitment highly differ between the years, but the highest mortality rates are seen in the year after a large seedling recruitment occurred. This high mortality is often caused by the one year old vegetation that was seeded in the previous year as seen in Figure 3.4b. This figure shows the vegetation mortality of one year old vegetation. It can be seen that the one year old vegetation is still very vulnerable to uprooting and flooding. This can be explained by the fact that this vegetation could only establishes itself due to the favourable conditions in the previous year. If in the next year longer periods of droughts or flooding occur, one year old vegetation has a high chance of dying.

As explained in the previous chapter, during the dispersal period seedlings are dispersed on the river banks after a discharge peak. The discharge regime after the germination is also important because it determines if a seedling is able to survive. Results show that most germinated seedlings die due to drought stresses. This effect can be observed in Figure 3.5 which shows the seedling development in the years 1987 and 1989. The brown line shows the total seedling coverage while the other coloured lines show the cumulative change in seedling coverage per vegetation process. The dotted black line represents the discharge.

In the year 1989 the seedling recruitment was very successful because a significant amount seedlings survived the first year. This is due to the favourable discharge regime right after the seed germination. The peak in discharge is early in the seed dispersal period and the fall in discharge is relative gradually. Which means that the seedling root growth is able to keep up with the falling water table. This means that the surviving seedlings have sufficient long roots to resist the low discharges that start around mid-June. In 1987 there are several smaller discharge peaks during the seed dispersal period. At the end of the seed dispersal period the discharge is still relative high, so no seeds are dispersed on the lowest part of the river bank. This gives the seedlings a large disadvantage during low discharges. Figures 3.6 shows the seedling coverage on a map for both years at the peak of the seedling coverage and right after the largest drought mortalities. It can be seen that in 1987 the seedlings could not recruit the lower river banks. As a result most seedlings are removed by drought. In 1989 also a lot of seedlings are removed by drought, but because the fall in discharge is during the seed dispersal period, new seedlings have germinated on the lower river banks (Fig. 3.6d). Those 'younger' seedlings with smaller roots are still able to survive the low discharges because they are closer to the river channel.

Not only the discharge but also the vegetation characteristics of each species influence the places that a species can colonise. To determine the recruitment elevation of each species a base-flow groundwater level is used as reference elevation. A discharge of 45 m^3/s is used as base-flow, which is the median daily discharge in July. For all the seedlings that survive the first year, their elevation above base-flow groundwater level (BGL) is calculated in July. To calculate the base-flow groundwater level, for each year a separate Delft3D FM model run was done with a discharge of 45 m^3/s and the corresponding bed level data in mid-July. Figure 3.7 shows the probability distribution of the elevations above BGL where surviving seedlings are located in mid-July. It can be seen that the *S. alba* species is able to colonise the lower part of the river bank due to its flood and uproot resistance. The *P. nigra* species can however colonise the higher parts of the river banks because of its faster growth rate. The figure shows that most seedlings survive in the region between 0 and 1 meter above BGL.

Figure 3.8 shows the bed levels and vegetation cover in 2019. It can be seen that there is a clear age distribution of the vegetation within the floodplain. The older vegetation is generally found further away from the river channel, because the vegetation there is less quickly removed and therefore has a chance to develop.

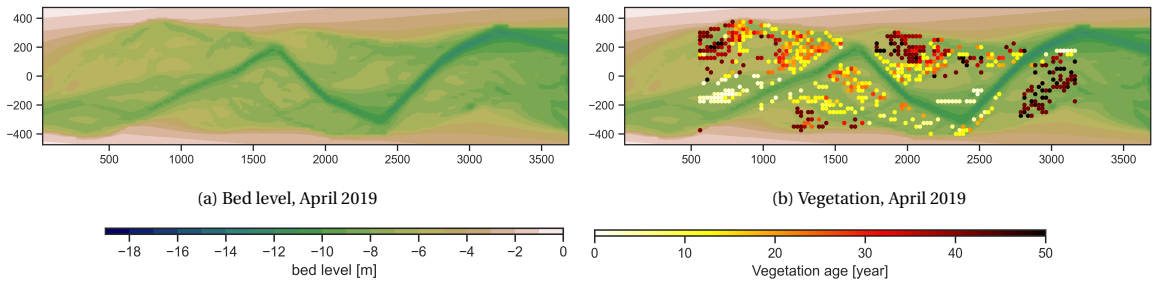

(a) Bed level, April 2019

(b) Vegetation, April 2019

Figure 3.8: The morphology and vegetation cover in April 2019. Each dot represents a Delft3D FM cell with vegetation. The vegetation age is calculated as the weighted average of all the existing vegetation in a Delft3D FM cell.

The youngest vegetation is found closer to the river channel and located on the lower parts of the floodplain. This age distribution along the floodplain is in line with that found along the Allier river (Van Oorschot et al., 2016).

The results show that the seedling recruitment has a large influence on the total vegetation coverage if successful. The recruitment of seedlings is again largely dependent on the occurring discharge. As expected, the results show that young vegetation till one year old is the most vulnerable, especially to drought. Older vegetation is more resistant, but can still be removed or killed due to flooding and uprooting.

4

Sensitivity analysis

4.1. Introduction

To get a better understanding of the importance of the different vegetation processes in the vegetation model a sensitivity analysis is performed. The vegetation model is partly based on the model of Van Oorschot et al. (2016) for which they already did an extensive sensitivity analysis. In their analysis they focussed on different types of vegetation with different ecological strategies.

The sensitivity analysis in this study will focus on separate vegetation processes instead of different vegetation types. This will give a better insight in how a vegetation process influences the model results. The selection of processes fro this sensitivity analyses is based on either the importance of a process in the model, the uncertainty of the parameters used for a process or a combination of both. Additionally the effect of the morphology on the vegetation is investigated in three different scenarios.

4.2. Scenarios

The following processes are investigated in this sensitivity analysis:

- Flooding
- Uprooting
- Seedling growth
- Seed dispersal period
- Morphology

A short overview of the different scenarios used in this sensitivity analysis and their corresponding vegetation parameters can be found in Tables 4.1 and 4.2. The vegetation parameters of the default scenario are based on the literature described in Chapter 2. For each selected vegetation process a set of scenarios is defined and their results are compared with the default scenario.

4.2.1. Flooding

Two different flooding scenarios are created for this sensitivity analyses. Flooding is the most important vegetation removal process in the model. It is therefore important to investigate the effect of different flooding parameters, even more because the flooding thresholds found in literature bear some uncertainties. Vegetation removal due to flooding process is controlled by two parameters, the flooding threshold and the flooding slope. The flooding threshold is a threshold in days that indicates after which time period flooding mortality occurs. The flooding slope determines the rate in which the vegetation is removed after the flooding threshold is reached. In this sensitivity analysis the flooding threshold is changed while the flooding slope is kept the same. The used flooding thresholds can be seen in Table 4.2.

Scenario	Abbr.	Dispersal period		Seedling stem growth parameters (Eq. 2.2)		Seedling root growth parameters (Eq. 2.5)	
		S. alba	*P. nigra*	*S. alba*	*P. nigra*	*S. alba*	*P. nigra*
Default	-	15 April-15 June	1 May-1 July	a=6.42, b=-0.0506, c=0.848, d= 0.002	a=6.74, b=-0.0534, c=1.05, d= 0.005	k=0.015, c=0.5, d=0.02	k=0.012, c=0.6, d=0.03
Fast Seedlings	FGS	Default	Default	a=5, b =-0.0506, c=1.1, d=0.002	a=5.3, b=-0.0534, c=1.2, d= 0.04	k=0.017, c=0.7, d=0.04	k=0.014, c=0.8, d=0.06
Slow Seedlings	SGS	Default	Default	a=7.8 ,b=-0.0506 , c=0.6 , d=0.001	a=8.1 ,b=-0.0534 , c=0.75 , d=0.0025	k=0.013 , c=0.3 , d=0.01	k=0.01 , c=0.4 , d=0.015
Seperate Dispersal	SD	1 May -31 May	1 June - 1 July	Default	Default	Default	Default
Equal Dispersal	ED	15 April -1 July	15 April - 1 July	Default	Default	Default	Default

Table 4.1: The growth and dispersal parameters per vegetation species used in the different scenarios. Scenarios not shown in this table have the same growth and dispersal parameters as the Default scenario.

			S. alba					*P. nigra*				
			Seedling	Young sapling	Sapling	Adult	Old Adult	Seedling	Young sapling	Sapling	Adult	Old Adult
Parameter	Scenario	Abbr.	1	2	7	40	10	1	2	7	130	10
Flooding threshold	Default	-	50	100	120	130	130	30	70	70	80	80
	Flood resistant	FR	75	150	180	195	195	45	105	105	120	120
	Flood susceptible	FS	25	50	60	65	65	15	35	35	40	40
100% flooding mortality	Default	-	107	200	320	330	230	80	137	237	247	180
	Flood resistant	FR	132	250	380	395	295	95	172	272	287	220
	Flood susceptible	FS	82	150	260	265	165	65	102	170	175	140
Uproot factor	Default	-	0.3	0.2	0.2	0.2	0.2	0.2	0.1	0.1	0.1	0.1
	Uproot resistant	UR	0.7	0.6	0.6	0.6	0.6	0.5	0.4	0.4	0.4	0.4
	Uproot susceptible	US	0.05	0.05	0.05	0.05	0.05	0	0	0	0	0

Table 4.2: The different vegetation characteristics used in the scenarios. There are five different life stages defined: Seedling, Young sapling, Sapling, Adult, Old adult. Each life stages has different characteristics. Scenarios not shown in this table have the same vegetation characteristics as the default scenario.

4.2.2. Uprooting

Uprooting is the second most important vegetation mortality cause after the flooding process. Removal due to uprooting occurs in the model when a certain percentage of the roots beneath the germination level are exposed by erosion, which is specified by the uproot factor. The used uproot factor is chosen to be relatively low as it was found in literature that the largest part of a riparian root system often develops in the deposited soil above the germination level (see Sec. 2.2.6). It is therefore assumed that only a low percentage of the roots beneath the germination level needs to be uprooted to remove the vegetation.

The uproot factor is a rough estimate and it is uncertain what the effect of a different uproot factor is. Two scenarios each with a different uproot factor are used to investigate this effect. The Uproot resistant (UR) scenario has more uproot resistant vegetation with a relative large uproot factor. For the Uproot vulnerable (UV) scenario a very low uproot factor is chosen, this scenario represents a situation where vegetation is removed almost immediately when erosion occurs below the germination level.

Both scenarios will also give a better insight into the impact of uproot factor on seedling recruitment. A larger uproot factor could lead to more seedling recruitment due to its increased resistance to uprooting. In contradiction, a very small uproot factor will give little to no protection to uprooting, which could lead to a situation where a large part of the seedlings is washed away.

4.2.3. Seedling growth

The rate of the seedling growth largely determines its chance of survival, because the larger a seedling is, the higher its resistance to mortality processes such as drought, burial, and wash out. The seedling survival rate will eventually determine how much new vegetation will be established in the model. Starting with an initial situation without vegetation, a faster seedling growth rate will probably lead to a fast colonization of vegetation.

The growth rate of seedlings also indirectly influences the bed level range at which it can survive. For instance vegetation with faster root growth is better resistant to drought and is therefore able to survive on higher bed levels. This results in a larger part of the floodplain that can be colonised and could lead to a higher overall vegetation cover. To investigate the effect of the seedling growth rate, two different scenarios are used: one with a high shoot and root growth rate and one scenario with lower growth rates. Table 4.2 shows the used growth parameters for both scenarios.

4.2.4. Seed dispersal

The seed dispersal period is, like the seedling growth, an important parameter for seedling recruitment. The seed dispersal period determines in which weeks seeds are dispersed and thus in which period seeds are able to germinate on the river bank. Altering this period can have large effects on the seedling recruitment. A shorter dispersal period gives a vegetation species a smaller time window for successful establishment.

Another important effect to investigate is that of equal and separate seed dispersal periods when modelling two or more vegetation species. For instance, if vegetation species' seed dispersal periods differ from each other, the species with the earlier seed dispersal period could colonize most part of the available space for seedling recruitment. In this case the species with a slightly later dispersal period have less chance to establish because most available space is already partly covered with the first vegetation species. To check whether this effect actually occurs two different seed dispersal scenarios are used, one with equal dispersal periods (ED scenario) and one with separate seed dispersal periods (SD scenario). The seed dispersal periods in the SD scenario last a month for each species which is significant less than the default scenario. This will also give insight in the importance of length of the seed dispersal period.

4.2.5. Morphology

To get a better understanding of the effect of vegetation on the morphology and vice-versa two scenarios were used. The first scenario is called the No coupling (NC) scenario. This scenario uses the same model and vegetation setting as those in the default scenario, but does not use the coupling between the vegetation model and Delft3D FM. All processes in the vegetation model still work in the same way, but the vegetation is now unable to affect the flow and morphology of the river. In the Delft3D FM model no vegetation will be simulated and only its output will be used in the vegetation model.

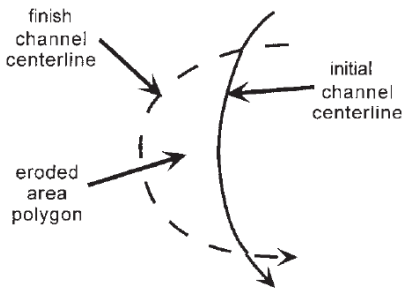

Figure 4.1: Eroded-area polygon. An eroded-area polygon is created by intersecting two channel centrelines from different time periods. The river channel shifting rates are calculated by dividing the polygon area by the average stream length of the initial and finish centerline. This method proved to be, a simple, reproducible measure of the magnitude of shift in channel location normal to the original channel centreline. The figure and method is adapted from the study of Micheli et al. (2004).

The second scenario uses does use the coupling between Delft3D FM and the vegetation model but does not update the morphology. In this way the effect of a static morphology can be investigated. This scenario is referred to as the No bed level update (NBLU) scenario

Finally a third scenario is used to investigate the effects of using an initial sediment layer in Delft3D FM. The default scenario uses an initial sediment layer thickness of 5 m. To investigate the effects of this model setting a scenario is ran where a infinitely thick sediment layer is used. This scenario is referred to as the infinite sediment layer (ISL) scenario.

4.3. Data analysis

Due to the differences in vegetation properties and model settings, each scenario will develop different morphologies and vegetation coverages. Due to the strong interaction between vegetation and morphology it can be difficult to compare the different scenarios.

The development in time of the overall vegetation coverage is the main parameter used to compare the different scenarios in the sensitivity analysis. The vegetation coverage gives a good insight of what the effects of vegetation properties or model settings are on the vegetation development.

Often the differences in morphology play large role in the development of vegetation. In those cases map plots of the bed level are often used to explain why the vegetation development differs between scenarios. Also the yearly river channel shifting rate is calculated to indicate how dynamic the river behaves. The yearly river channel shifting rate is determined as follows: Each year a centerline is drawn through the main river channel. This centerline is drawn based on the maximum discharge within a model cross-section (see Appendix A.11 for more information). This results in a different channel centerline for each year. The area between two centerlines of two sequential years form a so called eroded area polygon. The river channel shifting rates are calculated by dividing the polygon area by the average stream length of the initial and finish centerline (see Figure 4.1). This method to calculate the channel shifting rate is adopted from Micheli et al. (2004). Most years the shifting rate is relatively low and the larger values indicate sudden changes in the main river channel. In this study the average of the 15 highest observed yearly channel shifting rates are used to indicate how dynamic a scenario behaves. This shifting rate gives insight at which rate the channel moves and how dynamic a river is. The term CSRH15 is used as an abbreviation to indicate the average value of the 15 highest observed annual channel shift rates.

Another measure to compare the different scenarios is looking at the average fraction of the floodplain that is between 0 and 1 meter above BGL, previous Chapter showed that most seedlings are recruited within this area, also called recruitment band. The average fraction gives an indication of how much of the floodplain is suitable for the recruitment of vegetation. The value gives also information on the steepness of the river banks, because a smaller floodplain fraction between 0 and 1 meter above BGL indicates a steeper gradient of the river banks.

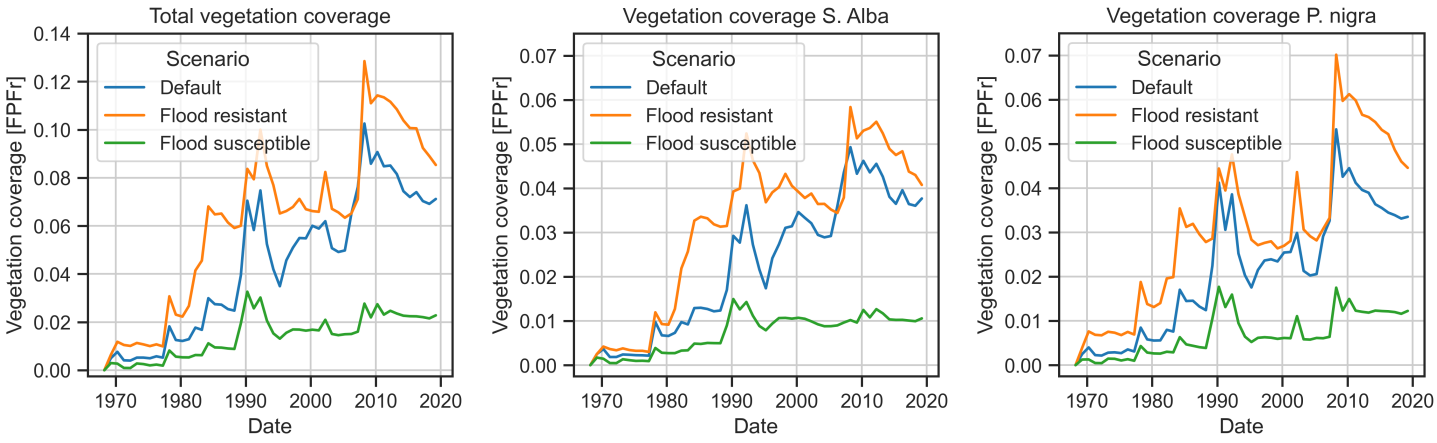

(a) Total coverage

(b) *S. alba* coverage

(c) *P. nigra* coverage

Figure 4.2: Figure (a) shows the total vegetation coverage in ha for the different flooding scenarios. Figures (b) and (c) show the vegetation coverage subdivided by the vegetation species *S. alba* and *P. nigra*

4.4. Results

4.4.1. Flooding

Figure 4.2 shows the vegetation coverages for the default scenario and the two different flooding scenarios. It can be clearly seen that the model is sensitive to a changing flooding threshold. As can be expected, a more flood resistant vegetation results in a higher overall vegetation coverage and vice versa for a more flood susceptible vegetation. It is interesting to see that the difference between the default and flood resistant (FR) scenarios is much smaller than between the default and flood susceptible (FS) scenarios. This is as expected because in the FS scenario the flooding thresholds are around those of hardwood species Glenz et al. (2006), which are known to be vulnerable in regularly flooded river floodplains.

The large difference in vegetation coverage is for a large part caused by differences in the yearly seedling recruitment. Figure 4.15 shows for each scenario the distribution of the yearly seedling recruitment. Looking at the flooding scenarios it becomes clear that the default and FR scenarios often have significantly more seedling recruitment in a year than the flood susceptible scenario. This difference can be explained by understanding how the seedling coverages develop throughout the year. The moment a seed is deposited on the river bank, a seedling germinates. This young seedling is still very small and therefore very vulnerable. Many seedlings die in their first months due to drought, burial and uprooting. In this period flooding is often not an important mortality cause. If a seedlings survives those first months it has grown sufficiently to be resilient to drought, burial and uprooting due to its larger roots and stem. However a seedling is at that moment still vulnerable to flooding. A flood susceptible seedling is therefore at a clear disadvantage. This can be seen in Figure 4.3a where the seedling coverage over time is shown accompanied with the vegetation cumulative vegetation removal caused by each process. Around November 1969, both flooding scenarios differ more or less equally from the default scenario as can be seen in Figure 4.3b. Figure 4.3b is a detailed plot of Figure 4.3a. Flooding mortality starts to play a role around January, killing a greater proportion of the flood-prone vegetation. This higher flooding mortality at the end of the year reoccurs often, leading to a lesser overall seedling recruitment in the FS scenario.

The relatively large difference between the default and FS scenario is also caused by a large difference in mortality rates of the vegetation older than 1 year. This can best be seen by looking at the yearly mortality rate of the vegetation. The yearly mortality rate is calculated by taking the total vegetation removal in a year in FPFr and dividing the result by the vegetation coverage in FPFr at the start of a year. This yearly mortality rate can be calculated for each process. Figure 4.4a shows the distribution of the yearly mortality rates for all the removal processes combined. It becomes clear that the total yearly mortality rates are significantly higher for the FS scenario. This increase in the total yearly mortality rate is caused by significantly higher flooding mortalities.

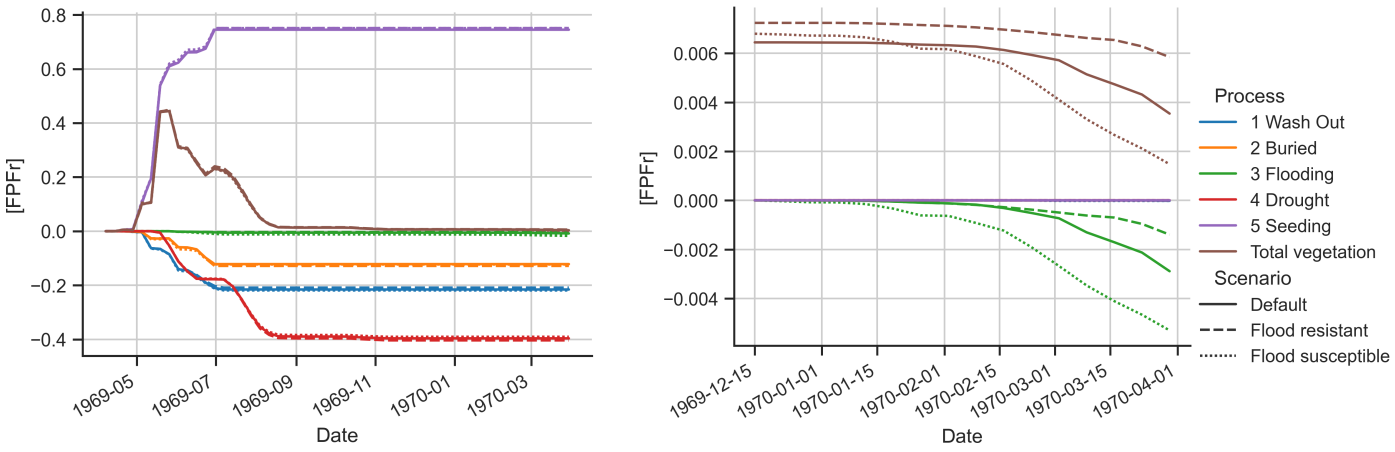

(a) (b)

Figure 4.3: Figure (a) shows the seedling development in time from 1-4-1969 till 1-4-1970 for the default, flood resistant and the flood susceptible scenarios. The brown lines shows the seedling coverage over time as a fraction of the floodplain (FPFr). The blue, orange, green en red lines represent the the cumulative removal of vegetation in FPFr, where the purple line represent the cumulative seed deposition. The continuous lines denote the default scenario, the dashed lines denote the flood resistant scenario and the dotted lines denote the flood susceptible scenario. Figure (b) shows a detailed section of figure (a), as the difference between the scenarios is minimal. The cumulative sum in (b) is calculated from 15-12-1969.

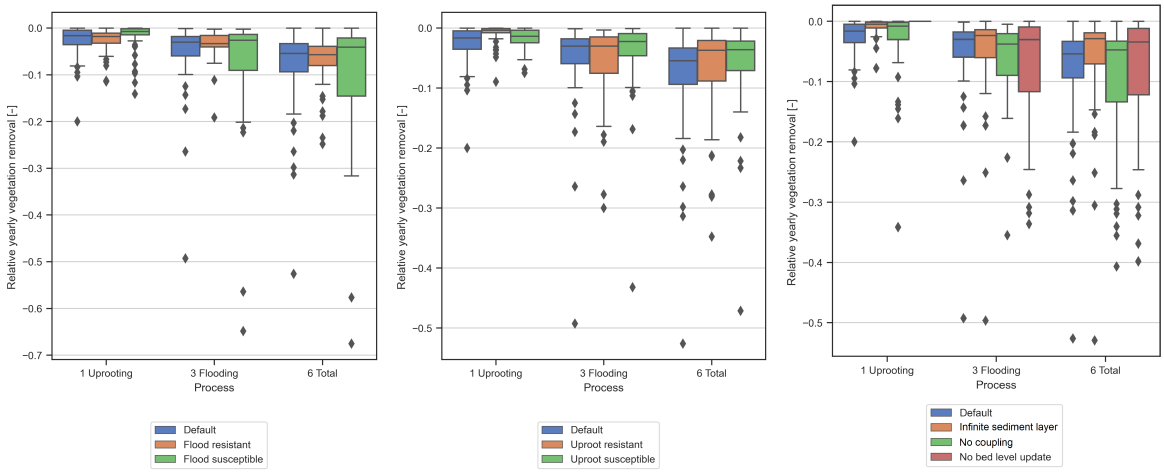

(a) Flooding scenarios (b) Uprooting scenarios (c) Morphology scenarios

Figure 4.4: Boxplot of the relative yearly vegetation removal rate for uprooting, flooding and all mortality processes combined. The relative yearly vegetation removal is calculated by taking the yearly vegetation removal in FPFr and divide this by the vegetation coverage in FPFr at the start of a vegetation year. Within each box, the black line denote the median value; boxes extend from the 25th to the 75th percentile of the distribution of values; vertical extending lines denote adjacent values (i.e., the most extreme values within 1.5 interquartile range of the 25th and 75th percentile of each group); dots denote values outside the range of adjacent values.

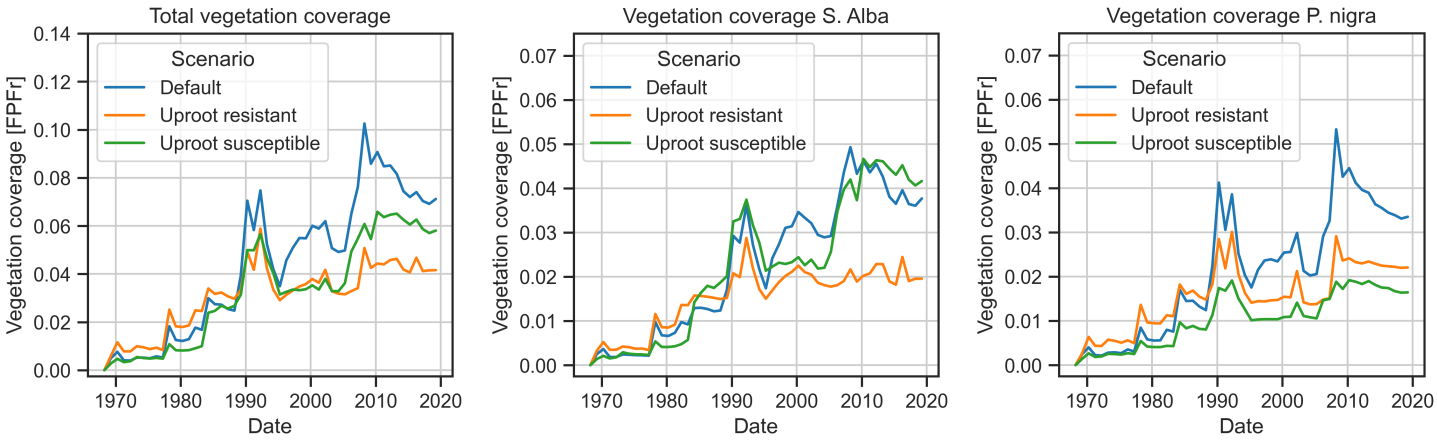

(a) Total coverage (b) *S. alba* coverage (c) *P. nigra* coverage

Figure 4.5: The vegetation coverage of the default and the two uprooting scenarios. Figures (b) and (c) show the vegetation coverage subdivided by the vegetation species *S. alba* and *P. nigra*

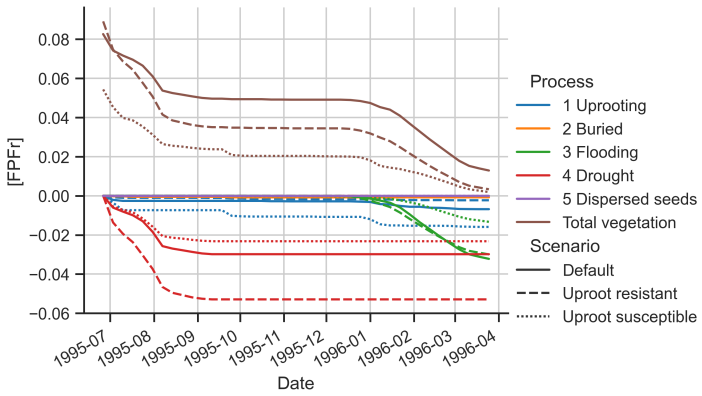

Figure 4.6: The combined seedling development of the *S. alba* and *P. nigra* species in time from 12-6-1995 till 1-4-1996. The brown lines shows the seedling coverage over time as a fraction of the floodplain (FPFr). The blue, orange, green en red lines represent the the cumulative removal of vegetation in FPFr, where the purple line represent the cumulative seed deposition. The continuous lines denote the default scenario, the dashed lines denote the uproot resistant scenario and the dotted lines denote the uproot susceptible scenario.

The different vegetation characteristics and thus coverages result in different morphology developments. The higher vegetation coverage in the default and FS scenarios leads to higher channel shifting rates than the FS scenario (Table 4.3). This means that the default and FR scenorios show less channel narrowing, which means that a larger part of the floodplain is between 0 and 1 meter above BGL. This gives both scenarios an extra advantage over the FS scenario, because in these regions new vegetation can establish itself. The large difference in vegetation coverage between the FS scenario and the default and FR scenarios is thus caused by a combination of lower seedling recruitment rates, higher yearly mortality rates and lower dynamics in morphology. The difference in vegetation coverage between the default and FR scenario is significantly smaller. This indicates that mainly lower flooding thresholds influence the vegetation coverage.

4.4.2. Uprooting

Figure 4.5 shows the vegetation coverage for the default, uproot resistant (UR) and uproot susceptible (US) scenarios. From 1968 till 1988 the vegetation coverage develops as expected, with a higher vegetation coverage for the uproot resistant vegetation and vice versa for the uproot susceptible vegetation. From 1988 the highest vegetation coverages are seen in the default scenario, with an increased difference after the year 1996. This is an unexpected result, considering the fact that the uproot resistant vegetation has better characteristics than the default vegetation to survive uprooting.

This difference can be explained by taking a closer look at the seedling recruitment. An example the seedling recruitment in 1995 is used. Figure 4.6 shows the development in seedling coverage from 12-6-1995. The coloured lines below the x-axis show the cumulative vegetation removal in FPFr for each mortality process. At 12-6-1995 the UR scenario still has the highest seedling coverage of all the three scenarios. However, in the months June and July a significant higher part of the uproot resistant seedlings die due to drought in comparison with the other two scenarios. Those higher drought mortalities result in a significant lower seedling coverage for the UR scenario in comparison with the default scenario. The US scenario also has a low seedling coverage, but this is mainly caused by the higher uproot mortalities, which is to be expected considering the more uproot susceptible vegetation in this scenario.

The large difference in drought mortality between the UR and the other two scenarios can be explained by looking at the difference in bed levels between each scenario. Figure 4.7 shows for the default and UR scenario the bed levels at 12-6-1995 and also the seedling coverage before and after the high drought mortalities. It can be clearly seen that the UR scenario has narrower channels with steeper river banks in comparison with the default scenario. With the same discharge those narrow channels with steep river banks mean that a lower fraction of the floodplain is suitable for seedling recruitment. In comparison with the default scenario, a larger part of the floodplain in the UR scenario will have groundwater levels that are too deep for young seedlings to survive, which explains the higher drought mortalities.

This effect also occurs in other years because a smaller part of the floodplain in the UR scenario falls within the recruitment band of 0 and 1 meter above BGL (Table 4.3). It is interesting to see that the initial higher vegetation coverage in the UR scenario did not result in higher channel shifting rates. The more dynamic behaviour of the Default scenario resulted eventually in higher seedling recruitment rates which in turn resulted in a higher vegetation coverage. Apparently the higher uproot resistance of the vegetation in the UR scenario caused the river banks to be stabilised which reduced the river channel shifting rate. This is also the reason the US eventually has a higher vegetation coverage than the UR scenario, because its morphology is more dynamic which results in a wider recruitment band.

Figure 4.4b shows the overall yearly mortality rate per scenario and the mortality rates per process. It can be seen that the uproot resistant scenario has significantly lower uproot mortalities, which is to be expected. The default scenario has the highest yearly mortality rates, resulting from its relatively high seedling recruitment rate (see Figure 4.15). So even though the default scenario loses a larger percentage of its vegetation each year, this is compensated by the overall higher seedling recruitment rates.

4.4.3. Seedling growth

The seedling growth rate has a large impact on how fast a vegetation species colonizes the river bed, as can be seen in Figure 4.8. Looking at the fast growing seedlings (FGS) scenario, the vegetation cover is significantly higher in the first 20 years in comparison with the other two scenarios. As expected, a faster seedling growth rate results in higher seedling recruitment. Figure 4.9 shows the seedling development in the year 1968. At this moment, the bed levels of the different scenarios are still more or less the same, which allows for a good comparison in the seedling development between the scenarios. A faster growth rate gives seedlings a clear advantage against uprooting, burial and drought mortalities. At the end of the seed dispersal period, this results in a higher seedling coverage. Looking at the seedling development from mid-July and onwards it can be seen that the fast growing seedlings have a significantly higher coverage at the end of the year (Fig. 4.9b). However, the higher seedling growth rate in the FGS scenario does not give the seedlings a higher flood resistance, which explains the significant flooding mortalities in the winter period.

The seedling growth rate also has a large influence on the morphology. The fast colonisation in the FGS scenario leads to a very static river. The average value of the 15 highest observed yearly channel shifting rates is 6 m/year for the FGS scenario which means that no large channel shifts have occurred in the 52 years modelling time. In FGS scenario the river banks are rapidly colonised by vegetation which protects the river banks against erosion. This gives the river channel a very static behaviour and leads to narrowing of the river channel. However, this narrowing of the river channel in the FGS scenario has less effect on the vegetation cover, because the fast-growing seedlings can settle much higher above the groundwater level. (Table 4.3). Slow-growing seedlings have less effect on morphology because the recruitment band and channel shifting rates

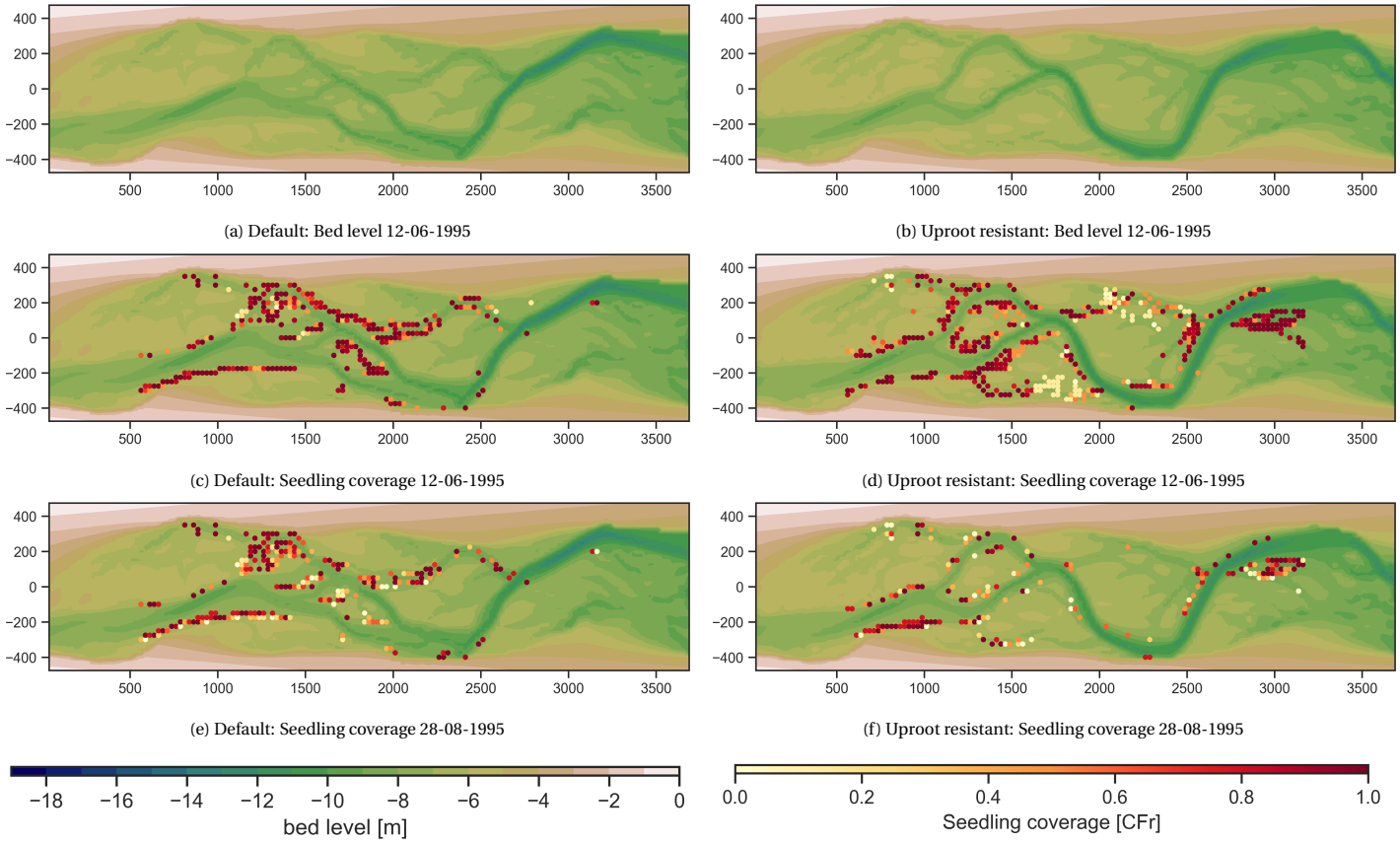

(a) Default: Bed level 12-06-1995

(b) Uproot resistant: Bed level 12-06-1995

(c) Default: Seedling coverage 12-06-1995

(d) Uproot resistant: Seedling coverage 12-06-1995

(e) Default: Seedling coverage 28-08-1995

(f) Uproot resistant: Seedling coverage 28-08-1995

(g) Bed level legend

(h) Seedling coverage legend

Figure 4.7: The bed levels and seedling coverage at 12-6-1995 for the default (a,c) and uproot resistant (b,d) scenarios. Figures e and f show the seedling coverage at 28-08-1995 after most of the drought mortalities in the year 1995 have occurred. The seedling coverage is shown as fraction of a Delft3D FM cell (CFr).

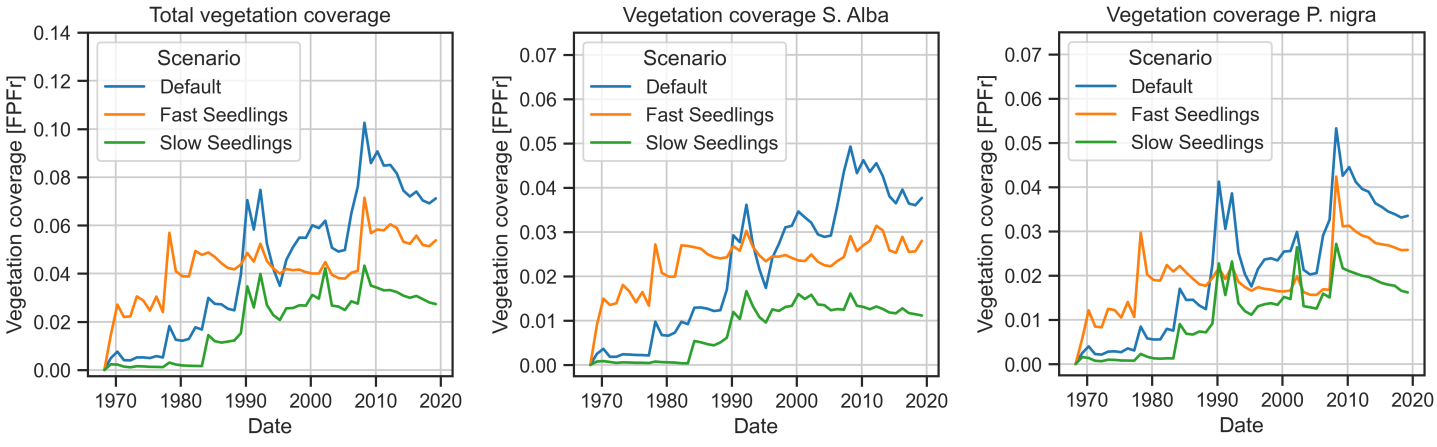

(a) Total coverage

(b) *S. alba* coverage

(c) *P. nigra* coverage

Figure 4.8: The vegetation coverage of the for the different seedling growth scenarios. Figures (b) and (c) show the vegetation coverage subdivided by the vegetation species *S. alba* and *P. nigra*

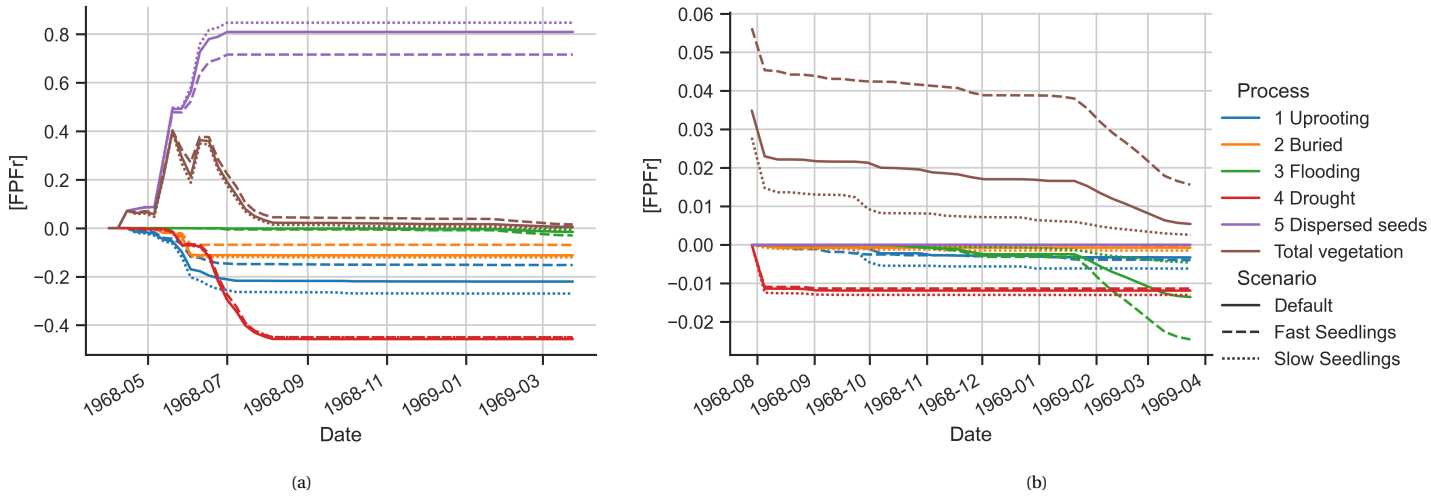

(a) (b)

Figure 4.9: Figure (a) shows the seedling development in time from 1-4-1968 till 1-4-1969. The brown lines shows the seedling coverage over time as a fraction of the floodplain (FPFr). The blue, orange, green en red lines represent the the cumulative removal of vegetation in FPFr, where the purple line represent the cumulative seed deposition. The continuous lines denote the default scenario, the dashed lines denote the fast-growing seedlings scenario and the dotted lines denote the slow-growing seedlings scenario. Figure (b) shows a detailed section of figure (a). The cumulative sum in figure (b) is calculated from 27-07-1968.

are similar to those of the default scenario. (Table 4.3). However, the slow growth of the seedlings leads to a significantly lower seedling recruitment rate (Fig. 4.15). This eventually leads to half the vegetation coverage than in the default scenario.

4.4.4. Seed dispersal

Figure 4.10 shows the vegetation coverage over time for the default scenario and the two different seed dispersal period scenarios. Only looking at the total vegetation coverage (Figure 4.10a) no large differences are seen till around the year 2005. However when looking at the species *S. alba* and *P. nigra* separately, there are significant variations in coverage. In the case of separate dispersal periods especially the coverage of the *S. alba* is heavily influenced by reducing the seed dispersal period to only the month May.

Figures 4.11a and 4.11b show the seedling development of both species in the year 1977, the moment that the first differences in coverage occur. The figures show that the moment of dispersal has a large influence on the seedling coverage. In the case of separate dispersal the *S. alba* trees only releases seeds in May, which gives the *S. alba* a clear disadvantage because of the high discharges at the begin of June (see Fig. 4.12). These high discharges causes high seedling mortalities. By the end of June most of the *S. alba* seedlings have died in the separate dispersal (SD) scenario. This is in contrast with the default and equal dispersal (ED) scenarios, which still have *S. alba* recruitment till respectively 15 June and 1 July (Table 4.1).

The SD scenario shows a higher seedling coverage than the default scenario for *P. nigra* species at the end of March 1978 (Figure 4.11b). Even when considering the fact that the seed dispersal period for the *P. nigra* species starts later in the year and is also shorter in the SD scenario. This difference is caused by how seedling recruitment is incorporated in the vegetation model. Consider for example a Delft3D FM cell has become dry during a time that both the *S. alba* and the *P. nigra* disperse their seeds. The available free space in that cell is then shared equally between both species. This differs when for instance only the *P. nigra* species disperses it seeds, in that case the Delft3D FM cell is filled for 80 percent with *P. nigra* seedlings. The 80 percent corresponds with the maximum area fraction a vegetation species can occupy in a Delft3D FM cell (see Sec. 2.4.1 and Table 2.1). In the SD scenario a higher amount of *P. nigra* seedlings are dispersed, which explains the higher *P. nigra* coverage for the SD scenario in Figure 4.11b

From 2005 onwards, the vegetation coverage of the SD scenario becomes suddenly larger than the other two scenarios. The year 2005 has an ideal discharge regime for seedling recruitment, as the discharge decreases gradually during the months May and June (Figure 4.12). Especially the SD scenario benefits from this ideal discharge regime, due to the differences in bed levels between the scenarios. Figure 4.13 shows bed levels of

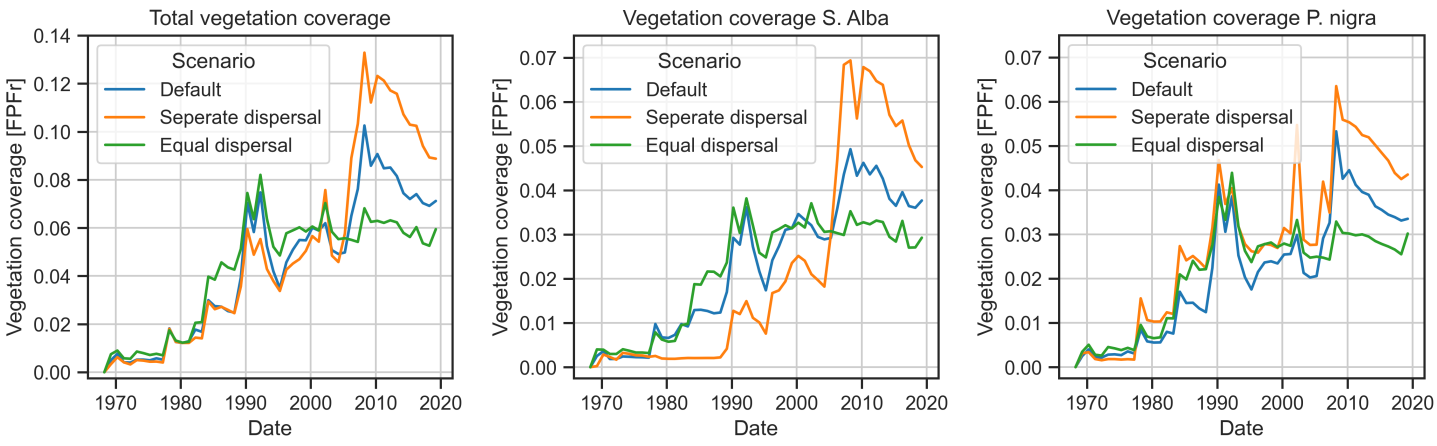

(a) Total coverage

(b) *S. alba* coverage

(c) *P. nigra* coverage

Figure 4.10: The vegetation coverage of the for the different seed dispersal scenarios. Figures (b) and (c) show the vegetation coverage subdivided by the vegetation species *S. alba* and *P. nigra*

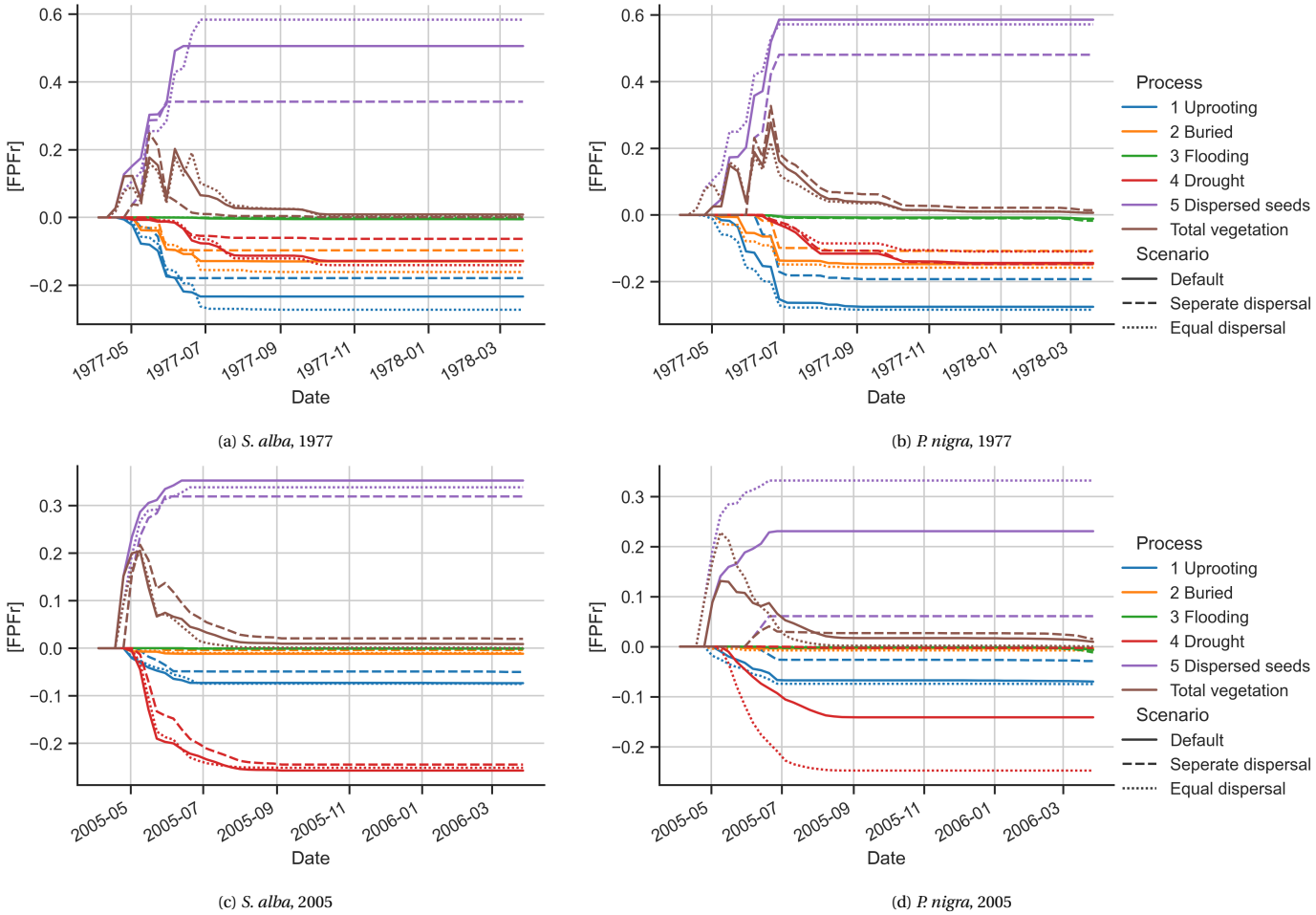

(a) *S. alba*, 1977

(b) *P. nigra*, 1977

(c) *S. alba*, 2005

(d) *P. nigra*, 2005

Figure 4.11: Seedling development of the default, separate dispersal and equal dispersal scenarios for two different years. The figures show the seedling development in time from 1-4-1977 till 1-4-1978 (a,b) and 1-4-2005 till 1-4-2006(c, d) for the *S. alba* and *P. nigra* species. The brown lines shows the seedling coverage over time as a fraction of the floodplain (FPFr). The blue, orange, green en red lines represent the the cumulative removal of vegetation in FPFr, where the purple line represent the cumulative seed deposition. The continuous lines denote the default scenario, the dashed lines denote the separate dispersal scenario and the dotted lines denote the equal dispersal scenario.

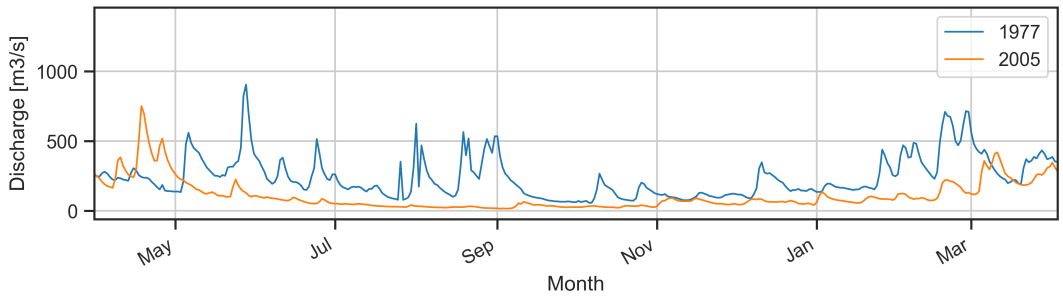

Figure 4.12: Discharge between 1-4-1977 and 1-4-1978 (blue), and between 1-4-2005 and 1-4-2006 (orange).

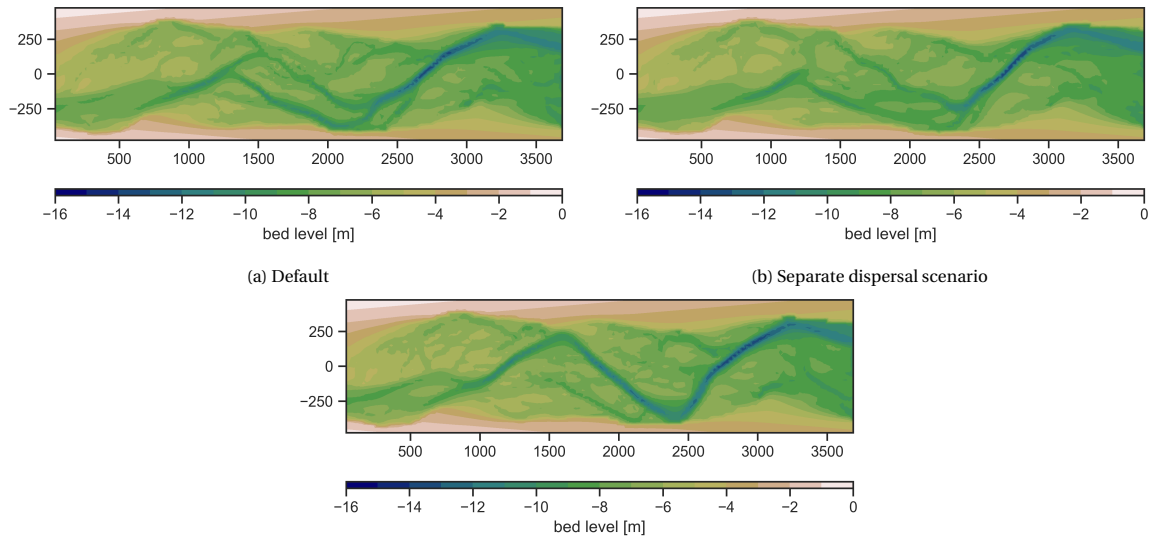

(a) Default

(b) Separate dispersal scenario

(c) Equal dispersal scenario

Figure 4.13: The bed level at April 2005 for the Default, Separate dispersal and Equal dispersal scenarios

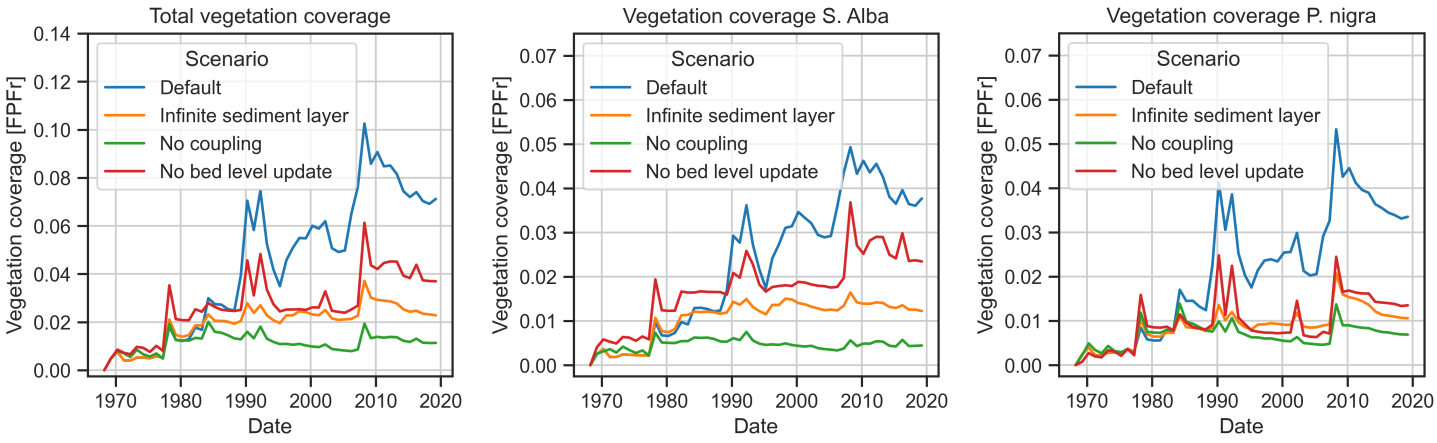

(a) Total coverage

(b) *S. alba* coverage

(c) *P. nigra* coverage

Figure 4.14: The vegetation coverage over time for the different morphology scenarios. Figures (b) and (c) show the vegetation coverage subdivided by the vegetation species *S. alba* and *P. nigra*.

all three scenarios in April 2005. It can be seen that the SD scenario has more gradual river bank slopes in comparison with the other two scenarios, especially the ED scenario. This results in a larger recruitment area for the SD scenario, as 28 percent of the floodplain bed area is between 0 and 1 meter above BGL in 2005. For the default and ED scenarios this is respectively 24 and 15 percent. Those more gradual slopes give the SD scenario an advantage against drought stresses.

The discharge regime in 2005 explains the high seedling recruitment of the *S. alba* species (Figure 4.12). In comparison with the year 1977, this time a larger part of the *S. alba* seedlings recruited in the month May is able to survive. This is largely due to the lack of high discharges in the month June. The lower discharges also cause drought stresses, but are less problematic in the SD scenario due to the more gradual river banks.

It is also interesting to see that even while the total amount of seed dispersal of the *P. nigra* species is significantly lower for the SD scenario, the SD still has the largest *P. nigra* seedling recruitment in 2005. This is again caused by the fact that the SD scenario has significantly lower drought stresses. Because most of the *P. nigra* seedlings that are dispersed before June in the default and ED scenarios die due to drought stresses. This is especially true for the ED scenario, which has the steepest river banks and therefore the highest drought mortalities.

4.4.5. Morphology

As seen in the earlier sections, morphology and vegetation interact strongly with each other. This section shows the results of the three different morphology scenarios as defined in section 4.2.5. Due to the differences between each scenario, the scenarios are treated separately.

The vegetation coverage in the Infinite sediment layer (ISL) scenario shows relatively similar vegetation development in the first 15 years as the default scenario (Figure 4.14). After that period the vegetation cover of the ISL scenario stays around 0.025 FPFr. This is because around 1983 the default scenario hits the bottom of the initial sediment layer. Because the channel cannot erode any further, it initiates erosion of the river banks which eventually leads to the forming of new channels (Fig. 4.16). Around 1993 only a few cells touch the bottom of the sediment layer. However, in the ISL scenario the erosion is not stopped by the sediment layer which deepens the river channel. This deepening prevents the forming of new channels and causes the channel to become very static. This steepens the riverbanks which also reduces the places where seedlings can survive. This also explains the low seedling recruitment and therefore the low vegetation coverage in the ISL scenario.

The default scenario with the sediment thickness layer displays a more dynamic and therefore more natural morphology than the ISL scenario. A possible reason for this is that in the Delft3D FM model a uniform

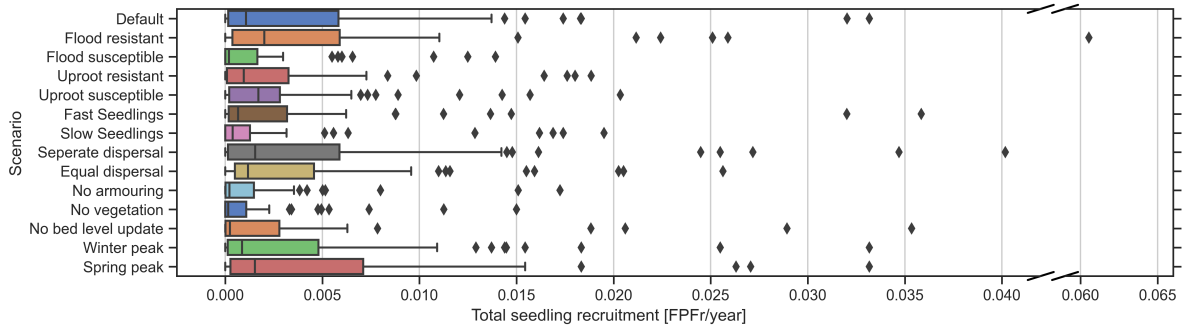

Figure 4.15: The distribution of yearly seedling recruitment rate in fraction of the floodplain per year [FPFr/year]. The shown seedling recruitment rate is the cumulative seedling rate of both the *S. alba* and the *P. nigra* species. Within each box, the black line denote the median value; boxes extend from the 25th to the 75th percentile of the distribution of values; vertical extending lines denote adjacent values (i.e., the most extreme values within 1.5 interquartile range of the 25th and 75th percentile of each group); dots denote values outside the range of adjacent values.

sediment fraction is used. This is a simplification that makes it impossible to model the morphological process of bed armouring. Armouring of the river bed is a process where the combination of different sediment fractions can make the river bed immobile and thus resistant to erosion. This happens when the smaller sediment fractions are eroded by the flow from the river bed, while the larger and heavier fractions stay behind on the river bed. This creates a non-erodible layer of sediment that acts as a armour layer for the sediment below. This process of armouring is also observed in the Allier River (Kleinhans et al., 2002). The bottom of the sediment layer in the default scenario prevents erosion of the deepest parts of the main river channel and acts therefore as a kind of armour layer, which could explain why the default scenario shows a more realistic river pattern.

The No coupling (NC) scenario shows the importance of the coupling between vegetation and morphology. The NC scenario has the lowest vegetation coverage, which is caused by a combination of very low seedling recruitment rates and high mortalities due to flooding and uprooting (Figures 4.15 and 4.4c). Due to the uncoupling between the vegetation model and Delft3D FM, the vegetation is unable to influence the river flow, which explains the higher mortality rates. As a result, the vegetation can only survive at the higher levels of the riverbanks, because at the lower levels it is too vulnerable to the river flow. The existing vegetation is also unable to protect the younger and therefore weaker vegetation. The result is that seedlings can only survive at higher levels (Table 4.3). However, this is an unfavourable place for seedlings because there they are more vulnerable to drought. This partly explains the lower seedling recruitment rates in the NC scenario. The other reason is that the morphology of the NC scenario shows little dynamics, resulting in steep river banks (Table 4.3), which is unfavourable for the seedling recruitment rate.

Looking at the scenario without bed level updates (NBLU) the vegetation coverage in the first 15 year is higher than in the default scenario. This caused by the fact that the vegetation in the NBLU scenario has an advantage over the default scenario, because the mortality processes uprooting and burial do not occur. However, the static bed levels in the NBLU scenario eventually become a disadvantage at the moment the default scenario develops multiple river channels. Those new river channels create new habitat for the vegetation to establish itself, which eventually increases the recruitment of new vegetation. Eventually the static morphology in the NBLU scenario causes the seedling recruitment rate to drop, which diminishes the advantage of no uprooting and burial mortalities.

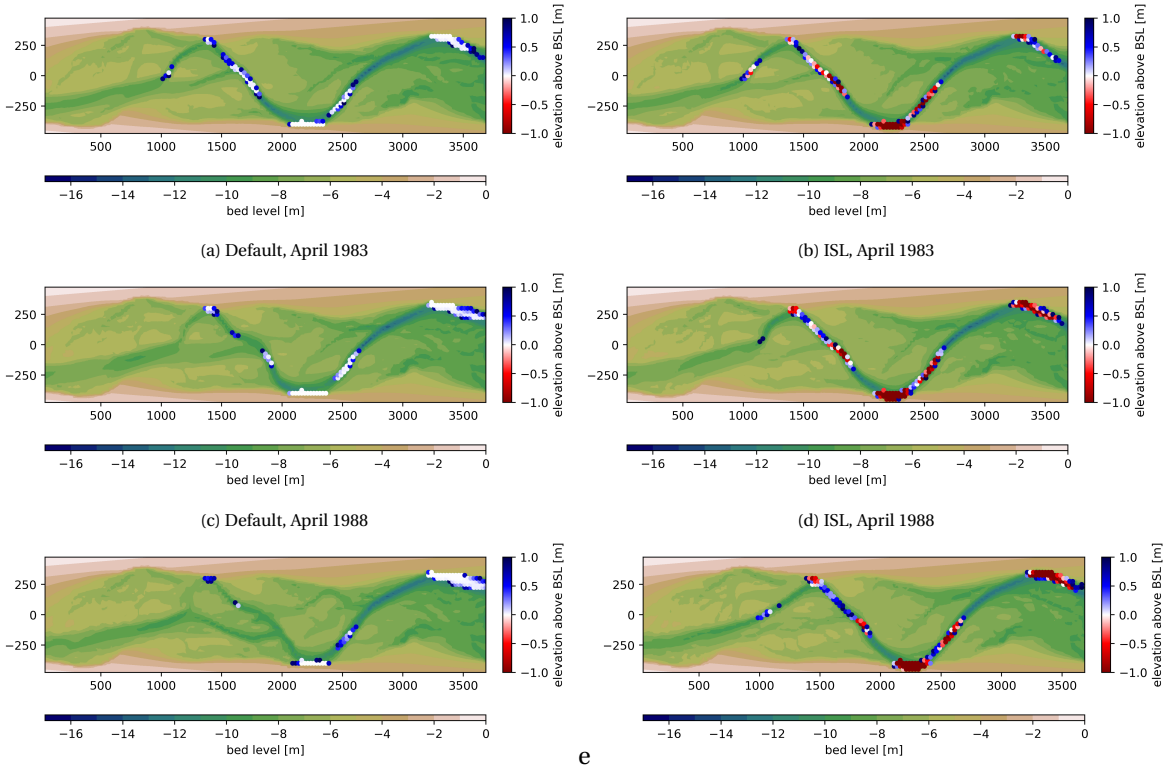

(a) Default, April 1983

(b) ISL, April 1983

(c) Default, April 1988

(d) ISL, April 1988

(e) Default, April 1993

e

(f) ISL, April 1993

Figure 4.16: The figures show the bed levels of the default and ISL scenarios. The dots represents the elevation above the bottom of the sediment layer (BSL). Only the cells are shown where the elevation above BSL is below 1 meter.

Parameter	Unit	Default	FR	FS	UR	US	FGS	SGS	SD	ED	ISL	NC	NBLU
Median vegetation coverage[1]	FPFr	0.067	0.08	0.019	0.039	0.052	0.043	0.029	0.089	0.059	0.023	0.011	0.03
Median *P. nigra* coverage[1]	FPFr	0.036	0.042	0.01	0.019	0.036	0.025	0.013	0.046	0.031	0.014	0.004	0.019
Median *S. alba* coverage[1]	FPFr	0.031	0.039	0.009	0.019	0.015	0.019	0.016	0.042	0.028	0.01	0.007	0.011
Mean bed level fraction between 0 and 1 meter above BGL[1]	FPFr	0.19	0.18	0.14	0.16	0.18	0.11	0.19	0.19	0.17	0.13	0.1	0.14
Median *S. alba* germination height above BGL[1,2]	m	0.43	0.47	0.51	0.48	0.43	0.78	0.33	0.42	0.43	0.64	0.62	0.64
Median *P. nigra* germination height above BGL[1,2]	m	0.56	0.56	0.6	0.64	0.52	1.1	0.37	0.57	0.57	0.84	0.92	0.64
Median *S. alba* height above BGL[1]	m	0.92	1.03	0.89	1.02	0.86	1.45	0.95	0.87	1.04	1.23	1.57	0.89
Median *P. nigra* height above BGL[1]	m	1.12	1.27	1.05	1.28	1.06	1.59	1.09	1.05	1.23	1.5	1.62	1.08
Mean shifting rate[3]	m/year	23	35	14	15	18	6	26	22	19	8	7	4

[1] first 25 years are excluded from the dataset as the vegetation is still developing in those years

[2] of the seedling surviving their first year

[3] average over the fifteen highest observed yearly shifting rate values

Table 4.3: Statistics of vegetation and morphodynamic parameters values for all scenarios in the sensitivity analysis. The scenarios are: default, flood resistant (FR), Flood susceptible (FS), uproot resistant (UR), uproot susceptible (US), fast growing seedlings (FGS), slow growing seedlings (SGS), separate seed-dispersal period (SD), equal seed-dispersal period (ED), infinite sediment layer (ISL), no coupling (NC) and no bed level update (NBLU).

5

Extreme discharge events

As stated in section 1.1 most river discharge regimes will be impacted by climate change in future. It is expected that there will be an increase in frequency and intensity of heavy rainfall events over many land areas (IPCC, 2014). Studies found that this could lead to an increase of extreme flood events (Hirabayashi et al., 2013; Van Vliet et al., 2013; Schneider et al., 2011). In this chapter the effect of an extreme flood event on the riparian vegetation coverage and morphology will be investigated.

To investigate the effect of extreme discharge events, the same Allier model schematization is used as the previous chapters. To simulate such an event, a manually generated extreme discharge event is used. This discharge event is not directly based on the predicted change in discharge regime due to climate change for the Allier catchment. The purpose of this study is to investigate the effects of an extreme discharge event and it falls outside the scope of this study to investigate the precise climate change effects on the river Allier.

5.1. Scenarios

To investigate the effect of an extreme flood two different scenarios are examined. Each scenario is based on the default scenario but has one extra flood added to its hydrograph. The first scenario has its extreme flood in the spring of 1997 and the second scenario has its extreme flood in the winter of 1997 (Figure 5.1). The year 1997 is selected because at that time the vegetation has established itself in the model. Two scenarios are used to see if a different timing of the extreme flood has an effect on the results.

To create a realistic extreme discharge event for the Allier river data of historic peak discharges were used. The highest measured peak discharges for the Allier river occurred in the 19th century and were around 1,900 m3/s Gautier et al. (2000). This maximum value is then used to create a extreme flood event. This is done by taking a flood-wave in 1984 and intensify this flood-wave by a factor 1.5 so its peak becomes equal to 1,900 m3/s.

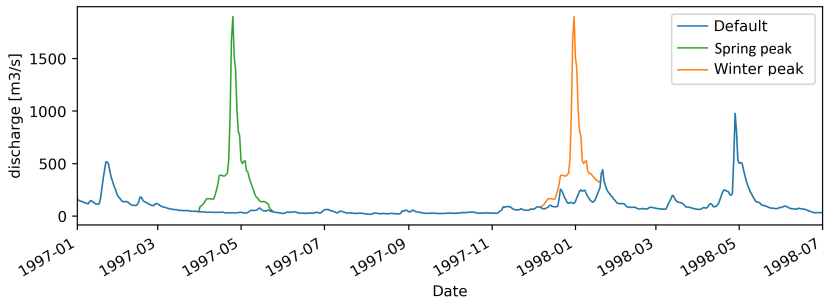

Figure 5.1: The peak discharges used in the Winter peak and Spring peak scenarios. Except for the additional discharge peak, both scenarios are similar to the default scenario.

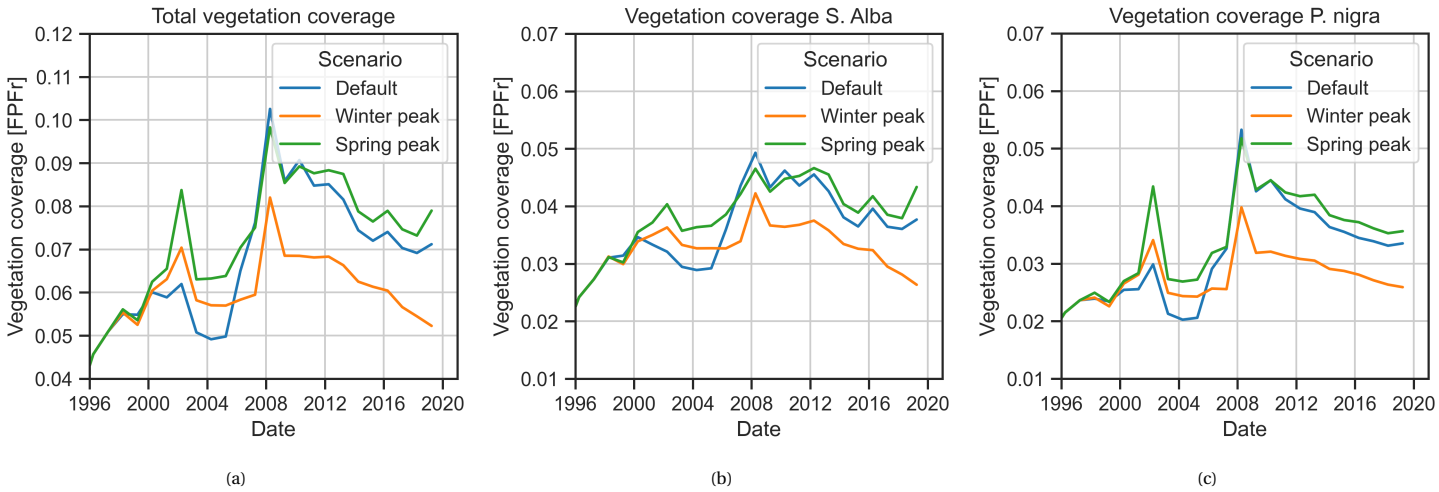

Figure 5.2: The total vegetation coverage in ha for the different extreme flood scenarios (a). Figures (b) and (c) show the vegetation coverage subdivided by the vegetation species *S. alba* and *P. nigra*

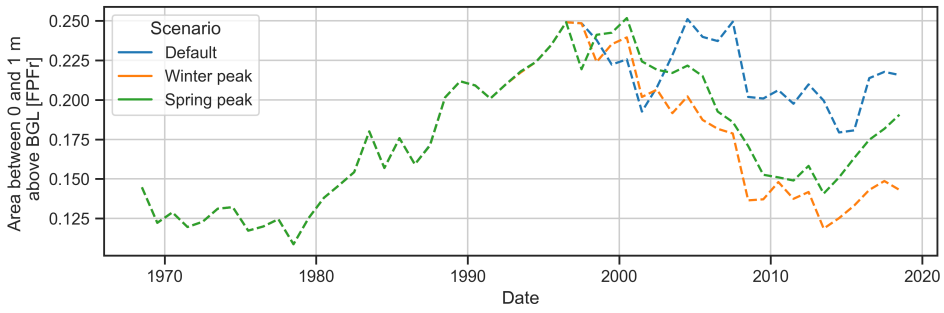

Figure 5.3: The size of the recruitment band in time. The recruitment band is defined as the fraction of the floodplain between 0 and 1 meter above base-flow groundwater level (BGL).

5.2. Results

Figure 5.2 shows the vegetation coverage for the default scenario and the spring and winter peak scenarios. The floods do not have a direct impact on the vegetation coverage, as almost no change in vegetation coverage can be seen in 1997 (year of flood peak). However, in the long term the extreme flood event does have an impact on vegetation coverage. Around the year 2000 there is an increase in vegetation coverage for both floods scenarios, while this increase is not seen in the default scenario. Around 2007 the vegetation coverage of the spring peak scenario shows more or less the same vegetation coverage as the default scenario. This is caused by a steep increase in the vegetation coverage in the default scenario after 2005 and onwards. The winter peak scenario shows after 2006 a lower vegetation coverage than the default scenario.

This difference in vegetation coverage is largely caused by differences in the morphology between the scenarios. This can be best showed by looking at the size of the recruitment band, i.e., the fraction of the floodplain elevation above 0 and 1 meter BGL (see Fig. 5.3). While both peak scenarios show an initial decrease of the recruitment band size directly after the extreme peaks, the recruitment band size quickly increases in the following years. Around 2000 the recruitment band is in both peak scenarios larger than in the default scenario which gives them an advantage in the recruitment of new seedlings.

The difference in vegetation coverage directly after 2000 can be seen most clearly in the vegetation coverage development of the *S. alba* species. Both peak scenarios show an increase in *S. alba* coverage while the default scenario shows a slight decrease. Figure 5.4a shows for all the three scenarios the seedling development of the *S. alba* species in the year 2000. At the beginning of July the seedling coverage is similar for each scenario. In July and August a part of the seedlings die due to drought. Especially the seedlings in the default scenario are prone to drought, which is to be expected due to the smaller size of the recruitment band in 2000. Figure

5.5 shows the water levels at the start of July, at that moment the discharge is around 40m^3/s. The figure also shows the cells of the floodplain that are situated between 0 and 1.5 m above groundwater level. It can be seen that in both peak scenarios a second northern river channel is formed. Because of this secondary channel, the groundwater levels of both extreme flood scenarios are higher, especially in the surrounding area of the northern channel. This results in significant lower drought mortalities in both peak scenarios, especially for those located in the region around the northern channel (Fig. 5.6). Eventually, this lead to higher seedlings seedling survival rates in both peak scenarios, and explains the increase in vegetation coverage.

The fast colonisation of vegetation in both peak scenarios eventually affects the morphology. In both peak scenarios the southern river channel is eventually colonised by vegetation. This colonisation leads to sedimentation in the southern river channel which eventually forces most of the river flow through the northern channel (Fig. 5.8). This abandonment of the southern river channel reduces leads to a reduction of the recruitment band size in both peak scenarios, which continues until 2015.

The reduction of the recruitment band size in the peak scenarios has an effect on the seedling recruitment rate. In the year 2005 the default scenario has the highest seedling recruitment and shows a large increase in the vegetation coverage. The larger seedling recruitment in the default scenario can be explained due to its larger size of the recruitment band (see Fig. 5.3). This results in lower seedling mortalities due to drought in the default scenario (Fig. 5.4b). Both peak scenarios have a lower recruitment band size than the default scenario, resulting in higher drought mortalities. However, the spring peak scenario has two main differences with the Winter peak scenario, explaining its higher seedling recruitment. The first difference is that the size of the recruitment band is larger for the spring peak scenario, which results in slightly lower drought mortalities (Fig. 5.4b). The second difference is that the southern river channel becomes dry during the seed dispersal period. This means that seeds are dispersed on the lowest parts of the southern channel river bed (see Fig. 5.7c). Those seedlings at the lowest parts of the southern channel river bed grow in a relatively safe area, due to the lack of current in this river channel section. The seedlings in the southern channel are also less likely to die as a result of drought, as they are dispersed on the lowest part of the river bank, close to the water groundwater level. In conclusion, the larger recruitment band in combination with the lower mortality risks in the southern channel ensures a higher survival rate of the seedlings in the spring peak scenario than in the winter peak scenario (Figures 5.4b and 5.7)

The results show no large effect on the vegetation coverage directly after the modelled extreme floods. The results also show that both extreme flood events have a positive effect on the vegetation cover in the years after the flood event. However a large part of this colonisation takes place in the southern river channel. This leads to sedimentation in the southern river channel and eventually forcing most of the river through the northern channel. This eventually leads to a decrease of the recruitment band in the peak scenarios and therefore to lower seedling recruitment rates. The results also show that a smaller recruitment band does not necessarily lead to a lower vegetation cover. After all, the spring peak scenario shows the same high vegetation cover as in the standard scenario, which is mainly due to the successful colonization of the southern channel.

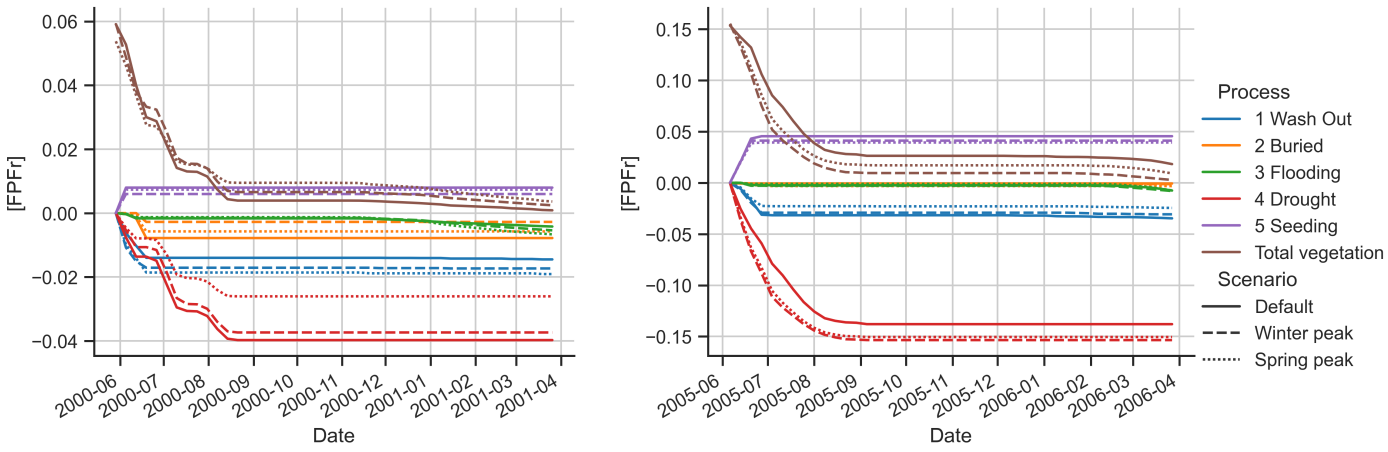

(a) *S. alba*, 2000

(b) *S. alba* and *P. nigra* combined, 2005

Figure 5.4: The seedling development of the *S. alba* species starting at 1-6-2000 (a) and the seedling development of the *S. alba* and *P. nigra* species combined starting at 1-6-2005 (b). The brown lines shows the seedling coverage over time as a fraction of the floodplain (FPFr). The blue, orange, green en red lines represent the the cumulative removal of vegetation in FPFr, where the purple line represent the cumulative seed deposition. The continuous lines denote the default scenario, the dashed lines denote the winter peak scenario and the dotted lines denote the spring peak scenario.

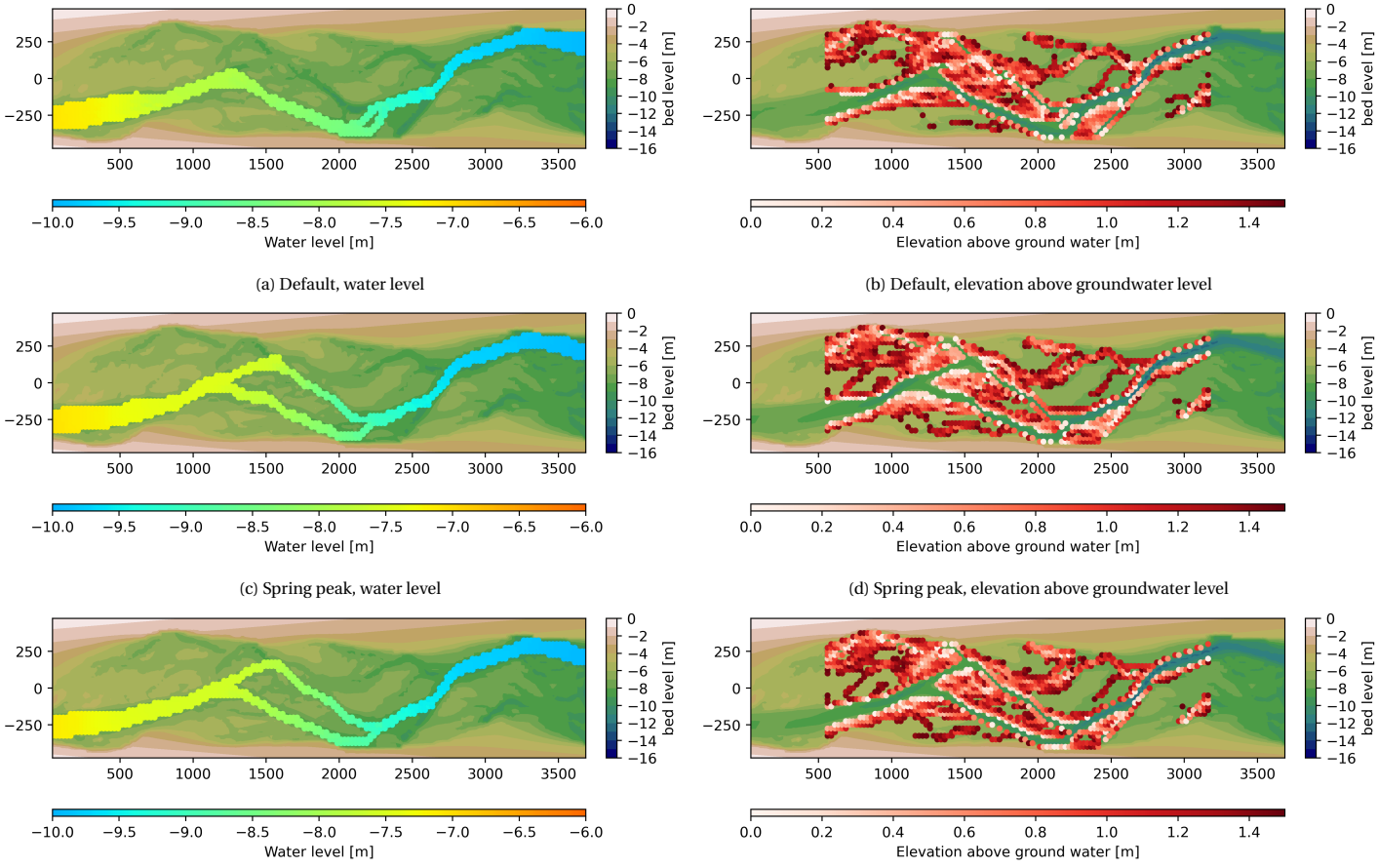

(a) Default, water level

(b) Default, elevation above groundwater level

(c) Spring peak, water level

(d) Spring peak, elevation above groundwater level

(e) Winter peak, water level

(f) Winter peak, elevation above groundwater level

Figure 5.5: The water levels (a,c and e) at 3-7-2000 for the Default, Spring peak and Winter peak scenarios. The discharge is around 40m^3/s. Figures b,d and f shows the areas of the floodplain that are between 0 and 1.5 meter above the groundwater level at 3-7-2000.

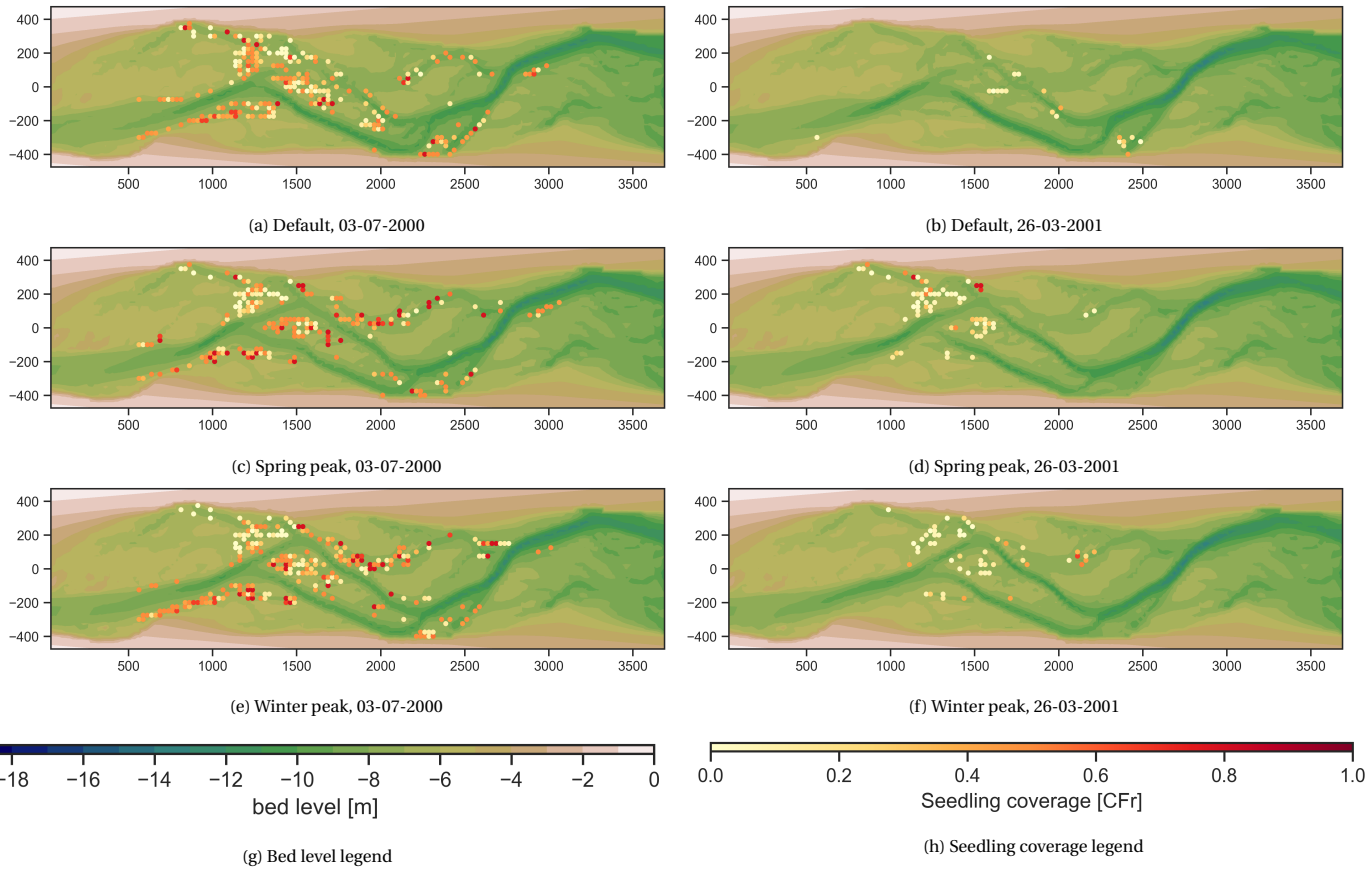

(a) Default, 03-07-2000

(b) Default, 26-03-2001

(c) Spring peak, 03-07-2000

(d) Spring peak, 26-03-2001

(e) Winter peak, 03-07-2000

(f) Winter peak, 26-03-2001

(g) Bed level legend

(h) Seedling coverage legend

Figure 5.6: The seedling coverage of the *S. alba* species at 03-07-2000 and 26-03-2001. The seedling coverage is shown as fraction of a Delft3D FM cell (CFr).

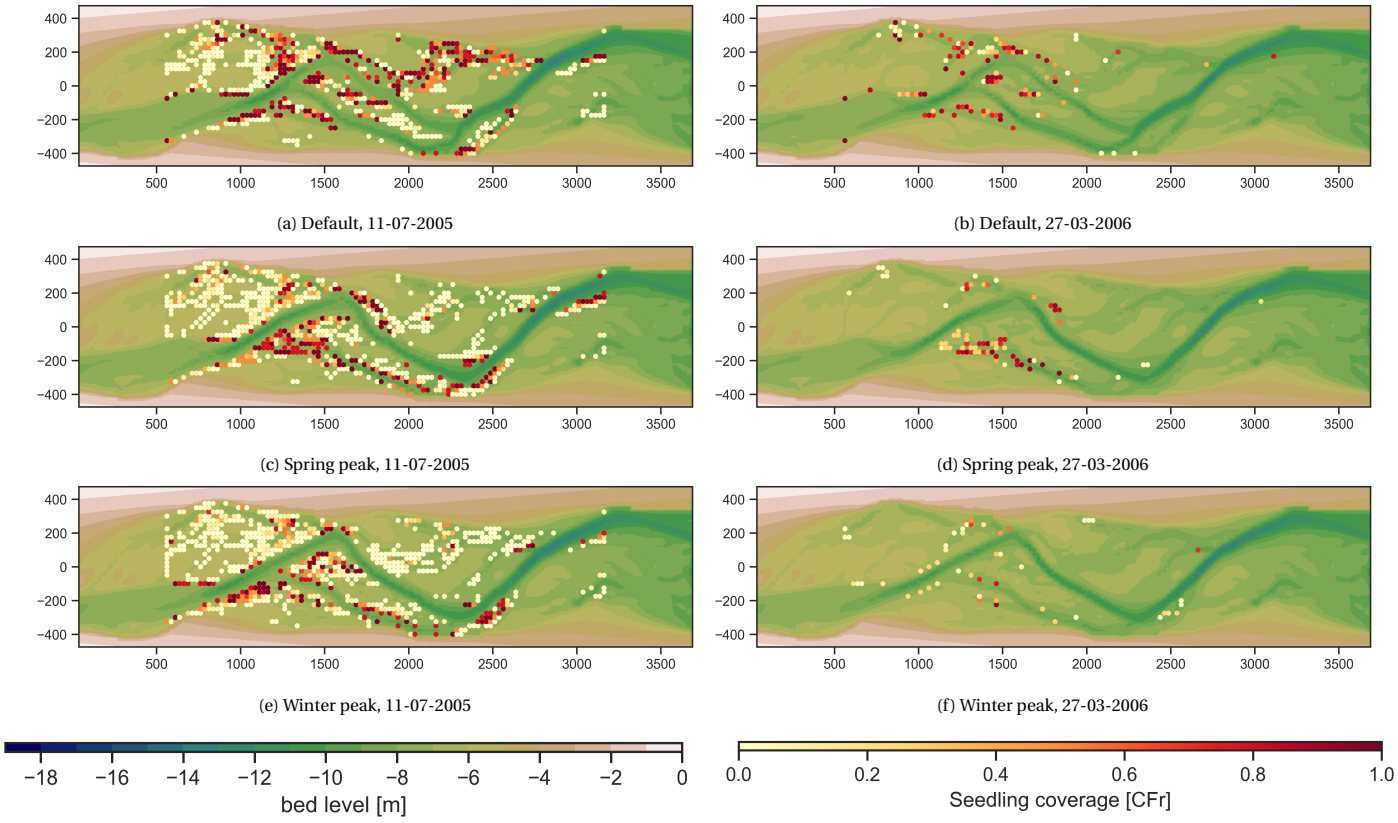

(a) Default, 11-07-2005

(b) Default, 27-03-2006

(c) Spring peak, 11-07-2005

(d) Spring peak, 27-03-2006

(e) Winter peak, 11-07-2005

(f) Winter peak, 27-03-2006

(g) Bed level legend

(h) Seedling coverage legend

Figure 5.7: The total seedling coverage of the *S. alba* and *P. nigra* species combined at 11-07-2005 and 27-03-2006. The seedling coverage is shown as fraction of a Delft3D FM cell (CFr).

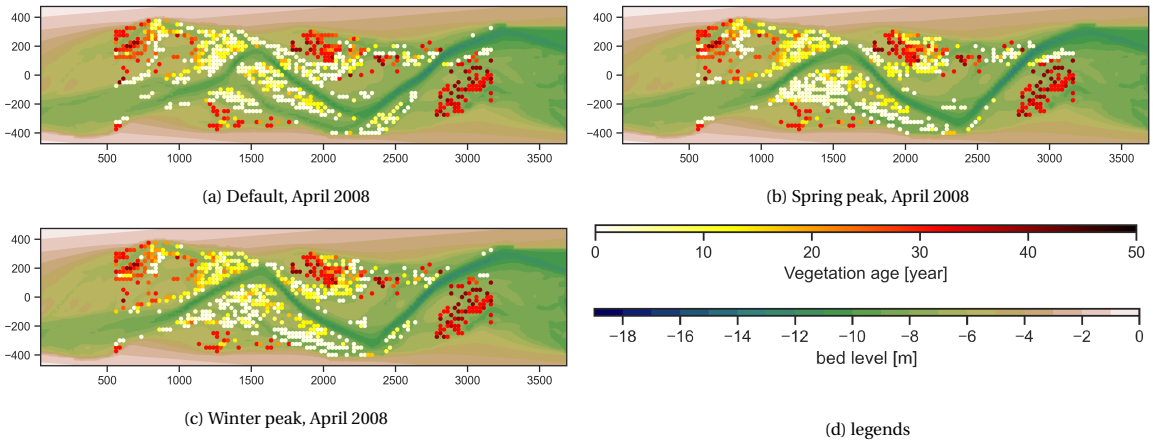

(a) Default, April 2008

(b) Spring peak, April 2008

(c) Winter peak, April 2008

(d) legends

Figure 5.8: The vegetation age in April 2008 for the default and the extreme discharge scenarios. The vegetation age is calculated as the weighted average of all the existing vegetation in a Delft3D FM cell.

6

Discussion

In order to critically reflect on the results presented in the previous chapters and to contrast these findings to riparian vegetation studies, the discussion has been separated into three main sections. The first main section discusses the results of the vegetation model. This section consists of three sub-sections and discusses: 1) the results of the default run and the sensitivity analysis, 2) the results of the extreme discharge events and 3) the simplifications within the vegetation model. The second main section discusses the morphological model. Third and final, the model applicability for end-users is discussed.

6.1. Vegetation modelling

6.1.1. General

In this study a process-based approach is used to develop the vegetation model. Vegetation properties such as drought and flooding thresholds are based on existing literature as much as possible, in order to get a realistic representation of vegetation behaviour in the model. This approach differs from the model developed by Van Oorschot et al. (2016), in which the mortality thresholds are parametrized to broadly fit the age distribution of pioneer, bush and forest vegetation as deduced by Geerling et al. (2006). The model used in this study uses a model-schematisation based on the Allier River and is not intended to describe the exact morphological behaviour of the Allier River. This means that there are differences in morphology between the river model and the actual Allier River. The results in this study showed that the vegetation coverage depends heavily on the combination of the occurring discharge and morphology of the river, which makes it difficult to compare field observations directly with the model results. The model can, however, be used to gain insight into how a river system reacts to, for example, extreme discharge events, different discharge regimes, and the introduction of invasive species.

The results show that natural vegetation patterns arise from the modelled interaction between dynamic vegetation and morphodynamics. The age distributions in the floodplains found in this study are similar to those found in the field (Van Oorschot et al., 2016): 1) young vegetation is mostly found on the lower areas near the channels and 2) older vegetation is found on the higher parts of the floodplains, further away from the channels. This is a realistic result considering that new vegetation can only establish itself at places where its short roots can reach the groundwater level. Because the groundwater level is directly related to the occurring water level(Mahoney and Rood, 1998), those places are often close to the river channel. The results show that new vegetation colonises at elevations of 0 to 1 m above base-flow groundwater levels (BGL), which is in correspondence with those observed in the field (Rivaes et al., 2013; Mahoney and Rood, 1998). Once established, Salicacea species are known for efficiently collecting sediment, creating sedimentation at places with vegetation (Corenblit et al., 2009). This means that older vegetation will eventually occur at a higher levels above BGL, which is also shown in this study (Table 4.3).

Results show that seedling survival throughout the first summer is low. The vast majority of seedlings die due to drought stresses. The surviving seedlings do so because their roots are able to reach the groundwater table. The discharge directly after the seed germination determines the seedling's survival chances, if the

water table decline is too fast high seedling mortalities occur due to drought (eg. Fig 3.5). However, discharge peaks directly after the seed germination can cause high uprooting, burial and flooding mortalities. These results are in line with field observations and previous studies, which found that drought is indeed the most important seedling mortality cause but that river disturbances just after germination lead to even higher seedling mortality rates due to uprooting and flooding (eg. Mahoney and Rood (1998); Karrenberg et al. (2002); Corenblit et al. (2014); Scott et al. (1997b)).

This research shows that detailed seedling growth is important to correctly model the survival chances of a seedling. Older and therefore larger seedlings are more resistant to mortality processes such as burial, uprooting and drought. By including a detailed simulation of seedling growth in their first year, it is now possible to take this higher resistance of older seedlings into account. This is a step forward in vegetation colonization modelling compared to other advanced vegetation modelling studies that did not take seedlings growth into account (Van Oorschot et al., 2016; Martínez-Fernández et al., 2018).

This study confirms that it is important to include multiple species when modelling riparian vegetation, because each species has its own colonisation pattern. Due to its faster root growth, *P. nigra* species is able to colonise at higher elevations above BGL than the *S. alba* species. In turn, the *S. alba* species has a higher uproot and flood resistance, which gives it the ability to colonise at lower elevations above BGL. The modelled colonization height of these two species resembles the observed patterns of the Allier River, where *P. nigra* species indeed colonise on higher grounds and *S. alba* species colonise the more wetter lower parts of the floodplain (Hortobagyi, 2018).

Hortobagyi (2018) also found that the *P. nigra* species are the more dominant vegetation, and occurs in larger quantities in the Allier River. This is in contradiction with the results found in this study, where the coverage of the *S. alba* and *P. nigra* species is relatively the same. This could be due to the fact that for the *P. nigra* species a too low flood mortality threshold is used in this study. No flood mortality threshold for adult *P. nigra* trees could be found in literature (see Sec. 2.2.5), therefore an estimation had to be made. This means that this flooding threshold bears some uncertainties and it is a possibility that the chosen value is an underestimation.

The sensitivity analyses shows that the vegetation coverage is sensitive to variations in the vegetation properties. The results shows that an increase in vegetation coverage generally leads to an increase the dynamics of the river system (Table 4.3). The inclusion of riparian vegetation leads to the formation of river islands, secondary channels and chute cut-offs, while scenarios with little or no vegetation result in a static channel. The fact that riparian vegetation increases the dynamic behaviour of a river is consistent with other research that has shown that riparian vegetation can play an important role in maintaining a dynamic morphology (Gurnell, 2014). Vegetation can act as so-called eco-engineers by creating pioneering landforms, such as small islands and natural levees (Francis et al., 2009; Gurnell et al., 2012). These pioneering landforms often give an impulse to riparian vegetation because they create new places where the vegetation can settle. If conditions are favourable, these pioneering landforms can develop into larger landforms such as benches, lateral bank extensions, islands, and lateral floodplain extensions (Gurnell, 2014). Riparian vegetation can thus receive positive feedback by increasing the river dynamics, which increases the number of favourable areas for the establishment of vegetation.

However, an increase in the river dynamics was not found in the case when the colonisation rate of the vegetation became high, as seen in the FGS scenario. In this scenario, the banks of the river are rapidly colonized due the higher growth rate of the seedlings. Because the riverbanks are quickly overgrown, the river channel becomes more or less static as the banks are protected against erosion by the vegetation. This is in line with flume experiments which showed that bank erosion rates decrease for increasingly vegetated banks (van Dijk et al., 2013). Field observations also found that rapidly growing (invasive) vegetation can cause braiding rivers to become less dynamic (Javernick, 2013). Even while this study uses a meandering river instead of a braiding river as case-study, still a reduction in dynamic behaviour of the river was found.

The analysis of using different seed dispersal periods shows that the length of the seed dispersal period in combination with the discharge has a major influence on the vegetation coverage. Seedlings need a gradually decreasing discharge to settle successfully and if this does not occur during the seed dispersal period they

cannot survive. The shortening of the seed dispersal period makes the vegetation even more sensitive to the occurring discharge. This can be seen in the development of *S. alba* coverage in the SD scenario, where the *S. alba* seed dispersal period is shortened to the month of May. In the first 35 years, *S. alba* coverage is therefore considerably lower than in the standard scenario, where the *S. alba* seed dispersal period lasts from mid-April to mid-June. Interesting to see is that shortening *P. nigra*'s seed dispersal period to only the month June in the SD scenario shows no significant effect for *P. nigra* coverage in the first 35 modelling years. This means that in the first 35 years the seedling survival changes are very small in the months before June. This changes, however, in the years 2005, 2006 and 2007, where a rapid increase of both *S. alba* and *P. nigra* species can be seen in the SD scenario. As a result, the total vegetation coverage of the SD scenario becomes suddenly higher than the default scenario, but this increase can also, partly, be explained by the larger recruitment band size of the SD scenario in these years. This shows that the successful seedling recruitment is closely related to the morphology, discharge and moment of seed dispersal.

6.1.2. Extreme flood events

The simulation of extreme floods shows an increase in the vegetation coverage in the years immediately after the extreme floods. Establishment of cottonwood 1-3 years following an flood has also been reported elsewhere (Friedman and Lee, 2002; Baker, 1990; Stromberg et al., 1991; Scott et al., 1997a; Kalischuk et al., 2001). An extreme flood provides an impulse to the dynamics of morphology, which in both scenarios leads to the forming of a secondary northern river channel. This creates more places where vegetation can settle which eventually results in a higher vegetation coverage in the years following the extreme flood.

In both flood scenarios the southern river channel becomes heavily colonised by vegetation. This leads to sedimentation in the southern channel and eventually results in the abandonment of the southern channel and a decrease of the recruitment belt (Figures 5.8 and 5.3). These results are in line with field observations which report a narrowing of the river channel due to the increasing vegetation coverage following a extreme discharge event(Friedman and Lee, 2002). However, the results in this study show that this narrowing is of a temporary nature, because in both cases the proportion of bed levels between 1 and 0 above BGL seems to rise again after 20 years after the flood. This indicates that the river channel is widening again.

While the long-term effects of extreme floods are well represented by the model, there is uncertainty in the ability of the model to simulate the direct effects of an extreme flood. The model results show little vegetation removal during an extreme flood, but these results are difficult to validate with field data. This is because there are not many studies on the direct effects of extreme discharge events on riparian vegetation. An extreme discharge event is unpredictable and to investigate the effects on vegetation, both pre and post-flood coverage must be known. The pre-flood vegetation coverage is often unknown, and therefore few studies have addressed the immediate impact of a extreme flood (Bendix, 1998). Bendix (1998) found that a one in ten year flood did not lead to significant removal of vegetation in the Piru and Sespe creeks, California, where the riparian zone is dominated by Salix, Populus and Alnus species. In contrast, another study showed that extreme floods led to a strong widening of the channel immediately after the flood, which did remove some trees (Friedman and Lee, 2002). They also found that the long-term effects of extreme floods eventually increased the total width and density of riparian forests and maintained the abundance of young trees. This study, however, showed no significant widening of the river channel in the two extreme discharge scenarios. The lack of this effect could explain the low removal of vegetation, as a widening of the channel indicates erosion of the riverbanks, resulting in uprooting of the vegetation on these riverbanks. However, a field study showed that woody vegetation is able to prevent erosion of the riverbank during major floods (Beeson and Doyle, 1995). Other studies also showed that woody vegetation is able to prevent sudden widening of the river channel across the floodplain during major floods in systems that are close to a transition from single- to multi-thread planform (Griffin and Smith (2004); Smith (2004) as reviewed by Gurnell (2014)). Another reason why no widening was visible, could be because around 1993 the proportion of bed level between 0 and 1 meter above BGL was already quite high (see Fig 5.3). This could also be a reason why an extreme flood did not show a strong widening of the river channel in the model results.

The low removal of vegetation in the model during extreme floods can also be due to the fact that the model uses relatively large grid cells. This means that local scour effects such as horseshoe vortices like those around a bridge pier are not modelled, which can be an important process for large trees during removal by large floods (Tanaka and Yagisawa, 2009).

6.1.3. Simplifications

Although the current model is a step forward in vegetation modelling, some simplifications had to be made within the model. The below paragraphs describe the most important simplifications within the vegetation model and how they are expected to effect the model results.

Drought

The results show that the drought process plays an important role in the colonization of vegetation, because young seedlings are very vulnerable to drought. Drought stress occurs when the roots cannot reach the capillary zone above ground water, where the ground water is directly connected to the occurring water levels. This is a more realistic description of the drought process and a step forward compared to other advanced riparian vegetation modelling studies, where they used the uninterrupted time that the vegetation was not flooded as a drought indicator Van Oorschot et al. (2016); Martínez-Fernández et al. (2018). Even while the drought process is improved, it is still a simplification of reality and does not take all factors into account. An example is the weather conditions, during rainfall it is possible that vegetation can survive even if the roots do not touch the modelled capillary zone. Conversely, seedlings under particularly hot and dry conditions are probably more likely to die from drought than assumed in the model. Another assumption is that the thickness of the capillary fringe layer is the same throughout the entire model domain. In an actual river the sediment composition may vary, resulting in variations of the capillary fringe layer (lower for gravel, higher for fine sand) (Mahoney and Rood, 1998). This means that in some cases the drought stress can be both under- and overestimated, which can have consequences for the places where the vegetation settles.

Flooding

For the flooding mortality, the number of continuous days of flooding is used as the mortality threshold. This threshold is the same throughout the year in the current model. However, studies show that Salicaceae species are less resistant to flooding during the growing season than outside the growing season (Glenz et al., 2006). The current model uses flooding thresholds based on those found in the growing season, but with relatively low flooding slopes so that flooding mortalities occur very gradually. However, this means that flooding mortalities are currently overestimated outside the growing period and underestimated within the growing period. A improvement within the vegetation model would therefore be to let the flooding thresholds vary throughout the year.

Uprooting

The uproot mortality process is based on the principle that a part of the original roots must be exposed by erosion. The original roots are those that grow below the initial germination level. However, when a part of a tree stem is buried under sediment, the tree will develop new roots in this new sedimented layer, the so-called adventious roots (see Fig. 2.4). However, these adventious roots can become the most important part of the root system (Holloway et al., 2017), because Salicaceae species have been remarkably acknowledged to be efficient traps of fine sediment (Corenblit et al., 2009). This means that in some cases, trees have long since been removed or died when these adventitious roots are exposed by erosion. As a result, the model may in some cases underestimate the uproot mortality of older trees in the model, because they have a larger chance of being partly buried under sediment.

Another simplification that influences the uprooting of trees is caused by the method in which bank erosion is modelled. In Delft3D FM a very simplified way of bank erosion is used (see Sec. 3.2). Normally, trees can be undermined by bank erosion, causing them to fall into the water (Keller and Swanson, 1979; Rutherfurd and Grove, 2004). Because bank erosion cannot be modelled properly, this process of undermining trees can not take place in the model. The model, therefore, likely underestimates the removal of trees due to uprooting.

Seedling growth

Although including seedling growth process has improved the model considerably compared to previous model studies, there are also uncertainties and simplifications. An important simplification is that the vegetation model can only specify one germination date per cell. Due to this simplification the following effect may occur when there are different discharge peaks during the dispersal period: 1) after the first peak, seedlings are sown on the river bank and get their germination date. This germination date is important because it determines the age and size of a seedling. 2) At the moment a second discharge peak occurs and some of the seedlings have died in the during this peak, new seedlings will be sown in the same cell after the water

level retreats. This also means that the germination date of this cell is updated, so the age of the more mature seedlings is reset and they get the same properties as the new seedlings. The older seedlings will lose their advantage of longer roots and higher stem height, causing the drought, uprooting and burial mortalities in these cases to be overestimated for the older seedlings. This could mean that (e.g. in 1987 Fig. 3.5) a smaller proportion of seedlings might die, than modelled in the model. However, the effects of this simplification are probably not very large. At the time when a cell is flooded for the second time within the seed dispersal period, the earlier established seedlings have a high chance to die by uprooting or burial. This because these earlier established seedlings are still very small and thus vulnerable.

Species used
In the presented vegetation model only two tree species are used as vegetation, so no herb layer or grasses are modelled. Riparian trees need bare, moist riverbanks for their establishment (Mahoney and Rood, 1998). When these banks are covered with grass or herbs it is more difficult for riparian trees to establish themselves. This competition between vegetation is not included in the current model, which may lead to an overestimation of the total vegetation coverage of trees. The model also does not include hardwood species that often grow higher up on the floodplain. Ignoring these in the model means that those areas are slightly more susceptible to erosion during the highest floods (Van Oorschot et al., 2016). However, in reality there is also competition between softwood and hardwood, replacing softwood with hardwood (Schnitzler, 1995). This competition between hardwood and softwood is not included in the model. Because softwood is not replaced by hardwood, some of the hardwood is therefore still included in the model.

6.2. Morphological model

This study found that in the case without vegetation the river channel became more or less static and hardly showed any dynamic behaviour. This finding is contrary to previous studies which have suggested that without vegetation channel shifting rates increase (Beeson and Doyle, 1995; Burckhardt and Todd, 1998) and can even become braided (Schumm, 1985; Tal and Paola, 2010; Gurnell, 2014). This inconsistency is probably caused by the fixed upstream boundary condition in the Delft3D FM model. Propagating bars from upstream or migrating meander bends are excluded in the model as the upstream boundary is fixed. This results in a static river channels. Schuurman et al. (2013) showed in his research that a moving upstream inflow boundary is essential for modelling a dynamic river.

The model uses grid cell sizes of 25x25 m, the relative large grid cell size could however affect the vegetation. Firstly, this can have an effect on drought, because each cell is represented as a horizontal tile. This can result in relatively large differences in bed levels between cells, while in reality the river bank has a more gradual slope. This means, for example, when a cell has a fairly high bed level, the vegetation in that cell can die from drought. While in reality a part of the vegetation in the lower levels of the cell would have survived. However, the reverse can also happen, that the cell is relatively low, allowing a larger part of the vegetation to survive than in reality. Secondly, another disadvantage of the large grid cells is that smaller channels cannot form, while the results indicate that multiple shallow channels can have a positive effect on the seedling recruitment.

The grid cell size has also an effect on how vegetation is simulated within Delft3D FM. In the Delft3D FM model individual trees, plants and small scale vegetation patches are lumped within a cell. This means that their physical properties are combined to a grid-cell averaged value (see Sec. 2.3). Using large grid cell sizes mean that those properties are also averaged over a relative large area. Therefore flow concentration and erosion between small scale vegetation patches can not be modelled.

The used model grid domain has probably also an effect on the model results. The grid domain is relatively short in length. This means that for instance a local change in vegetation can have a relatively large influence on the total vegetation coverage. An example of this is the overgrowth of the abandoned southern river channel in the Spring peak scenario, which causes a large increase in the total vegetation coverage. Therefore, it is important to realize that in this model those kinds of local effects can have a relatively large effect on the results at certain times. This is why Table 4.3 mainly uses the median value, so that outliers are not included in the statistics. An recommendation would be to use a longer grid in a future studies.

Although a major step has been taken in investigating the sensitivity of different vegetation properties, the effects of different Delft3D FM settings and parameters have not yet been investigated systematically. This means that some uncertainties in the results may not yet have been discovered. Important to investigate is the effect of different sediment transport formulas, sediment sorting, transverse slope concepts and morphological acceleration factors. It is also important to note that the Delft3D FM model in this study uses the simple ThestSD scheme to calculate bank erosion: a dry grid cell erodes when erosion occurs in a neighbouring wet grid cell. In this study 50 percent of the erosion is assigned to the adjacent dry cells. Changing this percentage could influence the vegetation uprooting mortalities, as vegetation is often located on those dry cells close to the river channel.

6.3. Model applicability

The current model is based on real-life processes in hydrology and physiology should be applicable for a range of Salicaceae species and for different vegetated meandering rivers, large and small. However, the condition is that the modelled vegetation reproduces itself by means of seeds distribution by the river flow and germinating on dry riverbanks. Although the model is developed with data from the Allier river, it is very easy to modify vegetation characteristics or to add other vegetation species, as long as the mortality thresholds and growth characteristics of the vegetation are known.

In this study the vegetation-development model is coupled with Delft3D FM using the BMI Python module, which makes it possible to directly read variables from Delft3D FM memory into the Python vegetation model. A simulation of 50 years using the coupled model developed in this study takes around 12 hours of computation time on a single processor core[1]. It was found that on a computer with 4 cores and a memory of 16GB up to 3 simulations could be performed simultaneously without affecting the computation times. This is significantly faster than the model used in the study of Van Oorschot et al. (2016), where a simulation of 300 years takes around 3 to 5 weeks depending on the amount of vegetation species modelled (pers. comm. M. van Oorschot). This significant reduction in computation times makes the developed coupled model in this study better applicable for modelling many model runs with small variations. Consequently it makes the model more applicable for river management purposes, as a envelope of model results is more informative than a single, never exactly right model outcome.

The vegetation development model should also applicable on braided rivers, because the colonization and mortality processes occur in the same way in a vegetated braided river as in a meandering river. Studies have shown that Delft3D 4.0, which is the predecessor of Delft3D FM, is capable of modelling braided sand-rivers with the right combination of the sediment formula, spiral flow and transverse slope concepts (Schuurman et al., 2013, 2018). Therefore, it is assumed that modelling sand-braided rivers is also possible with Delft3D FM.

The current coupled model is less suitable to model braided gravel rivers, because of two reasons. First of all, earlier modelling studies showed that bank erosion is important when modelling braided gravel rivers within Delft3D 4.0 (Javernick, 2013; Williams et al., 2016; Kasprak et al., 2019). Javernick et al. (2016) looked at a vegetated braided gravel river and found that a realistic vegetation pattern was only possible by using a separate bank erosion repose scheme (pers. comm. L.A. Javernick). In this repose scheme, the slope across each cell boundary is calculated, and material is moved downslope in locations where the slope angle exceeds the repose slope. However, this Repose module has been specially developed for Delft3D 4.0 and cannot be used in Delft3D FM. This indicates that the modelling of vegetated braided gravel rivers is currently not possible with Delft3D FM.

The second reason that the current coupled model is less suitable to model braided gravel rivers is because gravel braided rivers require relatively small grid cell sizes of around 1-2 meters (eg. Javernick (2013); Williams et al. (2016); Kasprak et al. (2019)). This means that the computation times of those models are high and therefore those models are only used to simulate flood events. However, vegetation development takes months to years, depending on the vegetation species. To model vegetation development within a braided gravel river would require huge computation times.

[1] Specifications: Intel Xeon Gold 6144 CPU @ 3.50GHz

7

Conclusions and recommendations

7.1. Conclusions

The objective of this study was to gain a better understanding of how extreme discharge events can affect the channel and vegetation patterns of a vegetated meandering river. This was studied by means of a literature study and the development of a dynamic vegetation model which was coupled with a hydro-morphodynamic model. This chapter presents the conclusions of this study by means of answering the research questions posed in chapter 1. The main research question is answered first, followed by the sub-questions of second research question.

What effect can an extreme flood event have on the long-term riparian vegetation development and larger-scale morphology of a meandering river and what is the recovery time of such an event?
Based on this study it can be concluded that the direct effects of an extreme flood are relatively low, with almost no vegetation removed during such a flood. However, the extreme floods cause an increase in the amount of areas suitable for seedling colonization within the river floodplain. This causes an increase in the seedling recruitment rate in the years directly after an extreme flood and in a higher vegetation coverage.

The higher vegetation coverage in the years after an extreme flood causes a narrowing of the river channel and eventually forces the river to become single-threaded. This results in a reduction of the amount of suitable areas for seedling colonization and consequently to a decrease in seedling recruitment. Depending on how successfully the secondary streams are colonized with vegetation, this leads to equal or lower vegetation coverage than in the scenario without extreme floods. However, the results show that the reduction in the number of suitable areas for seedling colonization is likely to be temporary, as there is an upward trend in recruitment band size after about 20 years of extreme flooding.

What processes influence channel and vegetation patterns and need to be included in the numerical and vegetation-development model?
The vegetation development has a strong feedback loop with its environment and includes three main drivers: 1) the river flow, 2) river morphology and 3) the vegetation development itself. Riparian vegetation is able to influence the river flow and prevent erosion of the bed level. In turn, river flow causes vegetation mortality but also enables the recruitment of new vegetation. The morphology provides habitat for the vegetation but also causes vegetation mortality. These three drivers are essential to reliably simulate riparian vegetation. In this study, Delft3D Flexible Mesh (Delft3D FM) is used to model the river flow and morphology. The vegetation development is modelled in a separate Python model and coupled with Delft3D FM, so that all the three main drivers are included in the coupled model.

In the vegetation model six different vegetation processes are used to model riparian vegetation development: seedling recruitment, growth, flooding mortality, drought mortality, uprooting mortality and burial mortality. The combination of those processes define whether the vegetation coverage will increase, decrease or stays the same.

Recruitment of new riparian vegetation happens mainly through the reproduction of seeds. During the seed dispersal period thousands of seeds float on the river surface and in combination with receding water levels, those seeds can successfully germinate on the river banks. Without receding water levels seeds can not be dispersed on the river bank. Successful seedling recruitment is therefore depended on the discharge conditions during the seed dispersal period.

Uprooting, burial, flooding and drought are the main mortality processes for riparian vegetation. In its first year riparian vegetation is the most vulnerable to those processes, especially drought. Riparian vegetation older than one year is most vulnerable to flooding and uprooting, and occasionally to drought. Burial does not occur on older vegetation.

Growth is an important processes because it determines the properties of the vegetation. The physical properties like the stem height, diameter and root length depend on the age of the vegetation. But also properties such as the flood and drought resistance increases when vegetation gets older. In the vegetation model all those properties are updated once a year, because they change relatively slowly in vegetation. A exception is made for vegetation younger than one year, for which the stem height and root length are updated weekly. This is done because young riparian vegetation grows rapidly in its first year and has therefore large changes in its mortality resistance

How can the processes and computational efficiency of the vegetation-development model of Van Oorschot et al. (2016) be improved?
This study a new vegetation development model is developed. A part of the vegetation processes used are based on a model developed by Van Oorschot et al. (2016). The new vegetation model is improved in several ways which are described below.

The first important improvement of this study is the modelling of seedling recruitment. Seedlings are rather vulnerable in their first year, which requires an accurate and realistic simulation of their survival rate during this period. This determines if (and where) the vegetation cover will increase. Two important processes contribute to the modelling of seedling survival: drought stresses and seedling growth. Earlier studies showed that drought stresses are the main mortality cause for seedlings. This study made a major improvement in modelling those drought stresses, because it is the first to link drought stresses to the occurring groundwater levels within a coupled vegetation morphology model. With this improved method, drought mortalities of the vegetation are simulated in a much more realistic way. An improvement for the simulation of seedling growth was made by more frequent updates of the young vegetation. This makes it possible to take the higher mortality resistance of more mature seedlings into account. Because of these two improvements, it is possible to simulate reliable seedling recruitment rates in the current model.

The second improvement is related to the uprooting process in the vegetation-development model. In previous models the roots needed to be entirely exposed by erosion before the vegetation would be removed. In the new model, only a user-defined percentage of the root length needs to be exposed in order to remove the vegetation. This method of including the uprooting process is more in line with various field observations, is more flexible and can be considered a better representation of reality.

The last major improvement in this study is made in the coupling method between the vegetation model and the hydro-morphodynamic model. In this study the vegetation-development model is coupled with Delft3D FM using the BMI Python module, which makes it possible to directly read variables from Delft3D FM memory into the Python vegetation-development model instead of using text files. This makes the coupled model in this study 7 to 10 times faster than the model of Van Oorschot et al. (2016).

How sensitive are the model results on the formation of vegetation and morphological patterns to the model settings?
The model that is developed in this study is able to realistically model riparian vegetation. The model results of the default scenario show realistic vegetation patterns and vegetation age distributions compared to field observations reported in literature and observed in the Allier river. The results show that in the Allier river in France the vegetation creates and maintains an active meandering system, and thereby confirms the earlier

findings of Van Oorschot et al. (2016). Simulating dynamic vegetation results in a more dynamic river because it influences the flow and morphology of the river, ultimately resulting in islands, chute cut-offs and secondary channels. This is in contrast to the no coupling scenario where the influence of vegetation was not included in the hydro-morphodynamic model, leading to a very static behaviour of the river channel. Another effect of the coupling was that a much higher vegetation cover was observed. This is because the coupled vegetation is able to influence the flow and erosion of the river, leading to much lower vegetation mortality.

The sensitivity analysis showed a strong interaction between vegetation and morphology, and found that vegetation characteristics can have a large influence on the river morphology in the model. In general, a higher vegetation coverage leads to a more dynamic river behaviour in the model. An exception, however, is vegetation with characteristics that allow them to colonize the river banks very quickly. In this case the rapid colonization leads to stabilization of the river banks, which in turn leads to a static behaviour and narrowing of the river channel. This effect is most pronounced in the scenario with fast growing seedlings, where the rapid seedling growth rate causes a rapid colonization of the river banks.

The total modelled vegetation coverage is most sensitive to the flooding threshold of the vegetation, especially when this threshold is lowered. The flooding threshold strongly influences both the mortality as the seedling recruitment rates. The uproot resistance of the vegetation has a much smaller effect on the vegetation coverage. Results also showed that the moment and length of seed dispersal period has a large influence on seedling recruitment rate. An earlier and shorter seed dispersal period can significantly reduce the chances of successful seedling recruitment.

7.2. Recommendations

7.2.1. Model improvements

In the current model, root growth is linked to the age of the vegetation. The model could be further improved by linking the root growth to to the historical groundwater levels. This method would be more in line with studies that have shown roots of riparian trees to often reach up to the groundwater level (Scott et al., 1997b, 2000; Shafroth et al., 2000; Sprackling and Read, 1979).

This modification in the model could also help to improve the uprooting mortality process. In the current model, adventious roots are not included in the uprooting process. However, studies show that these adventious roots can form an important part of the root system (e.g., Holloway et al., 2017). The model can be improved by including these adventious roots in the uprooting process. For example, by storing the maximum occurring bed level per tree and assuming that the adventious roots reach up to this maximum bed level. In combination with historical groundwater levels, the total root length can then be estimated. This total root length can then be used to see when vegetation is removed by uprooting.

Another important improvement to the vegetation model is to apply different flooding mortalities in and outside the growing season. Studies have shown that vegetation is less resistant to flooding during the growing season than outside the growing season (Glenz et al., 2006). In the present study this distinction is not made. Therefore, flooding mortalities are currently overestimated outside the growing period and underestimated within the growing period. A solution is to slow down the counting of the continuous days of flooding in a cell outside the growing period. For example, if every day of a flooding outside the growing season is counted as half a day, the resulting flooding mortalities will be significantly lower.

An improvement of the Delft3D FM software is to specify multiple trachytopes within one Delft3D FM cell trough the Python interface. At this moment only one trachytope is specified within a Delft3D FM cell. This results in an averaging of vegetation properties within a single cell (see Sec. 2.3). As a result, the Delft3D FM model can then more accurately take into account the difference in height of the vegetation, which will lead to more realistic flow patterns. Another improvement would be the development of a more realistic bank erosion scheme within Delft3D FM. In natural rivers, trees can be removed by bank erosion due to undermining of the roots, causing them to fall into the water (Keller and Swanson, 1979; Rutherfurd and Grove, 2004). Currently it is not possible to correctly simulate this process due to the simplified bank erosion scheme within Delft3D FM.

7.2.2. Future research

Future research efforts should be aimed at investigating the effects of multiple extreme flood events, as studies predict that the frequency of extreme floods can increase due to climate change (Hirabayashi et al., 2013; Van Vliet et al., 2013; Schneider et al., 2011). For instance, it would be interesting to investigate if a second extreme flood event is able to diminish the narrowing of river caused by the first extreme flood. Flume experiments showed that multiple extreme floods can have a more devastating effect on the vegetation, because the vegetation is already weakened by the first flood (Luz Fernandez et al., 2018). In further research it can be investigated if the current model shows similar effects. Additionally, the intensity of an extreme flood and its effect on vegetation and morphology should be studied. This because the intensity of an extreme flood determines its effect on the morphology and consequently on the vegetation.

It is highly recommended to further extend the sensitivity analysis of the current model. Especially the effects of different Delft3D FM settings and parameters have not yet been investigated systematically. It is therefore advised to investigate the sensitivity of the model to different sediment transport formulas, sediment sorting, ThetSD values, transverse slope concepts and morphological acceleration factors. In addition, the grid dependency of this model should be investigated. Using smaller grid sizes could for instance increase the amount of secondary channels, which could affect the vegetation coverage.

The current model shows an unrealistic static behaviour when no vegetation is included. In order to improve the morphological behaviour of the model, it is recommended to use a moving upstream inflow boundary. It is also recommended to extend the length of the model domain. In that way, local effects will have a smaller effect on vegetation coverage. This will make the model more accurate in predicting general changes in the vegetation coverage.

7.2.3. Model applicability

With few modifications (see Sec. 6.3), the model can be applied to other meandering vegetated rivers and used to investigate long-term effects of changing discharge regimes, human interventions, and river adjustments on riparian vegetation. Because of the model's relatively fast computation times it is possible to quickly investigate multiple scenarios with slightly different vegetation characteristics and discharge regimes. This makes the model applicable for river management purposes, as an envelope of model results is more informative than a single, never exactly right model outcome. Furthermore, crucial biological processes, like drought and growth processes, were added or improved which improved the reliability of seedling recruitment rates. While many vegetation processes are simulated in the model, it is not possible to implement all complex interactions. As a result, it remains unclear what the absolute value for vegetation coverage is. However, the relative difference between scenarios with different vegetation characteristics or discharge regimes can be well simulated.

Because of the improved simulating of the seedling recruitment rates the model also provides management opportunities with respect to vegetation recruitment. Especially at dammed vegetated rivers where the flow is artificially managed, the current model could be used to investigate which discharge regime is needed to promote seedling recruitment. In the case of invasive vegetation species, it could be investigated which discharge regime would dissuade the seedling recruitment of a invasive species.

A

Vegetation model

The vegetation model is a python-based model and coupled with the morphodynamic Delft3D FM model. The vegetation model is partly based on the model of Van Oorschot et al. (2016) but also uses new vegetation processes. The model can simulate riparian vegetation colonization, growth, mortality and interacts with the river flow. This Appendix gives a more technical explanation of how the model is build and how each process is incorporated in the vegetation model. See Chapter 2 for a literature review of each process.

A.1. Vegetation coverage

For each vegetation species a two dimensional array is used to define the vegetation coverage. Table A.1 shows an example of such a array, each row represents a cell in DFM and each column represents the age in years of the vegetation. For example DFM cell 3 is coveraged for 40 percent with zero to one year old seedlings and for 10 percent with three to four year old trees. Multiple vegetation ages and even species can therefore exist in one DFM cell.

For each vegetation characteristic a similar two dimensional array is used. Table A.2 shows such an array with the stem height as example. In the vegetation model the first column represents the seedling height, which can differ depending on the age of the seedling. The rest of the columns have the same values because the stem height is then depended on Equation 2.1. It is important to note that for every age and cell the stem height is specified, even if there is no vegetation coverage in that cell.

	Age 0-1	Age 1-2	Age 2-3	Age 3-4
DFM cell 1	0	0.2	0	...
DFM cell 2	0	0	0	...
DFM cell 3	0.8	0	0.1	...
DFM cell 4	0.4	0	0	...
DFM cell 5	...	...	...	...

Table A.1: An example of a two dimensional array of the vegetation coverage in the model

	Age 0-1	Age 1-2	Age 2-3	Age 3-4
DFM cell 1	0.5	1.0	2.3	...
DFM cell 2	0.002	1.0	2.3	...
DFM cell 3	0.3	1.0	2.3	...
DFM cell 4	0.4	1.0	2.3	...
DFM cell 5	...	...	...	...

Table A.2: An example of a two dimensional array used in the model to define the vegetation characteristics per year. In this example the stem height is used as vegetation characteristic.

A.2. Vegetation processes

The model exists of seven main processes:

- Seedling recruitment
- Uprooting
- Burial
- Flooding
- Drought
- Growth
- Seedling growth

The effect of each process depend on the vegetation characteristics which can vary per species. In this study two vegetation species are simulated in the model, but the amount of species can easily be changed. For each vegetation species the user has to specify the corresponding vegetation characteristics. Tables 2.1 and 2.2 show the vegetation characteristics that are used in this study for the default scenario and need to be specified in the model.

A.3. Seedling recruitment

Recruitment of new vegetation takes place during the seed dispersal period. If a cell is currently dry and was wet in the previous time step, seeds are deposited in cells that have room for establishment. Dry and wet cells are defined by a wetdry threshold of 0.05 m. When cells are already completely filled with older vegetation, new vegetation cannot settle. Vegetation is added to a cell with a maximum fraction defined by the ini_fraction, in this study an ini_fraction of 0.8 was used (similar to that in the study of Van Oorschot et al. (2016). For each newly colonized vegetation type, the current bed level of the grid-cell is recorded. This value is called the germination level and used to determine the amount of future sedimentation and erosion in the grid-cell which is used for calculating the mortality due to burial or uprooting. The following actions are performed during colonization:

- Summing fractions of all vegetation types and ages per grid-cell
- Check if current time is within seed dispersal window of one of the defined vegetation types
- Check available space in each grid-cell
- Check if grid-cell is now dry; water depth < 0.05 and was previously wet; maximum water depth t-1 > 0.05
- If all conditions are met: vegetation is added to the grid-cell up to the maximum defined fraction
- Colonization takes place in small steps to ensure evenly divided vegetation when there are multiple vegetation types.

Vegetation characteristics	
Changes every year	Depends on the life stage
Stem height	Stem density
Root length	Area fraction
Stem diameter	Drought threshold
	Drought slope
	Flooding threshold
	Flooding slope
	Uproot factor

Table A.3: Overview of all the vegetation characteristics. These are divided between the characteristics that change every year and those that depend on the life stage.

A.4. Growth

Apart from the seedling stage, vegetation growth is relatively slow. Therefore vegetation properties for vegetation older than 1 year are updated once a year. The vegetation properties depend on the age vegetation. The vegetation age determines the corresponding vegetation properties.

Table A.3 gives an overview of all the vegetation characteristics in the model. Physical properties such as shoot length, shoot diameter and root length are specified with a growth formula (see Equation 2.1) and change every year. Vegetation characteristics such as flooding and drought thresholds do not necessarily change every year, because these depend on the life stage a vegetation is in. This is also determined by the age of the vegetation, but vegetation can be in the same life stage for several years.

For each vegetation characteristic a two dimensional array is used in the model. Table A.2 shows an example of such a two dimensional array used in the model to define the vegetation characteristics per year. In this example the stem height is used as vegetation characteristic. This array is directly linked with the fraction array (Table A.1). Vegetation growth is achieved in the model by sliding the fraction values in the fraction array one column to the right. The new column on the left side will exist of zeros, which can eventually be filled with new seedlings. The fraction values on the last right side, which represent the oldest vegetation, will be removed because they have reached their maximum age.

The same operation happens for the array which stores the germination height ($seedheight$), because this array is directly linked to the vegetation coverage in the fraction array.

A.5. Seedling growth

Seedling growth is fast and it is therefore important to model in more detail (see section 2.2.3). Therefore the root length and stem height of seedlings depend on the moment of germination and change throughout the year. The seedling growth is defined using the following steps:

1. First the age in days of the seedlings in each DFM cell is calculated using the date of germination.

2. With now known seedling age for each cell the corresponding stem height is calculated for using Equation 2.2

3. Using the seedling age also the root length is calculated with Equation 2.5.

A.6. Mortality slopes

The mortality processes Flooding and Drought use mortality function instead of a single threshold, see Figure 2.5. Using a mortality function gives the opportunity to use a gradually increasing vegetation. The mortality function is created using a mortality threshold (MT) and a mortality slope (MS) as can be seen in the Figure. The model checks every timestep if a cell is flooded or dry and keeps track of the consecutive days of flooding and drought of each cell. If the consecutive days of either flooding or drought exceed the corresponding flooding or drought thresholds, mortality is induced by reducing the fraction of the vegetation in that cell using the mortality function:

1. First it is checked if there was already a fraction reduction in the previous vegetation time step due to the same mortality process.

2. If so, first the previous survival percentage ($SP_{previous}$) is calculated with the consecutive days (CD) of either flooding of drought from the previous vegetation time step:
$SP_{previous} = \left(100.0 - \left(CD_{previous} - MT\right) * MS\right)$

   (a) If $SP_{previous}$ is higher than 100 percent, it is set back at 100 percent.

   (b) If $SP_{previous}$ is exactly zero it is set to 0.0001

3. Now the new mortality percentage is calculated with the updated consecutive days (of either flooding or drought):
$SP_{new} = (100.0 - (CD_{new} - MT) * MS)$

4. If SP_{new} is higher than 100 percent, it is set back at 100 percent.

5. Now the survival rate (SR) can be calculated, the SR represents the amount of vegetation that will survive after the process:
$SR = SP_{new}/SP_{previous}$

   (a) If SR is negative it is set to 0.

6. With the survival rate the new vegetation fraction in a cell can be easily calculated by: $fraction = fraction \cdot SR$

Example Consider a vegetation species with a flooding threshold of 50 days and a flooding slope of 1, a cell that has been flooded for 100 days, a vegetation fraction of 0.3 in that cell and a vegetation time step of 10 days. The previous survival percentage was $SP_{previous} = (100.0 - (90 - 50) * 1) = 60$ and the new survival percentage is $SP_{new} = 50$. This gives a survival rate of $SR = SP_{new}/SP_{previous} = 0.833$. The new fraction becomes therefore: $fraction = 0.3 \cdot 0.833 = 0.25$. Note that in this specific case the vegetation fraction in this cell could never been higher than 0.6, because in the previous vegetation time steps a part of the vegetation has already been removed due to flooding!

A.7. Flooding

Prolonged flooding of vegetation can be a cause of vegetation modelling and is therefore included in the model. The consecutive days of flooding is counted for each cell and used in combination with a user specified threshold to see if the vegetation will die due to flooding. The flooding process uses the following steps to calculate the flooding mortalities.

1. First for each cell is checked if it is flooded (eq. A.1). A cell is considered flooded if: (1)the mean water depth (wd_mn) during the vegetation time step is 5 cm or higher and (2) the mean depth averaged velocity (vel_mn) during the vegetation time-step is higher then 0.01 m/s. The velocity threshold is used to eliminate cells that were flooded during a flood but are not completely drained after the flood and act as some unrealistic pools of water.

$$flooded \text{ if } wd\_mn > 0.05 \text{ and } vel\_mn > 0.01 \tag{A.1}$$

2. For all cells that are not flooded, the consecutive days of flooding are set to zero.

3. The next step is to calculate the survival percentage of the previous vegetation time step ($SP_{previous}$, see Sec. A.6)

4. After that the consecutive days of flooding are updated.

5. Then the new mortality percentage (SP_{new}) is calculated with the updated consecutive days.

6. After that the survival rate (SR) is calculated and used to calculate the new vegetation fraction in each cell.

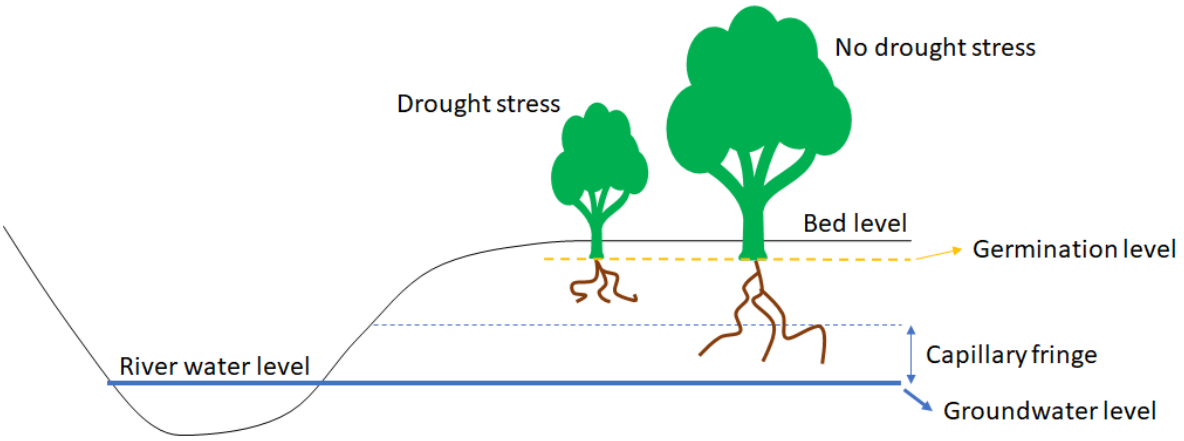

Figure A.1: Schematic representation of the groundwater level, capillary fringe and germination height related to vegetation drought stress.

A.8. Drought

Mortality by drought is calculated in a similar matter as the flooding mortality, only using the subsequent days that the vegetation in a cell can not reach the capillary fringe layer (cf) above the groundwater level (gwl) with its roots (Fig. A.1). To see if vegetation drought experiences stress equation A.2 is used:

$$\text{Drought stress if } gwl + cf < germination\_height - root\_length \tag{A.2}$$

Groundwater levels in the floodplain are not simulated in Delft3D FM. In the vegetation model the groundwater levels are therefore calculated by distance averaging the water level of the 3 nearest water containing grid-cells. A grid cell is considered water containing if the following requirements are met:

$$\text{water containing if } wd\_mn >= 0.1 \text{ and } vel\_mn > 0.1 \tag{A.3}$$

Hereby is wd_mn the mean water depth (wd_mn) during the vegetation time step and vel_mn the mean depth averaged velocity during the vegetation time-step. Higher threshold values are used in this equation than in equation A.1. It was found that higher thresholds resulted in a smoother calculated groundwater level, while lower values such as in equation A.1 sometimes still included unrealistic flooded cells somewhere higher on the floodplain. Those unrealistic cells have a large effect on the calculated groundwater levels and has therefore also a large effect on the drought mortalities. In the flooding process is a lower velocity threshold needed because most vegetation is located at the edges of the river channel where velocities are lower. The inclusion of unrealistic flooded cells somewhere higher up on the floodplain are less of a problem in the flooding process, as flooding mortalities happen on a larger time scales than the drought mortalities of young seedlings. Those unrealistic flooded cells are often caused by the drying or flooding of a secondary channel during a vegetation step. After the next vegetation step those cells often cause no problems because then they are either considered flooded or not flooded (depending if secondary channel became flooded or dry). This means that those unrealistic flooded cells have almost no effect on the flooding mortalities because these only start after 30 days at the earliest for *P. nigra* seedlings (see Table 2.1).

A.9. Uprooting

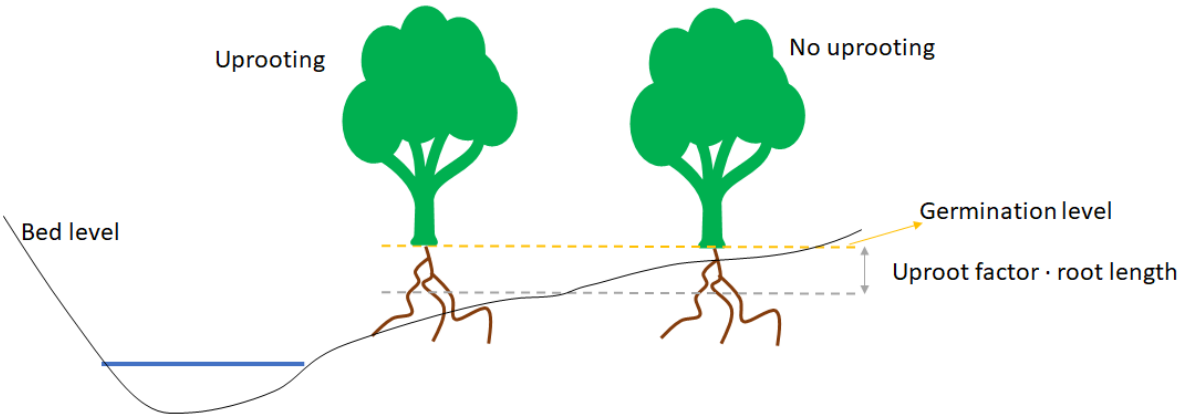

Figure A.2: Schematic representation of the uproot factor, germination level and root length related to the uprooting process.

Vegetation removal can be caused by erosion of the bed level. Uprooting takes place if the erosion is larger than the length of the vegetation root times an uproot factor (see Eq. A.4 and Fig. A.2). The uproot factor is the fraction of the root that has to be exposed to be uprooted.

$$\text{uprooting if: } (germination\_level - bedlevel) > root\_length * uproot\_factor \tag{A.4}$$

A.10. Burial

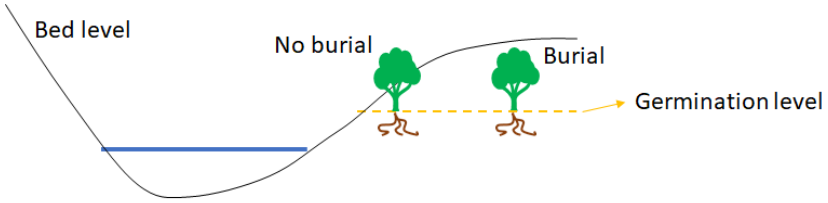

Figure A.3: Schematic representation of the burial process

Mortality by burial takes place when vegetation stem is completely covered with sediment (Eq. A.5 and Fig. A.3)

$$\text{uprooting if: } -1 * (germination\_level - bedlevel) > root\_length * uproot\_factor \tag{A.5}$$

A.11. Calculating centerline river channel

The centerline in a river is calculated based on the cross-sectional maximum flow velocity. The method used in this study largely based on the one used by Van Oorschot et al. (2016). Flow velocity values with large coordinate jumps, caused by chute bars temporarily having a higher flow velocity than the main channel were filtered out. This was done by calculating the absolute distance between two subsequent flow velocity values and as also the angle the centerline made between two subsequent flow velocity values. If this angle was less than 112.5 degrees or if the distance between two points was larger than $\sqrt{3125}$ the velocity point was considered to be wrong. In that case a new maximum velocity value in the cross-section was selected that did meet the required requirements. From this new velocity point it again checked whether the subsequent flow velocity point met the required requirements regarding the angle and absolute distance.

It was found that this method was able to provide a good representation of the centerline in the river. Figure A.4 shows an example of the calculated centerline, the red dots represent the cells with the cross-sectional maximum flow velocity. The black dots represent the newly selected cells based on the maximum angle and

distance. However in a small of cases this method was unable to correctly represent the centerline of the river. In those cases the centerline was manually removed from the dataset.

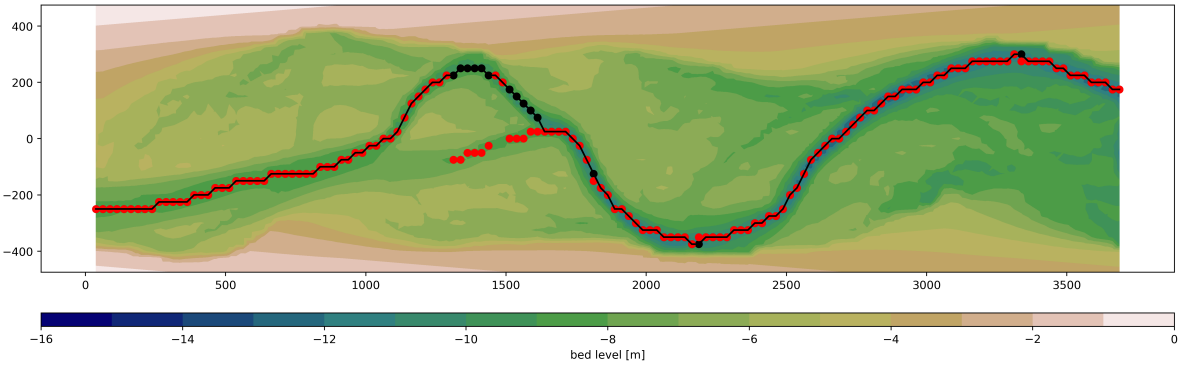

Figure A.4: Example of a calculated centerline in a river channel. The red dots represent the cells with the cross-sectional maximum flow velocity. The black dots represent the newly selected cells based on the maximum angle and distance.

Bibliography

Badhwar, G. (1984). Automatic corn-soybean classification using Landsat MSS data. II. Early season crop proportion estimation. *Remote Sensing of Environment*, 14(1-3):31–37.

Baker, W. L. (1990). Climatic and Hydrologic Effects on the Regeneration of Populus angustifolia James Along the Animas River, Colorado. *Journal of Biogeography*, 17(1):59.

Baptist, M. (2005). Modelling floodplain biogeomorphology. *Progress in Physical Geography*, 21(4):501–529.

Baptist, M. J., Babovic, V., Uthurburu, J. R., Keijzer, M., Uittenbogaard, R. E., Mynett, A., and Verwey, A. (2007). On inducing equations for vegetation resistance On inducing equations for vegetation resistance Sur l ' établissement des équations traduisant la résistance due à la végétation. *Journal ofHydraulic Research*, 45(4):435–450.

Beeson, C. and Doyle, P. F. (1995). COMPARISON OF BANK EROSION AT VEGETATED AND NON-VEGETATED CHANNEL BENDS. *Journal of the American Water Resources Association*, 31(6):983–990.

Bendix, J. (1998). IMPACT OF A FLOOD ON SOUTHERN CALIFORNIA RIPARIAN VEGETATION. *Physical Geography*, 19(2):162–174.

Braatne, J. H., Rood, S. B., and Heilman, P. (1996). Life history, ecology, and conservation of riparian cottonwoods in North America. *Biology of Populus and its Implications for Management and Conservation*, pages 57–86.

Burckhardt, J. C. and Todd, B. L. (1998). RIPARIAN FOREST EFFECT ON LATERAL STREAM CHANNEL MIGRATION IN THE GLACIAL TILL PLAINS. *Journal of the American Water Resources Association*, 34(1):179–184.

Bywater-Reyes, S., Wilcox, A. C., Stella, J. C., and Lightbody, A. F. (2015). Flow and scour constraints on uprooting of pioneer woody seedlings. *Water Resources Research*, 51(11):9190–9206.

Capon, S. J., Chambers, L. E., Mac Nally, R., Naiman, R. J., Davies, P., Marshall, N., Pittock, J., Reid, M., Capon, T., Douglas, M., Catford, J., Baldwin, D. S., Stewardson, M., Roberts, J., Parsons, M., and Williams, S. E. (2013). Riparian Ecosystems in the 21st Century: Hotspots for Climate Change Adaptation? *Ecosystems*, 16(3):359–381.

Corenblit, D., Steiger, J., González, E., Gurnell, A. M., Charrier, G., Darrozes, J., Dousseau, J., Julien, F., Lambs, L., Larrue, S., Roussel, E., Vautier, F., and Voldoire, O. (2014). The biogeomorphological life cycle of poplars during the fluvial biogeomorphological succession: a special focus on Populus nigra L. *Earth Surface Processes and Landforms*, 39(4):546–563.

Corenblit, D., Steiger, J., Gurnell, A. M., Tabacchi, E., and Roques, L. (2009). Control of sediment dynamics by vegetation as a key function driving biogeomorphic succession within fluvial corridors. *Earth Surface Processes and Landforms*, 34(13):1790–1810.

Corenblit, D., Tabacchi, E., Steiger, J., and Gurnell, A. M. (2007). Reciprocal interactions and adjustments between fluvial landforms and vegetation dynamics in river corridors: A review of complementary approaches. *Earth-Science Reviews*, 84(1-2):56–86.

Crow, P. and Houston, T. J. (2004). The influence of soil and coppice cycle on the rooting habit of short rotation poplar and willow coppice. *Biomass and Bioenergy*, 26(6):497–505.

Deltares (2018). *Delft3D-FLOW, User Manual*. Deltares, Delft.

Deltares (2020a). *D-Flow Flexible Mesh, User Manual*. Deltares, Delft.

Deltares (2020b). *D-Morphology, 1D/2D/3D, User Manual*. Deltares, Delft.

Dynesius, M. and Nilsson, C. (1994). Fragmentation and Flow Regulation of River Systems in the Northern Third of the World. *Science*, 266(5186):753–762.

Engelund, F. and Hansen, E. (1967). *A monograph on Sediment Transport in Alluvial Streams.* Teknisk Forlag, Copenhagen.

Flokstra, C. and Koch, F. G. (1980). Bed level computations for curved alluvial channels. IAHR Congress.

Francis, R. A., Corenblit, D., and Edwards, P. J. (2009). Perspectives on biogeomorphology, ecosystem engineering and self-organisation in island-braided fluvial ecosystems. *Aquatic Sciences*, 71(3):290–304.

Friedman, J. M. and Lee, V. J. (2002). Extreme floods, channel change, and riparian forests along ephemeral streams. *Ecological Monographs*, 72(3):409–425.

Garófano-Gómez, V., Metz, M., Egger, G., Díaz-Redondo, M., Hortobágyi, B., Geerling, G., Corenblit, D., and Steiger, J. (2017). Vegetation succession processes and fluvial dynamics of a mobile temperate riparian ecosystem: the lower Allier River (France). *Géomorphologie : relief, processus, environnement*, 23(3):187–202.

Gautier, E., Piégay, H., and Bertaina, P. (2000). A methodological approach of fluvial dynamics oriented towards hydrosystem management: case study of the Loire and Allier rivers. *Geodinamica Acta*, 13(1):29–43.

Geerling, G. W., Ragas, A. M. J., Leuven, R. S. E. W., van den Berg, J. H., Breedveld, M., Liefhebber, D., and Smits, A. J. M. (2006). Succession and Rejuvenation in Floodplains along the River Allier (France). *Hydrobiologia*, 565(1):71–86.

Glenz, C., Schlaepfer, R., Iorgulescu, I., and Kienast, F. (2006). Flooding tolerance of Central European tree and shrub species. *Forest Ecology and Management*, 235(1-3):1–13.

Griffin, E. R. and Smith, J. D. (2004). Floodplain stabilization by woody riparian vegetation during an extreme flood. In Bennett, S. J. and Simon, A., editors, *Riparian Vegetation and Fluvial Geomorphology*, pages 221–236. American Geophysical Union, Washington, DC, volume 8 edition.

Guilloy, H., González, E., Muller, E., Hughes, F. M. R., and Barsoum, N. (2011). Abrupt Drops in Water Table Level Influence the Development of Populus nigra and Salix alba Seedlings of Different Ages. *Wetlands*, 31(6):1249–1261.

Guilloy-Froget, H., Muller, E., Barsoum, N., and Hughes, F. M. (2002). Dispersal, germination, and survival of populus nigra L. (salicaceae) in changing hydrologic conditions. *Wetlands*, 22(3):478–488.

Gurnell, A. (2014). Plants as river system engineers. *Earth Surface Processes and Landforms*, 39(1):4–25.

Gurnell, A. M., Bertoldi, W., and Corenblit, D. (2012). Changing river channels: The roles of hydrological processes, plants and pioneer fluvial landforms in humid temperate, mixed load, gravel bed rivers. *Earth-Science Reviews*, 111(1-2):129–141.

Hirabayashi, Y., Mahendran, R., Koirala, S., Konoshima, L., Yamazaki, D., Watanabe, S., Kim, H., and Kanae, S. (2013). Global flood risk under climate change. *Nature Climate Change*, 3(9):816–821.

Holloway, J. V., Rillig, M. C., and Gurnell, A. M. (2017). Underground riparian wood: Buried stem and coarse root structures of Black Poplar (Populus nigra L.). *Geomorphology*, 279(73):188–198.

Hortobagyi, B. (2018). *Multi-scale interactions between riparian vegetation and hydrogeomorphic processes (the lower Allier River)*. PhD thesis, Université Clermont Auvergne.

Horton, J. L. and Clark, J. L. (2001). Water table decline alters growth and survival of Salix gooddingii and Tamarix chinensis seedlings. *Forest Ecology and Management*, 140(2-3):239–247.

IPCC (2014). *Climate Change 2013 - The Physical Science Basis.* Cambridge University Press, Cambridge.

Javernick, L. (2013). *Modeling Flood-induced Processes Causing Russell Lupin Mortality in the Braided Ahuriri River, New Zealand.* PhD thesis, University of Canterbury.

Javernick, L., Hicks, D. M., Measures, R., Caruso, B., and Brasington, J. (2016). Numerical Modelling of Braided Rivers with Structure-from-Motion-Derived Terrain Models. *River Research and Applications*, 32(5):1071–1081.

Johnson, R. R., Haight, L. T., and Simpson, J. M. (1977). Endangered Species vs . Endangered Habitats: A Concept. In *Importance, preservation and management of riparian habitat: a symposium*, pages 68–79. U.S. Dep. Agric.

Kalischuk, A. R., Rood, S. B., and Mahoney, J. M. (2001). Environmental influences on seedling growth of cottonwood species following a major flood. *Forest Ecology and Management*, 144(1-3):75–89.

Karrenberg, S., Edwards, P. J., and Kollman, J. (2002). The life history of Salicaceae living in the active zone of floodplains. *Freshwater Biology*, 47(4):733–748.

Kasprak, A., Brasington, J., Hafen, K., Williams, R. D., and Wheaton, J. M. (2019). Modelling braided river morphodynamics using a particle travel length framework. *Earth Surface Dynamics*, 7(1):247–274.

Keller, E. A. and Swanson, F. J. (1979). Effects of large organic material on channel form and fluvial processes. *Earth Surface Processes*, 4(4):361–380.

Kerns, B. and Peterson, D. (2014). *An Overview of Vegetation Models for Climate Change Impacts*. U.S. Department of Agriculture, Forest Service, Climate Change Resource Center.

Kleinhans, M. G., Wilbers, A. W., De Swaaf, A., and Van den Berg, J. H. (2002). Sediment supply-limited bedforms in sand-gravel bed rivers. *Journal of Sedimentary Research*, 72(5):629–640.

Klopstra, D., Barneveld, H. J., and Van Noortwijk, J. M. (1996). *Analytisch model hydraulische ruwheid van overstroomde moerasvegetatie*. Tech. Rep. PR051, HKV consultants, Lelystad, The Netherlands. Commissioned by Rijkswaterstaat/RIZA, The Netherlands.

Knopf, F. L., Johnson, R. R., Rich, T., Samson, F. B., and C., R. S. (1988). Conservation of Riparian Ecosystems in the United States. *The Wilson Bulletin*, 100(2):272–284.

Legionnet, A., Faivre-Rampant, P., Villar, M., and Lefèvre, F. (1997). Sexual and Asexual Reproduction in Natural Stands of Populus nigra. *Botanica Acta*, 110(3):257–263.

Luz Fernandez, R., Bodewes, B., McLelland, S., and Parsons, D. (2018). Presentation Impact of flood sequencing on the geomorphic-vegetation interaction in braided rivers.

Mahoney, J. M. and Rood, S. B. (1998). Streamflow requirements for cottonwood seedling recruitment—An integrative model. *Wetlands*, 18(4):634–645.

Martínez-Fernández, V., Van Oorschot, M., De Smit, J., González del Tánago, M., and Buijse, A. D. (2018). Modelling feedbacks between geomorphological and riparian vegetation responses under climate change in a Mediterranean context. *Earth Surface Processes and Landforms*, 43(9):1825–1835.

McDowell, N., Pockman, W. T., Allen, C. D., Breshears, D. D., Cobb, N., Kolb, T., Plaut, J., Sperry, J., West, A., Williams, D. G., and Yepez, E. A. (2008). Mechanisms of plant survival and mortality during drought: why do some plants survive while others succumb to drought? *New Phytologist*, 178(4):719–739.

Micheli, E. R., Kirchner, J. W., and Larsen, E. W. (2004). Quantifying the effect of riparian forest versus agricultural vegetation on river meander migration rates, central Sacramento River, California, USA. *River Research and Applications*, 20(5):537–548.

Onde, H. (1923). Les crues de l'Allier. *Revue de géographie alpine*, 11(2):301–372.

Peckham, S. D., Hutton, E. W., and Norris, B. (2013). A component-based approach to integrated modeling in the geosciences: The design of CSDMS. *Computers & Geosciences*, 53:3–12.

Pott, R. (2000). *Vegetationskundliche Untersuchung zu Fluktuation und Sukzession im Auenbereich des potentiellen Rückdeichungsgebietes Lenzen- Wustrow (Elbe)*. Sachstandsbericht im Verbundvorhaben Auenregeneration durch Deichrückverlegung, Hannover.

Rivaes, R., Rodríguez-González, P. M., Albuquerque, A., Pinheiro, A. N., Egger, G., and Ferreira, M. T. (2013). Riparian vegetation responses to altered flow regimes driven by climate change in Mediterranean rivers. *Ecohydrology*, 6(3):413–424.

Rutherfurd, I. D. and Grove, J. R. (2004). The Influence of trees on stream bank erosion: Evidence from rootplate abutments. *Riparian Vegetation and Fluvial Geomorphology*, (October 2018):141–152.

Schneider, C., Flörke, M., Geerling, G., Duel, H., Grygoruk, M., and Okruszko, T. (2011). The future of European floodplain wetlands under a changing climate. *Journal of Water and Climate Change*, 2(2-3):106–122.

Schnitzler, A. (1995). Successional status of trees in gallery forest along the river Rhine. *Journal of Vegetation Science*, 6(4):479–486.

Schumm, S. A. (1985). Patterns of Alluvial Rivers. *Annual Review of Earth and Planetary Sciences*, 13(1):5–27.

Schuurman, F., Marra, W. A., and Kleinhans, M. G. (2013). Physics-based modeling of large braided sand-bed rivers: Bar pattern formation, dynamics, and sensitivity. *Journal of Geophysical Research: Earth Surface*, 118(4):2509–2527.

Schuurman, F., Ta, W., Post, S., Sokolewicz, M., Busnelli, M., and Kleinhans, M. (2018). Response of braiding channel morphodynamics to peak discharge changes in the Upper Yellow River. *Earth Surface Processes and Landforms*, 43(8):1648–1662.

Scott, M. L., Auble, G. T., and Friedman, J. M. (1997a). Flood dependency of cottonwood establishment along the Missouri River, Montana, USA. *Ecological Applications*, 7(2):677–690.

Scott, M. L., Lines, G. C., and Auble, G. T. (2000). Channel incision and patterns of cottonwood stress and mortality along the Mojave River, California. *Journal of Arid Environments*, 44(4):399–414.

Scott, M. L., Shafroth, P. B., and Auble, G. T. (1997b). Responses of Riparian Cottonwoods to Alluvial Water Table Declines. *Environmental Management*, 23(3):347–358.

Shafroth, P. B., Stromberg, J. C., and Patten, D. T. (2000). Woody riparian vegetation response to different alluvial water table regimes. *Western North American Naturalist*, 60(1):66–76.

Siebel, H. N. and Blom, C. W. (1998). Effects of irregular flooding on the establishment of tree species. *Acta Botanica Neerlandica*, 47(2):231–240.

Siviglia, A. and Crosato, A. (2016). Numerical modelling of river morphodynamics: Latest developments and remaining challenges. *Advances in Water Resources*, 93(Part A):1–3.

Smith, J. D. (2004). The role of riparian shrubs in preventing floodplain unravelling along the Clark Fork of the Columbia River in Deer Lodge Valley, Montana. In Bennett, S. J. and Simon, A., editors, *Riparian Vegetation and Fluvial Geomorphology*, pages 71–85. American Geophysical Union., Washington, DC.

Splunder, I. V., Voesenek, L. A. C. J., Vries, X. J. A. D., Blom, C. W. P. M., and Coops, H. (1996). Morphological responses of seedlings of four species of Salicaceae to drought. *Canadian Journal of Botany*, 74(12):1988–1995.

Sprackling, J. A. and Read, R. A. (1979). Tree root systems in Eastern Nebraska. *Nebraska Conservation Bulletin*, 37:73.

Stromberg, J. C. (1997). Growth and survivorship of Fremont cottonwood, Gooding willow, and salt cedar seedlings after large floods in central Arizona. *Great Basin Naturalist*, 57(3).

Stromberg, J. C., Patten, D. T., and Richter, B. D. (1991). Flood flows and dynamics of Sonoran riparian forests. *Rivers*, 2(3):221–235.

Szałkiewicz, E., Jusik, S., and Grygoruk, M. (2018). Status of and Perspectives on River Restoration in Europe: 310,000 Euros per Hectare of Restored River. *Sustainability*, 10(1):129.

Tal, M. and Paola, C. (2010). Effects of vegetation on channel morphodynamics: Results and insights from laboratory experiments. *Earth Surface Processes and Landforms*, 35(9):1014–1028.

Tanaka, N. and Yagisawa, J. (2009). Effects of tree characteristics and substrate condition on critical breaking moment of trees due to heavy flooding. *Landscape and Ecological Engineering*, 5(1):59–70.

van Dijk, W. M., Schuurman, F., van de Lageweg, W. I., and Kleinhans, M. G. (2014). Bifurcation instability and chute cutoff development in meandering gravel-bed rivers. *Geomorphology*, 213:277–291.

van Dijk, W. M., Teske, R., van de Lageweg, W. I., and Kleinhans, M. G. (2013). Effects of vegetation distribution on experimental river channel dynamics. *Water Resources Research*, 49(11):7558–7574.

Van Oorschot, M., Kleinhans, M., Geerling, G., and Middelkoop, H. (2016). Distinct patterns of interaction between vegetation and morphodynamics. *Earth Surface Processes and Landforms*, 41(6):791–808.

van Rijn, L. (1993). *Principles of sediment transport in rivers, estuaries and coastal seas*. Aqua publications, Amsterdam.

Van Splunder, I., Coops, H., Voesennek, L. A. C. J., and Blom, C. W. P. M. (1995). Establishment of alluvial forest species in floodplains: the role of dispersal timing, germination characteristics and water level fluctuations. *Acta Botanica Neerlandica*, 44(3):269–278.

Van Vliet, M. T. H., Franssen, W. H. P., Yearsley, J. R., Ludwig, F., Haddeland, I., Lettenmaier, D. P., and Kabat, P. (2013). Global river discharge and water temperature under climate change. *Global Environmental Change*, 23(2):450–464.

Williams, R. D., Measures, R., Hicks, D. M., and Brasington, J. (2016). Assessment of a numerical model to reproduce event-scale erosion and deposition distributions in a braided river. *Water Resources Research*, 52(8):6621–6642.

Ying Liu, Gao, J., Lou, H., Zhang, J., and Cui, Q. (2011). The root anchorage ability of Salix alba var. tristis using a pull-out test. *African Journal of Biotechnology*, 10(73):16501–16507.

Zhang, X., Friedl, M. A., Schaaf, C. B., Strahler, A. H., Hodges, J. C., Gao, F., Reed, B. C., and Huete, A. (2003). Monitoring vegetation phenology using MODIS. *Remote Sensing of Environment*, 84(3):471–475.

Abbreviations

Notation	Description
BGL	Base-flow groundwater level
CFr	Fraction of a Delft3D FM cell
CSRH15	The average value of the 15 highest observed yearly channel shifting rates
Delft3D FM	Delft3D Flexible Mesh
ED	Equal dispersal period scenario
FGS	Fast growing seedlings scenario
FPFr	Fraction of the morphological active floodplain
FR	Flood resistant scenario
FS	Flood susceptible scenario
ISL	infinite sediment layer scenario
MvO2016	The vegetation-development model coupled with a morphodynamic model as developed in the study of Van Oorschot et al. (2016)
NBLU	No bed level update scenario
NC	No coupling scenario
P. deltoides var. *monilifera*	*Populus deltoides* var. *monilifera*
P. fremontii	*Populus fremontii*
P. nigra	*Populus nigra*
Q. robur	*Quercus robur*
S. alba	*Salix alba* (White Willow)
S. Albatristis	*Salix Albatristis*
S. babylonica	*Salix babylonica*
S. fragilis	*Salix fragilis*
S. gooddingii	*Salix gooddingii*
S. rubra	*Salix rubra*
S. viminalis	*Salix viminalis*
SD	Separate dispersal period scenario
SGS	Slow growing seedlings scenario
UR	Uproot resistant scenario
US	Uproot susceptible scenario

Nomenclature

Notation	Description	Symbol
a	vegetation age	$years$
B_i	braiding index	-
C	Chezy coefficient	$m^{1/2}/s$
C_b	Chezy coefficient of the bed roughness	$m^{1/2}/s$
C_{cb}	Chezy coefficient for non-submerged vegetation	$m^{1/2}/s$
C_D	Drag coefficient	-
C_v	Chezy coefficient for submerged and emerged vegetation	$m^{1/2}/s$
D	sediment grain diameter	m
D	stem diameter	m
F_v	logarithmic growth factor	-
G	vegetation size	m
g	acceleration of gravity	m/s^2
γ_s	grading factor	-
h	water depth	m
h_v	the height of the vegetation	m
k_s	Nikuradse roughness length	m
m	number of stems per square metre	$stems/m^2$
m	bar mode or number of braids	-
μ	dynamic viscosity	kg/ms
n	vegetation density ($n = mD$)	$stems/m$
ν	kinematic viscosity (=μ/ρ)	m^2/s
ϕ	grading factor	-
Re_*	the grain-size or particle Reynolds' number	-
ρ_s	density of sediment	kg/m^3
ρ_w	density of water	kg/m^3
S	the slope	-
τ_b	the bed shear stress	N/m^2
τ_t	the total fluid shear stress	N/m^2
τ_v	the vegetation resistance force per unit horizontal area	N/m^2
u_{cb}	uniform flow velocity through non-submerged vegetation	m/s
u_*	shear velocity	m/s